

A COMPARISON OF STELLAR ELEMENTAL ABUNDANCE TECHNIQUES AND MEASUREMENTS

NATALIE R. HINKEL¹, PATRICK A. YOUNG¹, MICHAEL D. PAGANO¹, STEVEN J. DESCH¹, ARIEL D. ANBAR¹, VARDAN ADIBEKYAN², SERGI BLANCO-CUARESMA³, JOLEEN K. CARLBERG^{4, 5}, ELISA DELGADO MENA², FAN LIU⁶, THOMAS NORDLANDER⁷, SERGIO G. SOUSA², ANDREAS KORN⁷, PIETER GRUYTERS^{7, 8}, ULRIKE HEITER⁷, PAULA JOFRE⁹, NUNO C. SANTOS^{2, 10}, CAROLINE SOUBIRAN¹¹,

Submitted for publication in the Astrophysical Journal

ABSTRACT

Stellar elemental abundances are important for understanding the fundamental properties of a star or stellar group, such as age and evolutionary history, as well as the composition of an orbiting planet. However, as abundance measurement techniques have progressed, there has been little standardization between individual methods and their comparisons. As a result, different stellar abundance procedures determine measurements that vary beyond quoted error for the same elements within the same stars (Hinkel et al. 2014). The purpose of this paper is to better understand the systematic variations between methods and offer recommendations for producing more accurate results in the future. We have invited a number of participants from around the world (Australia, Portugal, Sweden, Switzerland, and USA) to calculate ten element abundances (C, O, Na, Mg, Al, Si, Fe, Ni, Ba, and Eu) using the same stellar spectra for four stars (HD 361, HD 10700, HD 121504, HD 202206). Each group produced measurements for each of the stars using: 1) their own autonomous techniques, 2) standardized stellar parameters, 3) standardized line list, and 4) both standardized parameters and line list. We present the resulting stellar parameters, absolute abundances, and a metric of data similarity that quantifies homogeneity of the data. We conclude that standardization of some kind, particularly stellar parameters, improves the consistency between methods. However, because results did not converge as more free parameters were standardized, it is clear there are inherent issues within the techniques that need to be reconciled. Therefore, we encourage more conversation and transparency within the community such that stellar abundance determinations can be reproducible as well as accurate and precise.

Subject headings: solar neighborhood — stars: abundances — stars: fundamental parameters — techniques: spectroscopic — methods: data analysis — stars: individual (HD 361, HD 10700, HD 121504, HD 202206)

1. INTRODUCTION

Like many stars, the Sun is composed overwhelmingly of H and He ($\sim 98.5\%$ by mass), with the elements O, C, Fe, Ne, Si, N, Mg, S and the rest, in descending order, comprising the remainder (Lodders et al. 2009). How much of a star’s mass is in non-H/He elements (termed ‘metals’) and the proportions of the met-

als are very important parameters to constrain. Elemental abundances help astronomers constrain stellar ages (Bond et al. 2010; Nissen 2015) and trace Galactic chemical evolution (Timmer et al. 1995; Venn et al. 2004; Soubiran & Girard 2005). Most obviously, the abundances of elements in a star—and therefore its protoplanetary disk—help determine the composition of planets that form around that star.

In disks with varying chemical make-ups, different minerals will condense out of the gas, creating unique proportions of solids to form planets (Bond et al. 2008; Bond et al. 2010). Systems with more C than O could potentially form planets not of silicates but rather SiC (Kuchner & Seager 2005; Bond et al. 2010). That being said, it is worth noting that detailed observations show little variation from the solar value $C/O \sim 0.54$ ((Lodders et al. 2009), such that most stars have $C/O < 0.8$ (Nissen et al. 2014; Teske et al. 2014). More subtle mineralogical effects could be more common. The Mg/Si ratio in a planet can substantially change the mineral assemblage and mantle viscosity (Umemo et al. 2006; Ammann et al. 2011) and composition (Santos et al. 2015).

The widespread idea of chemical tagging, among stars with comparable dynamics, seeks to identify a subset of stars with very similar element abundance patterns. In this way, there is potential to find stars that formed in the same stellar cluster (e.g. Mitschang et al. 2014; Barenfeld et al. 2013), in particular stars that may have

Electronic address: natalie.hinkel@gmail.com

¹ School of Earth & Space Exploration, Arizona State University, Tempe, AZ 85287, USA

² Instituto de Astrofísica e Ciências do Espaço, Universidade do Porto, CAUP, Rua das Estrelas, 4150-762 Porto, Portugal

³ Observatoire de Genève, Université de Genève, CH-1290 Versoix, Switzerland

⁴ NASA Goddard Space Flight Center, Code 667, Greenbelt MD 20771, USA

⁵ Department of Terrestrial Magnetism, Carnegie Institution of Washington, 5241 Broad Branch Road, NW, Washington DC 20015, USA

⁶ Research School of Astronomy & Astrophysics, Australian National University, Cotter Road, Weston Creek, ACT 2611, Australia

⁷ Department of Physics and Astronomy, Uppsala University, Box 516, 75120 Uppsala, Sweden

⁸ Lund Observatory, Department of Astronomy and Theoretical Physics, Box 43, 221 00, Lund, Sweden

⁹ Institute of Astronomy, University of Cambridge, Madingley Road, Cambridge CB3 0HA, United Kingdom

¹⁰ Departamento de Física e Astronomia, Faculdade de Ciências, Universidade do Porto, Rua do Campo Alegre, 4169-007 Porto, Portugal

¹¹ CNRS/Univ. Bordeaux, LAB, UMR 5804, 33270, Floirac, France

formed with the Sun (e.g. González Hernández et al. 2010; Ramírez et al. 2014b; Nissen 2015). Chemical tagging studies benefit from measuring many elements, but especially those elements that vary the most from star to star (Ramírez et al. 2014b). Using 11 stars with both physical properties and abundance patterns similar to the Sun, or “solar twins”, Meléndez et al. (2009) looked for patterns among those refractory elements expected to be trapped in planets. They inferred that the Sun appears to be slightly depleted, relative to these solar twins, in elements trapped within the orbiting planets (Adibekyan et al. 2012). Comparatively, González Hernández et al. (2010) argued that they did not find such a discrepancy between solar twins that do and do not host planets. For all these reasons it is important to carefully measure elemental abundances in stars (Truitt et al. 2015).

Of all the non-H/He elements, the abundance of Fe is most easily measured in a star’s spectrum, owing to a large number of absorption lines at optical wavelengths. Its abundance (number or molar abundance) in a star’s atmosphere is usually reported normalized with respect to the abundance of H in the Sun, expressed as $[\text{Fe}/\text{H}] = \log_{10} [(\text{Fe}/\text{H})/(\text{Fe}/\text{H})_{\odot}]$. The iron-content of nearby, disk stars in the Milky Way spans a range, but the vast majority lie between $-0.5 < [\text{Fe}/\text{H}] < +0.5$, meaning stars have between 1/3 and 3 times the Sun’s abundance of Fe (e.g. Casagrande et al. 2011). When the Galaxy formed, ~ 1 Gyr after the Big Bang, the only dominant elements were H and He. But as the Galaxy evolved over time, supernovae, novae, asymptotic giant branch (AGB) stars, etc., enriched the interstellar medium with various elements. The range of metallicities is largely understood as reflecting the time of a star’s formation. Indeed, some of the oldest known stars, with metallicity < -2.0 dex, illustrate that the C/O has not been constant over Galactic history (Frebel & Norris 2015). Given the variety of nucleosynthetic sources occurring over the Galaxy’s lifetime, there is no reason to expect that both C and O, or any element, would be produced in exact proportion to Fe. It is widely recognized that in the Galaxy the ratio of α -elements (intermediate mass elements with even atomic number Z , as would be produced by successive α captures on elements from carbon up to the iron-peak) compared to Fe shows a trend towards super-solar values at low $[\text{Fe}/\text{H}]$ (e.g. Timmes et al. 1995). This is a result of differing contributions from core collapse and Type Ia supernovae over time. What has not been widely understood before the modern era of large surveys is the amount of variation of individual elements in stars of similar $[\text{Fe}/\text{H}]$. In other words, while the iron-content is easily measured and is even colloquially synonymous with total metallicity, it only broadly constrains the abundances of other elements. These other elements must be measured and understood in stars.

Many research groups have attempted to measure multiple elements, not just Fe, in stellar atmospheres (including many of the authors of this paper). Spectroscopic abundance data for 50 elements across > 3000 stars were compiled from 84 literature sources by Hinkel et al. (2014), who created the *Hypatia Catalog*. A surprising result of this compilation, similar to that seen in Torres et al. (2012), was that different stellar spec-

troscopy groups infer quite discrepant abundances for the same elements in the same stars. The variations in elemental abundances often exceed (by factors of 3 or more) the formal uncertainties in the measurements. Discrepancies between varying techniques were large enough, and found often enough, that the lack of agreement represents a crisis in the field of abundance determination by stellar spectroscopy.

Indeed, a number of recent papers have sought to compare different abundance methodologies in order to understand their inherent variations. For example, Bruntt et al. (2010) compared a variety of direct and indirect techniques used to calculate the fundamental parameters of bright, solar-like stars. The Gaia-ESO (Gilmore et al. 2012; Randich et al. 2013) survey team has also analyzed a combination of many methods to remove and understand systematic differences in stellar abundances. Smiljanic et al. (2014) conducted a spectroscopic analysis employing 13 different techniques who performed abundance measurements on 1300 FGK-type stars. In addition, Jofré et al. (2014); Heiter et al. (2015a) and Jofré et al. (2015) determined the iron-content, effective temperatures and surface gravities, and the abundances for α - and iron-peak elements, respectively, for 34 “Benchmark Stars” selected as the cornerstone for the Gaia-ESO survey’s data calibration. A variety of tests were performed on the spectra of these stars in order to understand the effect that, for example, data resolution, instrument, and local thermodynamic equilibrium (LTE) approximations may have on different techniques used to analyze the data.

In an attempt to reconcile the discrepancies, a Workshop Without Walls called “Stellar Stoichiometry” was held at Arizona State University, April 11-12, 2013, supported by the NASA Astrobiology Institute. The effects of elemental abundance variations on planet formation, planetary structure, and habitability were discussed (Young et al. 2014), but the emphasis was on resolving the abundance inconsistencies. To that end, workshop attendees from stellar spectroscopy groups were asked to participate before and after the workshop in a comparative study (affectionately called our “homework assignment” but what we will refer to here as the “Investigation”), in which they were provided a common set of 4 stellar spectra and asked to derive the abundances of several key elements in a variety of ways.

This paper reports the results of the comparative study, which was elaborated upon due to the findings and discussion from the initial workshop. In §2 we describe the comparative study: we list the participants and the numerical methods that each group used and then describe the common data set each group was asked to analyze. In §3 we present the results from the study, first discussing the stellar parameters and then we present the abundances of 10 key elements inferred by each group. In §4, we report on updated findings from the *Hypatia Catalog* exemplifying the magnitude of the discrepancies in abundance determinations. We also compare the results of the analysis with respect to literature abundances. In §5 we analyze some of the details of the Investigation, namely the error calculations by each group and the effect of varying line lists on the abundance results. We compare results between methods that used the curve-of-growth technique and those that used spectral fitting.

We also offer an overall recommendation to the field in order to establish more consistent results between future stellar abundances determinations. Finally, in §6, we summarize the findings of our Investigation.

2. DESCRIPTION OF THE INVESTIGATION

We chose four stellar spectra for our analysis: HD 361, HD 10700, HD 121504, and HD 202206, which are discussed in §2.1. Each group, introduced in §2.2, was asked to determine the abundances for each star in four different ways (or ‘analyses’). The end result was comprised of 16 abundance data sets for each group: four analyses for each of the four stars.

– *Run 1: Autonomous Method* - For the first run, we asked that the analysis be done in the way most typical for the participants, namely using their own line lists, stellar parameters, and customary abundance measuring techniques.

– *Run 2: Standard Stellar Parameters* - We provided all of our participants with standard stellar parameters (effective temperature T_{eff} , surface gravity $\log(g)$, and microturbulent velocity ξ) to use for each star during the second run, shown in Table 1. The standard parameters were chosen via an amalgamation of literature values that were consistent with each spectral type without giving preference to any one methodology. See Appendix C for more details.

– *Run 3: Standard Line List* - The participants were asked to use the provided line list (Table F2), which also specified excitation potentials, oscillator strengths, van der Waals damping constant, and the EW of each line. During this analysis, the groups determined their own stellar parameters. The line list was compiled from a variety of references (Column 7) with a similar wavelength range. See Appendix C for more details.

– *Run 4: Standard Stellar Parameters and Line List* - For the final run, we wanted to know whether standardizing both the stellar parameters and line list would force all of the abundance measurements to be nearly identical to within error. Therefore, the groups were told to use Tables 1 and F2 concurrently to determine the stellar abundances.

Each participating group was asked to document their entire produce and decisions during their analysis. We asked for the equivalent widths (EWs) to be recorded for every line where the curve-of-growth (CoG) method was used, such that we could do a more thorough comparison (§3.4). The line lists employed by the groups when one was not provided are shown in Tables F4-F9. All of the final abundance outputs are given as “absolute” abundances, $A(X)$, that were not normalized to the Sun, in order to reduce further cause for dispersion. Therefore, when we compare the results from this Investigation to literature sources (see §4), all of the abundances - including the literature sources - will be absolute and without a solar normalization.

2.1. Stellar Sample

The stellar spectra for this study were taken by Paul Butler and his team from the Carnegie Institute of Washington and were given to ASU for elemental abundance analysis. The spectra were observed through the Mag-

ellan Planet Search Program between December 2002–July 2009. Data were taken using the Magellan Inamori Kyocera Echelle (MIKE) spectrograph (Bernstein et al. 2003) on the 6.5 meter Magellan II telescope. The spectra have an average resolution of $\Delta\lambda/\lambda \sim 50000$ in the wavelength range 4700–7100 Å (red chip) with a S/N varying between 150–300, depending on the quality of the original spectra, with an average of ~ 200 . Individual orders were combined using the ODCOMBINE function in IRAF while wavelength calibration, carried out by the iodine absorption method (Marcy & Butler 1992), was done in IDL. The unified spectra were velocity shifted using DOPCOR with respect to the 6750.15 Å Fe I line scaled across the spectra. The function CONTINUUM was used to normalize the continuum. The calibrated data set was sent to the Investigation participants because it was considered not only typical for both resolution and S/N, but representative for standard stellar spectra (see §A) and thus, for determining typical variations.

As an aside, after the stellar abundances were sent to the participants, we discovered that there was a mismatch between the stellar spectra and the corresponding wavelengths in the region below 5050 Å. This directly impacted any element that had a line below this region, since the wrong absorption features would have been measured, namely Mg (4730.04 Å). Therefore, all groups were instructed to ignore any lines below the 5050 Å cutoff. We discuss this more thoroughly in §5.2.

We chose the four stars, HD 361, HD 10700, HD 121504, and HD 202206, based on a number of considerations. To begin, we wanted the MIKE spectra to be relatively common and “clean” for all of our stars, in order to reduce additional variation in the abundance determinations between groups. Despite analyzing a small sample, we sought to cover a range of stellar temperatures and/or stellar types which varied away from solar, but not so far that the stars were no longer comparable to each other. Gray et al. (2006) classified HD 361 as a G1V star while Morgan & Keenan (1973) used HD 10700, or Tau Ceti, as the standard G8V star. Comparatively, HD 121504 is a G2V (Houk & Cowley 1975), although may be considered more of a “G0.5V” given the systematic differences between the Houk & Cowley (1975) classifications with respect to the Morgan & Keenan (1973) grid in modern use. For similar reasons, while Houk & Smith-Moore (1988) classifies HD 202206 as a G6V, it may more closely resemble a “G8V.” For more information regarding the stellar subtype comparisons, we refer to the breakdown offered by Eric Mamajek¹.

2.2. Investigation Participants

As part of ASU’s NASA Astrobiology Institute-sponsored “Stellar Stoichiometry” Workshop Without Walls, a number of teams known for their stellar abundance research were contacted about participating in the Investigation. The aim was to accrue as many groups as possible, with as large a variety in stellar abundance techniques as possible. The six groups that participated in this Investigation were: Australian National University (ANU), Arizona State University (ASU), Carnegie Institution of Washington/Department of Terrestrial Magnetism (Carnegie), Observatoire de Genève (Geneva), In-

¹ [http://www.pas.rochester.edu/\\$\sim\\$emamajek/memo\\$_{\\\$}\\$_G2V.html](http://www.pas.rochester.edu/\simemamajek/memo$_{\$}$_G2V.html)

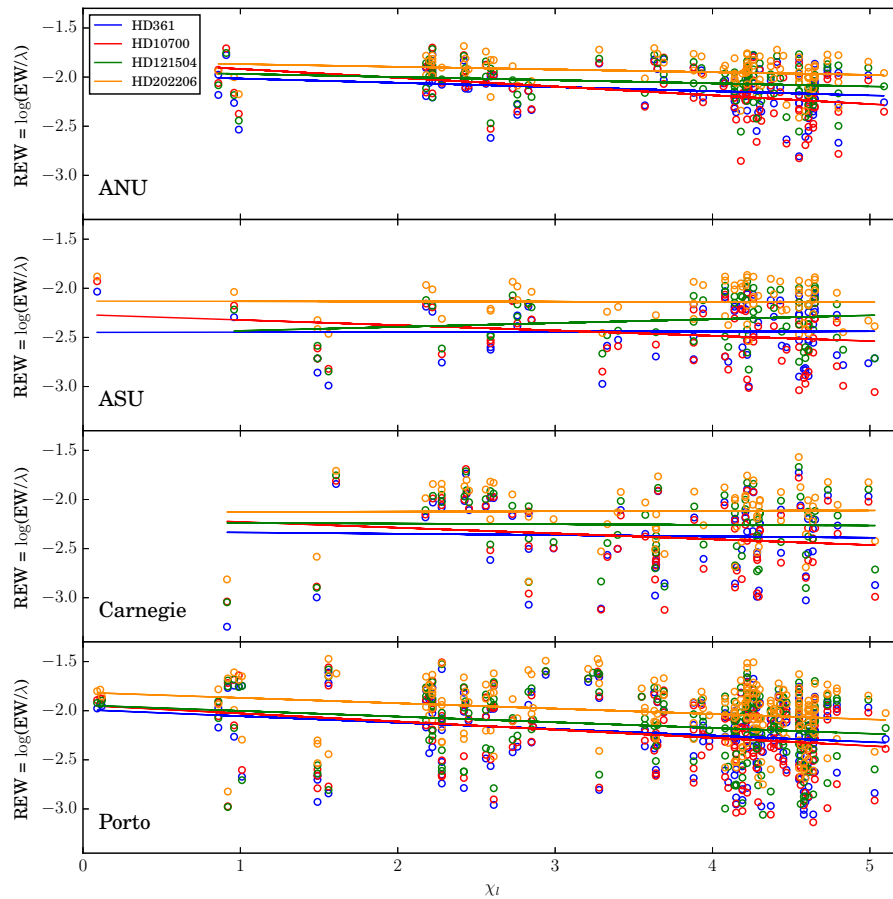


FIG. 1.— The reduced equivalent width (REW), which is determined by $\log(EW/\lambda)$, with respect to the excitation potential, χ_I , for the four CoG groups, as listed in the lower left-hand corner of each panel. Each star is represented by a different color, given by the legend in the top left corner. Linear regression lines are overlaid with respect to each star; the slopes are given in Table 3.

stituto de Astrofísica e Ciências do Espaço, Universidade do Porto (Porto), and Uppsala University (Uppsala). The names in parenthesis indicate the short-name that we use throughout the paper when referencing each group. We give an in-depth description of the methods used by the participants in Appendix B. A summary of these methods can be found in Table 2, which show that both Geneva and Uppsala employ a spectral fitting technique for determining stellar abundances while the rest use CoG. Finally, we note that only two groups participating in this Investigation overlapped with the analysis conducted by the Gaia-ESO team (i.e. Smiljanic et al. 2014; Jofré et al. 2014, 2015), namely the Porto and Uppsala groups.

3. INVESTIGATION RESULTS

Each of the 6 groups that participated in the Investigation generated one data set for each of the four stars per run analysis (see §2), including line lists, stellar parameters, EWs (in most cases), stellar abundances, and error bars. We have compiled all of this information into a number of figures and tables for better visualization. In

this section, we analyze the stellar parameters between Runs 1 and 3, element abundances for 10 elements from Runs 1–4, and conduct a line-by-line analysis for interesting elemental lines. Note that $[\text{Fe}/\text{H}]$ content was not fixed as part of the standard stellar parameters and will be discussed in §3.3 with the other element abundances.

3.1. Reduced Equivalent Width vs. Excitation Potential

When using the CoG method, the excitation and line-strength balance approach can only strictly work if there is no inherent correlation in excitation potential and line strength for the entire iron line sample utilized. If there is a correlation, then the solutions are not determinate without some additional constraint, in which case, solutions and their comparisons are meaningless. Fortunately, reducing or removing the correlation between these two parameters can be handled within the parameter calculation module of MOOG, utilized by all four CoG groups. To verify that the results were indeterminate, we have plotted the reduced equivalent width, or $\log(EW/\lambda)$, for all Fe I lines used by the four CoG groups (see Table 2) with respect to the excitation potential, χ_I ,

shown in Fig. 1. Note, that the REW and χ_I determinations were the same for all groups between Runs 1 and 2, and were provided for Runs 3 and 4, which is why we have only plotted one set of values regardless of run.

We generated a linear fit for the four stars as calculated by each group. The linear fits are overlaid on top of Fig. 1, with respective color for each star, and the slopes are given in Table 3. All of the slopes are below an absolute value of 0.09, with averages per group below an absolute value of 0.07 (last column). These are acceptable tolerances, especially considering the dispersion in the plots. Colucci et al. (2009) note that a small correlation of the REW Fe I lines with excitation potential, on par with those measured here, will not significantly affect the mean [Fe/H] abundance. In general, a correlation between REW and χ_I is most significant when a technique determines parameters in serial order, for example, constraining T_{eff} , fixing T_{eff} , constraining ξ , etc Sousa et al. (2014). None of the CoG groups determine parameters in this way, instead they find the best parameters in parallel where any possible correlations are considered during the minimization process. Overall, we found that there is no significant correlation between REW and χ_I , meaning that the resulting abundances are not indeterminate and are suitable for comparison.

3.2. Stellar Parameters

Unique stellar parameters were produced by each group for Run 1 (Autonomous) and Run 3 (Standard Line List), which can be found with their individual errors in Tables 4 and 5, respectively. We have also plotted the T_{eff} , $\log(g)$, and ξ values with respect to each other in Figure 2 (the A(Fe) comparisons will be discussed in §3.3). A representative error bar is given in the top right-hand corner for each plot, calculated by taking the median error for each star (to reduce the effect of outliers) and then taking the mean of all four stars. We signify an ‘outlier’ as a result which does not overlap any other data point to within either individual error or representative error, when the former was not reported. The standard stellar parameters, used during Run 2 (Standard Parameters) and Run 4 (Standard Line List and Parameters), are denoted as solid squares on all of the plots.

We go into more detail in Appendix D.1 regarding the trends seen in the stellar parameters. However, in general we found that both T_{eff} and $\log(g)$ varied somewhat between the Autonomous Method in Run 1 and Standard Line List in Run 3. The total ranges in both parameters for all groups became worse in Run 3 and we found that removing obvious outliers decreased the range in all stars to values smaller than those in Run 1. In fact, the ranges for Run 3 sans outliers were comparable to the average-median errors for both T_{eff} and $\log(g)$. We conclude that the standard line list had a polarizing effect on the methods analyzed in this study – making some calculations more similar and others vastly different. This may be related to the fact that a number of groups determined extremely similar $\log(g)$ values for all stars, regardless of spectral type, during the Autonomous Run 1. In contrast, the variation in ξ was constant or decreased for all stars between Runs 1 and 3, although those differences in the ranges were within the error budget. In other words, ξ was not noticeably affected by implementing a specific line list. We also found that the number of Fe

lines, as compared to the Standard Line List (see Table 2), did not impact the stellar parameters whether comparing between groups or between Run 1 and 3. This may be because the number of Fe lines implemented by all groups was above a critical number needed to consistently and precisely determine the stellar parameters of our sample.

As a further test, we compared the stellar parameters (T_{eff} , $\log(g)$, and ξ) determined by each group to the average for Runs 1 and 3. We found that everything but ξ was clearly correlated, as indicated in Figure 2, which was likely due to parameter degeneracies. Group-to-group biases confused the parameter correlations, but were realized again once outliers were removed. With outliers removed, the adopted standard line list tended to make results tighter and less correlated, supporting the degeneracy scenario. Remaining correlations are unexplained, but the strong T_{eff} -[Fe/H] correlation indicates that something rather fundamental is missing, possibly simply related to continuum placement or allowing [Fe/H] as a free parameter in Run 3.

3.3. Element Analysis

As mentioned in §2, we chose ten elements on which to focus our analysis: C, O, Na, Mg, Al, Si, Fe, Ni, Ba, and Eu. These elements cover a range of nucleosynthetic origins, from α -type to neutron-capture elements, so that we may better understand the reproducibility and standardizations employed in our study. All elements were measured by the majority, if not all, of our groups for more consistent comparisons. The abundance results for Runs 1–4 from all groups are reported in Tables 6–9. Note that, to avoid introducing more variability in the methods, the abundances are reported as absolute without any solar normalization. Therefore,

$$A(\text{El}) = \log_{10} N(\text{El})/N(\text{H}) + 12, \quad (1)$$

where $N(\text{El})/N(\text{H})$ is the atomic ratio of the element to hydrogen and normalized to 10^{12} hydrogen atoms on a logarithmic scale, such that $\log N(\text{H}) = A(\text{H}) = 12$. Abundance results are also plotted in Figures 3 and 4, using a similar legend as Figure 2. The y-axis ranges for all plots span the same distance (1.5 dex) for easier comparison between elements. While the individual group error estimations are given in Tables 6–9, we have included a representative error bar in the top-right corner of all of the individual plots in Figures 3 and 4. The representative error was calculated by first taking the median of all individual errors (to avoid outliers) determined for an element in a star per run. The median errors were then averaged across all stars and analyses, to calculate a unique representative error per element. Since we have provided all of the individual errors in Tables 6–9, these representative errors are meant to guide the eye of the reader without becoming distracting. In the rest of the discussion, similar to 3.2 and Appendix D.1, we will describe an ‘outlier’ as a result where a data point does not overlap to within individual error with any other data point (for example, the same star and run). If an individual error was not reported, we will use the representative error.

We have developed a metric to quantize how ‘good’ or similar the results are for a star per run. Assume

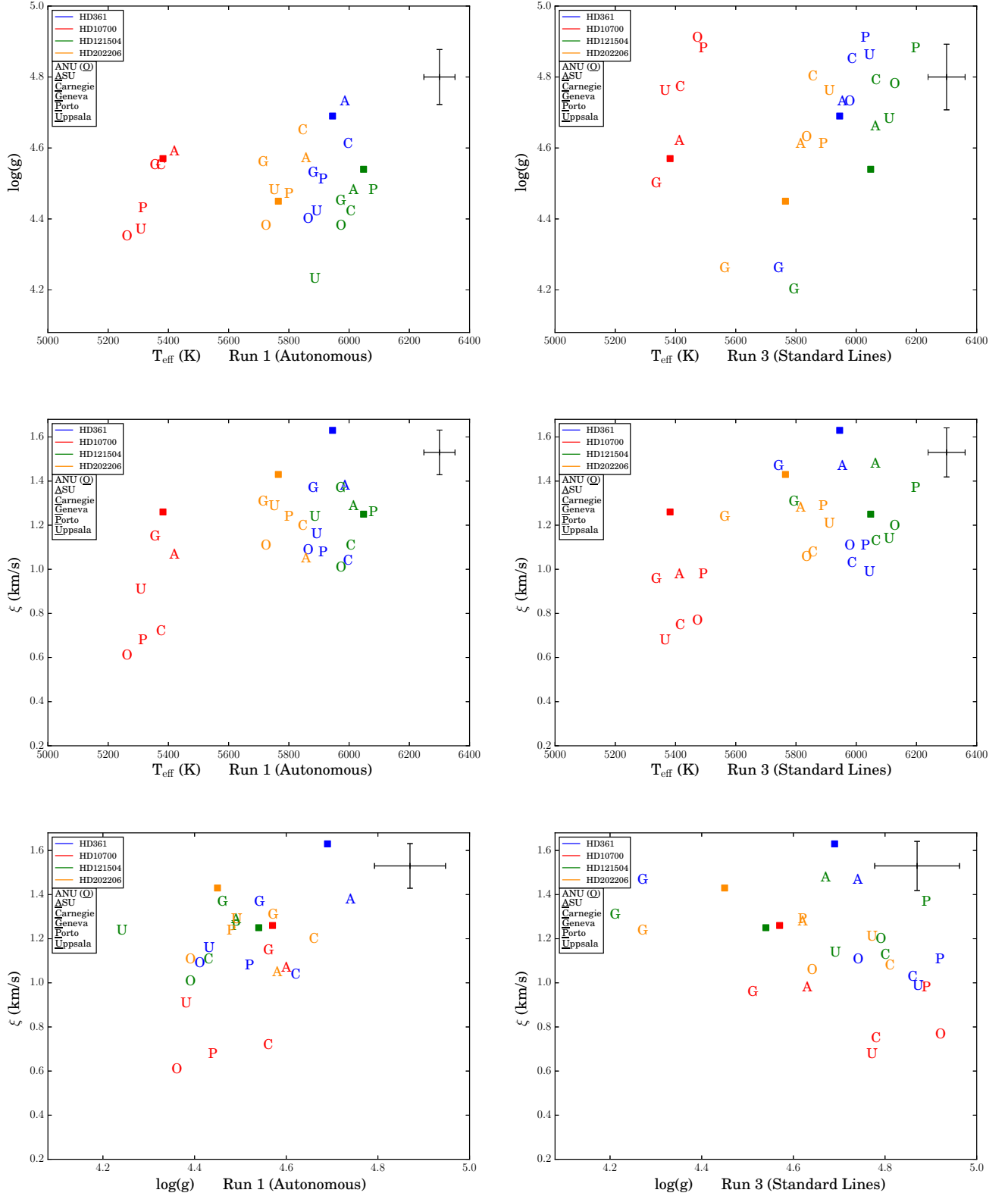


FIG. 2.— Stellar parameters for the Autonomous Method Run 1 (left column) and Standard Lines Run 3 (right column). On the top row is $\log(g)$ vs. T_{eff} , middle row is ξ vs. T_{eff} , and the bottom row is ξ vs. $\log(g)$. Colors are indicative of the star and each letter represents the group (see underlined letter in legend). There is a representative error bar in the upper right-hand corner for each plot. The standard parameters for each star, as given in Table 1, are denoted as solid squares.

that we have a total number, T , of groups who have provided T data points for the abundance of a star for a particular run (most commonly, $T = 6$). Qualitatively, we examine the distance between each individual data point with respect to the other data points, via permutation. In this way, we can calculate the average distance from each data point (i) with respect to the other data points (j). We then get the average distances for the T individual data points, which we sum. Shorter distances between points are ideal, thus we use an inverse exponential. In an ideal case where all data points are the same value, the individual-metric for each data point is 1 and the total metric (summing of the individuals) yields a value of T (for example, 6). The exponential has a varying constant per element, γ , such that if one standard deviation of the T data points is below the representative error for that element, then the metric is weighted positively. If, however, there are large gaps or outliers between the data points, the metric is weighted negatively – but with a limitation. We did not want an extreme data point or outlier to outweigh the other results, especially if the other data sets show good agreement. Thus after a point of “extremeness”, the bad point reaches a limit on how strongly it can affect the metric. To equally compare results when less than the T number of groups have measured an element, we scale the metric by $6/T$ – so 6 is the ideal maximum and values close to 0 are the minimum. More quantitatively, the metric is calculated via:

$$\frac{6}{T} \sum_{\substack{i=1 \\ i \neq j}}^T \left(\frac{1}{T} \sum_{\substack{j=1 \\ j \neq i}}^T \frac{1}{10^{\gamma |x_i - x_j|}} \right), \quad (2)$$

where x is the absolute abundance determination for a star. The results for each of the 10 elements discussed here can be found in Table 10, where the second column lists each element’s one standard deviation constant, γ .

When devising the metric, not only did we want a measurement of consistency between groups, but also the ability to compare the elements to each other. However, the use of different exponential constants for each element, γ , while mathematically rigorous, inhibits that functionality. Therefore, we have included normalized metric values (“Norm.” column in Table 10) where we have divided all metrics for a particular element (across all analyses and stars) by the maximum metric for that element. In this way, the reader does not have to reacclimate their sense of a “good” metric number between elements and can easily identify which star in which run yielded the most consistent abundance results. For example, the carbon abundances for HD 361 in Run 4 produced the most uniform measurements between groups as compared to any of the other carbon determinations (see Fig. 3, top left). The metric and normalized metric will be utilized when discussing the individual element results in §3.3.1–3.3.4 and within Appendix D.2–D.5.

3.3.1. α -Elements: C, O, Mg, & Si

Examining Figure 3, and with respect to more detailed discussion in Appendix D.2, the α -elements have varying consistency throughout each run. A likely contribution may be due to the number of lines measured for many of these elements. Carbon, oxygen, and magnesium can

range from one to three lines, with O and Mg often having only one reliable line. Silicon has many more lines, usually >8 , which tends to give a more robust result. Analyzing Table 10, the majority of stellar α -element abundance determinations were found to be the most consistent between groups. For example, the highest metric value for all four elements was usually during Run 2 – in 10 out of the 16 instances (four stars measured for four elements). Runs 1, 3, and 4 resulted in the best uniformity a total of 2 instances each.

Looking at the maximum metric, however, may neglect the possibility that a method works particularly well in one case, but poorly for others. Therefore, we take the mean and the median of the normalized metric per run for the four elements, which should be equal for a uniform distribution, to gauge the variation. We find that in all cases the median and the mean of the normalized metric are similar to each other within a 0.02 tolerance and span a range of 0.13 and 0.12, respectively. In both cases, Run 2 has the highest mean/median normalized metric, followed by Run 1, Run 3, and Run 4, respectively.

Therefore, standardizing the stellar parameters is ultimately favorable when calculating abundances for this set of elements and results in more consistent measurements between methods. However, it is unclear whether standardizing the line list was beneficial. In Appendix D.2 we go into more detail for the individual elements.

3.3.2. Odd-Z Elements: Na & Al

Per the last row in Figure 4 and the discussion in Appendix D.3, the odd-Z elements are improved when employing a standardized line list (Runs 3 and 4) in 6 out of eight cases. Looking at Table 10, most of the maximum metric values occur during Runs 3 and 4. In addition, the mean and median normalized metrics for the two elements, similar to each other by ≤ 0.03 and with a range of ~ 0.15 , are highest during Run 4.

Both elements have two lines in our spectra (see Table F2). Column 6 in Table F2 demonstrates that the EWs, specifically relevant to the CoG methods, for the first line of each element (6154.23 Å and 6696.03 Å, respectively) are similar to each other: 39.8 m Å and 38.1 m Å, respectively. However, the second lines (6160.75 Å and 6698.67 Å, respectively) are rather disparate: 58.4 m Å and 21.9 m Å, differing by a factor of ~ 3 . The weaker Al line may account for larger variation between groups.

3.3.3. Iron-Peak Elements: Fe & Ni

For both A(Fe) and A(Ni) in the top-row Figure 4, we found that all of the groups measured the abundances rather consistently, to within error, for all the analyses. See Appendix D.4 for more details. Both elements benefit from the combination of standardized line lists and stellar parameters (Run 4), although Ni also improved when standardizing only the stellar parameters (Run 2). While no results were poor, A(Fe) measurements were most uniform during Run 4, with lower metrics for Runs 1–3. In comparison, the A(Ni) determinations were most consistent for Run 2, relatively good for Run 4, and substantially worse for Runs 1 and 3. The general A(Ni) similarity between Runs 2 and 4 is reflected when taking the mean and median of the normalized metric values.

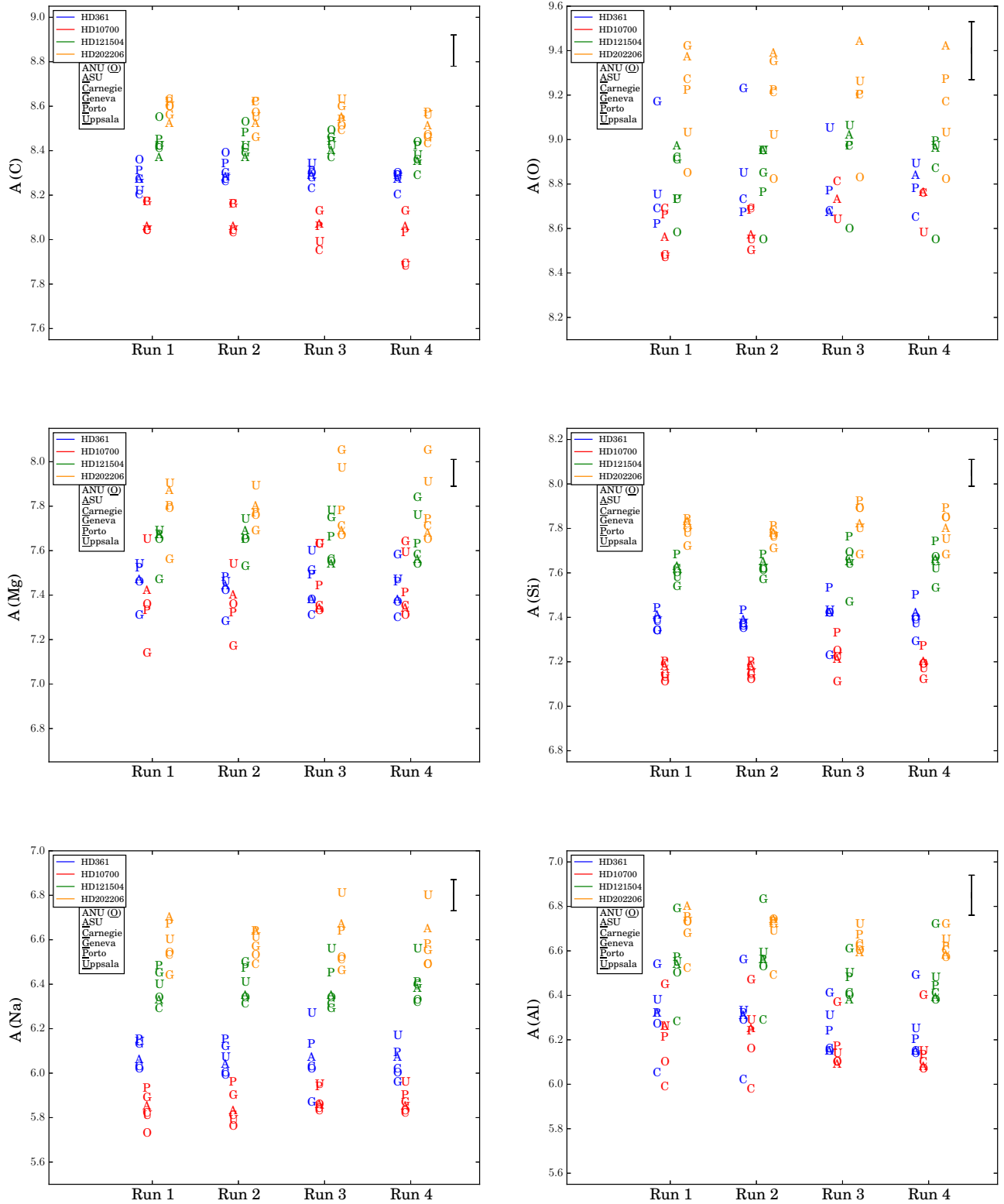


FIG. 3.— Absolute abundances of A(C), A(O), A(Na), A(Mg), A(Al), and A(Si) as determined for all four measurements analyses (Run 1 is Autonomous, Run 2 is Standard Parameters, Run 3 is Standard Lines, and Run 4 is Standard Parameters and Lines). Colors are indicative of the star and each letter represents the group (see underlined letter in legend). A representative error is given in the top-right corner, taken as the average of the median individual errors per star.

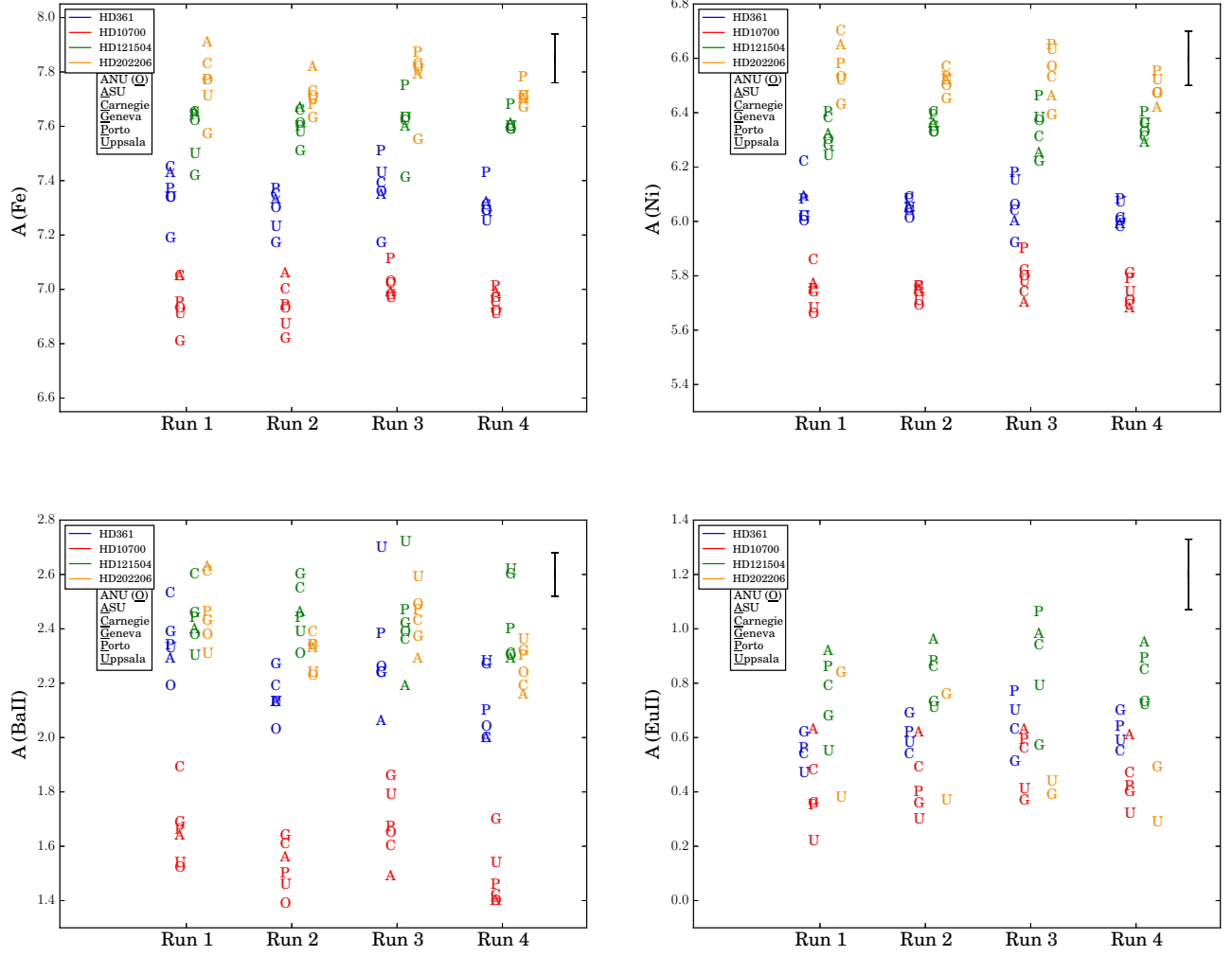


FIG. 4.— Similar to Figure 3, but for A(Fe), A(Ni), A(BaII), and A(EuII).

Namely, the mean and median, which were the same to within 0.01 for all runs, had the highest values for Run 2, followed by Run 4 (smaller by ~ 0.07), then Runs 1 and 3 (smaller by ~ 0.22). The total range was ~ 0.3 .

3.3.4. Neutron-Capture Elements: Ba & Eu

For the neutron-capture elements shown in the last row of Figure 4, there was no clear indication which standardization, if any, was better when looking at the maximum stellar metrics. This issue was made worse by the difficulty that many groups had measuring the weak Eu II line. We discuss both elements in more details in Appendix D.5. Unfortunately, analyzing the mean and median of the normalized metrics did not elucidate the situation, even when the Eu II values for HD 202206 were ignored. The variation in the mean and median determinations for each run made it clear that these distributions were not uniform: the mean values ranked the analyses from best to worst as Run 2, Run 4, Run 1, and Run 3 while the median indicated that the order should be Run 4, Runs 1 and 2 tied, and then finally Run 3. The only conclusion that can be drawn is that the standardized line list, on its own, is not conducive to making abundance measurements more uniform between groups.

3.4. Line Analysis

When trying to examine possible means of variation of elemental abundances, we initially hypothesized that the two biggest impacts on abundance determination would be the stellar parameters and the line list. We set up the four analyses to pinpoint any areas we believed introduced the greatest sensitivity. The differences between Run 1 and 2 and comparatively Run 3 and 4 should allow us to interpret the impact of stellar parameters. The differences between Run 1 and 3 should allow us to interpret the impact of the line lists chosen. Ideally, we imagined that there would be an increase in precision from Run 1 onwards; however this is not always the case.

After organizing the results we had a chance to examine the details of the individual line lists and the results that were calculated on a line-to-line basis. The line lists for each group for Runs 1 and 2 are included in Appendix F in Tables F4-F9. The standard line list used in Runs 3 and 4 is in Table F2. In this section we will look at a few selected lines to try and investigate the reasons for elemental variation, specific grouping of results, and improvements from one run to the next.

3.4.1. Iron

With the multitude of iron lines used by each group, which ranged from 60 to 298 Fe I lines (Table 2), we decided to only compare the lines for one star: metal-rich HD 202206. Table 12 shows a few selected Fe I lines for this star. The atomic parameters input for each line are the excitation potential (χ_l), the oscillator strength ($\log gf$), and the measured EW (mÅ) when given. The final 4 columns in this table are the absolute iron abundance values determined for each of the four analyses. For Runs 3 and 4, the atomic parameters are those given in the standard line list, per Table F2, which are not reproduced in Table 12 but implied via the two vertical lines. Throughout Table 12, we have provided the average iron abundance for the 7 individual selected lines

compared to the average over all iron lines, listed at the bottom.

Since the line list is the only thing standardized in Run 3, the individual line determinations can be used to understand the effect the atomic parameters have on individual lines. Additionally, it is possible to study the impact a single line may induce on the overall abundance measurement. The EWs measured by the CoG groups are the same for Runs 1 and 2 (column 5 of Table 12) and for Runs 3 and 4 (column 6 of Table F2). This is not the case for the spectral fitting groups, Geneva and Uppsala, whose methods do not produce individual EWs. The variations in technique make group comparisons difficult when analyzing on a line-to-line basis.

We include a detailed discussion of the seven individual Fe lines in Table 12 in Appendix D.6. Overall, despite similar atomic parameters, there is a scatter in the abundance determinations for Runs 1 and 2 that is likely due to the variation in methods and models. The utilization of a standardized line list is apparent in Run 3, which typically sees larger line-by-line abundance measurements. The variation in measurements between the first two analyses and Run 3 can be greater than the ± 0.09 dex representative error for iron. This is evident in the averages and total-averages listed in the table. However, during Run 4, when both the stellar parameters and line list are homogenized, the abundance determinations are more consistent with the first two runs. As seen in Fig. 4 (top-left) and in Table 10, the stars are most similar between groups in Run 4.

In general, the determinations between Runs 2 and 4 appear to be more consistent with each other to within error as compared to the Runs 1 and 3. This trend hints that stellar parameters are perhaps more influential in determining consistent abundances than standardizing the line list, at least for iron. The only remaining difference between these runs is the adopted [Fe/H] during the analysis, which was left as a free parameter and therefore varies between groups. The [Fe/H] content affects the temperature and electron density structure (important for stronger lines), the molecular equilibrium (important for C and O, as well as background H- opacity), and ionization equilibrium (important for neutral minority species, which may also depend on the H- opacity). Therefore, the [Fe/H] measurement itself may be an important missing ingredient for Runs 2 and 4.

3.4.2. Elements Other than Iron

When examining the abundances of elements other than iron it is important to note that most elements have very few absorption lines. The exceptions are silicon and nickel, which both show small ranges and great correlation between groups, as seen in Figures 3 (middle-right) and 4 (top-right). Similar to iron, here we briefly discuss the line-by-line breakdown of a select group of elements for HD 202206. Table 13 shows the line-by-line analysis of carbon, magnesium, sodium, aluminum and barium, with a more detailed discussion in Appendix D.7.

For the carbon lines, we find that there is a ~ 0.1 dex decrease in line-by-line abundance measurements when implementing the standardized line list. This indicates that the choice of carbon lines may outweigh the variation in stellar parameters or EW determinations. In general, while carbon abundance patterns emerge from

the line-by-line comparison, they are not consistent between lines or analyses. The lack of obvious trend was also true for the Mg and Ba II lines. Analysis of some Si lines imply that the EW measurement may be more significant than the oscillator strength, although that was not clear for all lines. When measuring Al, even though the groups agree on the average abundance for each star, they are systematically offset. Unfortunately, it's not clear in which direction they are offset. The solution to the Al abundances may be that we need to agree on which $\log(gf)$ values are best, which would give consistent results with each other.

4. LITERATURE ABUNDANCES

We chose the stars analyzed in this Investigation for a number of reasons, one of those was to enable a comparison to literature values. First, we discuss the *Hypatia Catalog*, a compilation of stellar abundance literature sources and the update it has undergone since Hinkel et al. (2014). Second, we will directly compare the measurements from §3.3 to the overall Hypatia 2.0 results as well as the individual data sources.

4.1. *Hypatia Catalog 2.0*

The *Hypatia Catalog*, originally introduced in Hinkel et al. (2014), is an amalgamation of stellar abundance data sets that have been renormalized to the same solar scale and homogenized to reduce systematic variations between techniques. The original catalog contained abundances for 50 elements within 3058 main-sequence (FGK-type) stars all within 150 pc of the Sun. Since then, *Hypatia* has been improved upon in multiple ways, which we are now calling *Hypatia 2.0*.

An additional 34 data sets have been added into *Hypatia* (see Table F1) which increased the stellar count by 1253 stars, making the total population 4311 main-sequence stars within 150 pc of the Sun. We have also included three new element and element-species, namely palladium (Pd), silver (Ag), and singly-ionized samarium (Sm II). A histogram showing the individual elements and the total number of stars in *Hypatia 2.0* for which they have been measured is shown in Fig. 5. The *Hypatia Catalog* will continue to be upgraded such that new data sets are included as they are released and the back-end functionality expanded. In subsequent papers, we will increase the tenths value of the version number in the former case and the ones value in the latter case, or if the two were simultaneous.

While the reduced abundance determinations, similar to those from Hinkel et al. (2014), will be made available on Vizier, we are excited to announce the creation of the Hypatia Catalog Database. The full multidimensional data found within the *Hypatia Catalog* will be available at www.hypatiacatalog.com as of Fall 2016. The online database will include catalog and abundance data manipulation, a variety of solar normalizations, planetary information (when available) from the Exoplanet Orbit Database (www.exoplanets.org, Wright et al. 2011), as well as a graphical/statistical interface. The community be able to take full advantage of these compiled resources, either within the interface or by downloading the data through a terminal.

The variety in stellar abundance techniques is nothing if not impressive. Over multiple decades, a number of dif-

ferent instruments with various resolutions, S/N, models, and programs have been utilized in order to determine elemental abundances. We go into more detail regarding the differences between observations and data reduction techniques in Appendix A. However, the problem arises when data sets are compared to one another. While data may be internally consistent, for example by measuring a unique solar abundance spectrum, it is unclear how those values will compare to data sets from other methods. As it stands, much of the abundance information that we get from different groups for the same stars often do not agree within error.

A part of the analysis of the *Hypatia Catalog* involved understanding the *spread* in the data – or the range of abundances determined by different groups but for the same element in the same star. Using *Hypatia 2.0*, we find there are 1244 stars that are so discrepant in their [Fe/H] measurements between groups, or with a spread above typical error, that it was impossible to homogenize them (see Hinkel et al. 2014). Interestingly, the analysis of the spread was taken *after* all of the data sets were renormalized to the same solar scale! The average spread in [Fe/H] for all of *Hypatia 2.0* is 0.18 dex which is nearly twice the standard error associated with [Fe/H]. Not even iron, the most frequently measured element in the field, can be well agreed upon between groups. It is because of this that we believe it is time to better understand the abundance measurement techniques that are employed by different groups, such that we can understand these systematic offsets and variations.

4.2. *Comparison to Literature*

The purpose of our Investigation is to test the effects of the various methodologies on the actual abundance measurements, in particular the determination of stellar parameters, the employed line list, the measurement of EWs, and the stellar atmospheres/abundance codes used by different groups. We cannot perform a controlled literature comparison to determine how other techniques or even other data sets/observations may vary, but we can compare the average values and spreads from our experiment to those of the literature as a whole. This enables us to estimate how much of the measurement variation could be accounted for by the particular methods tested here. A smaller spread in the Investigation results implies that some factor not present in any of our methods is affecting the values found by certain groups.

For the purpose of comparison and brevity, we will primarily focus on the averages and spreads of C, O, and Fe from the Investigation with respect to the those reported in the *Hypatia* catalog (Hinkel et al. 2014). Discussion of the other seven elements can be found in Appendix E, which are also summarized at the end of this section. While the abundance measurements were defined both with and without outliers, as described in § 3.3, comparisons here will be without outliers unless noted otherwise. In Table 11, all known (at the time of this writing) literature sources are listed with an associated *Hypatia* value, which is the median of the A(X) values by the groups who measure that element per Hinkel et al. (2014). Unfortunately, HD 121504 has no reported abundances in the literature for elements besides Fe and is not discussed. Carbon determinations behave similarly for the Investigation and the literature as a whole. For

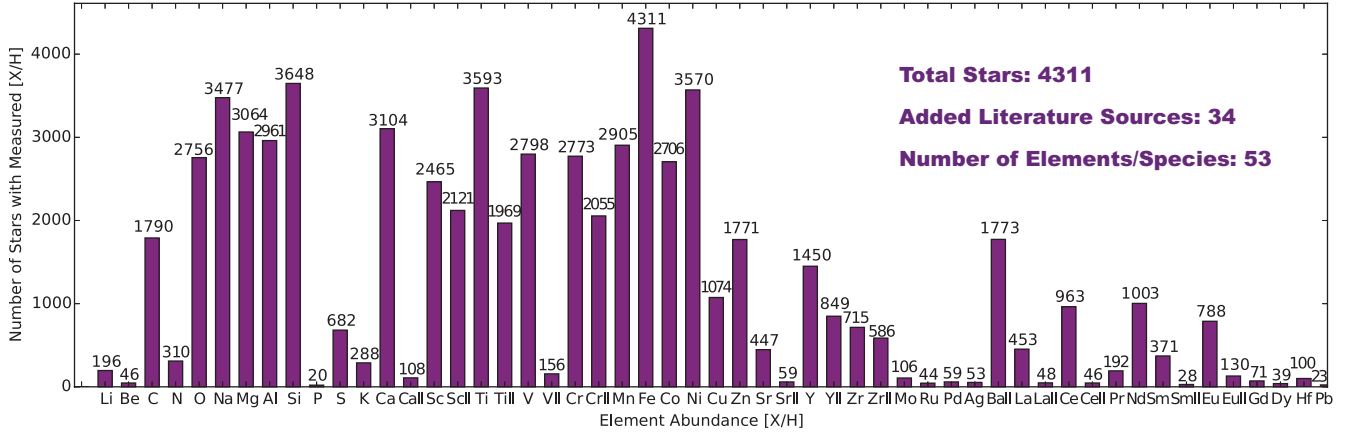


FIG. 5.— Number of stars in the updated *Hypatia Catalog* 2.0 with measured abundances for 53 different element species for stars all within 150 pc of the Sun. The catalog now includes an additional 1253 stars from 34 data sets, making the total 4311 stars.

the unconstrained Run 1 comparison, the results of the Investigation show a larger range in HD 361 as compared to *Hypatia*. However, the *Hypatia* ranges are larger for HD 202206 and HD 10700. Notably, the *Hypatia* values for the iron-poor star yielded a spread of 0.78 dex and average of 8.17 dex while the Investigation’s range was 0.13 dex. In the literature more than half of the spread is attributed to one group, Takeda et al. (2005, 2007). Removing this group results in average $A(C) = 8.28$ dex for the literature, a much more substantial discrepancy compared to the Investigation. Takeda et al. (2005, 2007) use an EW measurement routine and abundance finding code that is different from any of the other groups who participated here. Results for Runs 2-4 are similar to literature averages for HD 361 and HD 202206. For HD 10700 the average abundance found in Run 4 is 8.01 dex, with a larger range of 0.25. Otherwise, ranges tend to be fairly consistent across analyses.

Oxygen values are much more discrepant with those found in the literature, with average $A(O)$ differing by as much as 0.4 dex from the *Hypatia* values. For Runs 1 and 2, HD 10700 finds the best agreement, differing by only 0.08 dex in Run 1. HD 202206 sees the largest difference in these analyses, at $A(O) = 9.24$ dex vs. 8.82 dex. The difference for HD 361 is intermediate at 0.22-0.24 dex. There is a correlation between iron-content of the star and lack of agreement with literature values, though the sample is too small to be called robust. HD 10700 fares more poorly in Runs 3 and 4. From a difference smaller than the range, the disparity in $A(O)$ values rises to 0.24 dex in Run 3.

Imposition of the list of oxygen lines chosen for Runs 3 and 4 has an interesting effect. The fixed line list used only the 6156.8 Å OI line while the 6300 Å line is affected significantly by a blend with a NiI line (Nissen et al. 2014). The triplet at 7774 Å was outside the wavelength range of the spectra. Standardizing the oxygen lines has very little effect on the other two stars, leaving HD 202206 essentially unchanged and improving the agreement of HD 361 slightly. The spreads in these two stars are much larger than the *Hypatia* values for Runs 1 and 2. The spread for HD 10700 is the smallest in all

analyses and smaller than the *Hypatia* value of 0.33 dex. Consistency improves for HD 361 in Runs 3 and 4, but remains poor (~ 0.6 dex) for HD 202206 in all cases.

Iron abundances are fairly consistent between analyses, with maximum variations of 0.07 to 0.08 dex for all three stars. The Investigation’s $A(Fe)$ values for all three stars are similar to the literature averages and, in all cases, the *Hypatia* values fell within the range of the Investigation spreads. HD 361 is an interesting case. All five surveys from the literature use the same telescope and instrument, the 3.6m at La Silla with the High Accuracy Radial velocity Planet Searcher (HARPS). The surveys also use the same set of Fe lines, model atmospheres (ATLAS9), and abundance finding code (MOOG). The EWs are determined using IRAF’s SPLOT routine or ARES. Four out of the five surveys (Adibekyan et al. 2012; Bertran de Lis et al. 2015; Delgado Mena et al. 2010; Neves et al. 2009) determined solar-renormalized values of $A(Fe) = 7.35$ dex while González Hernández et al. (2010) report $A(Fe) = 7.391$ dex. The only difference discernible in the methodology is the use of differential analysis by González Hernández et al. (2010). The other groups all use the iron ratios from Santos et al. (2004), where the Anders & Grevesse (1989) solar abundance scale, which has since been superseded by much different solar abundances, was used for normalization, although $A(Fe)_\odot = 7.47$. All groups agrees very well with this study’s $A(Fe)$. The same pattern appears in HD 202206, with the same four groups reporting lower $A(Fe)$ abundances as compared to González Hernández et al. (2010). Again, all five groups agree well with the abundances found by this study. Only three of five groups have abundances for HD 10700, not including González Hernández et al. (2010), which have measurements similar to this study’s values and the *Hypatia* value.

For the most part, the abundances values found in the Investigation are consistent with the median of the literature values found in the *Hypatia Catalog*. At low metallicity, C diverges for all analyses but the spread is very large for both the Investigation and literature. The difference is not, therefore, as significant as it might first

appear, emphasizing the care that must be taken in the comparisons. When analyzing the spreads, the Investigation captures the range of variation seen in the literature. We find that O is the only case with radically different abundance values and the difference between the Investigation and *Hypatia* increases with metallicity. Imposition of a specific line list significantly affects measured O abundances, improving the high iron-content star, worsening the low, and leaving the approximately solar-iron star mostly unaffected. Given the problematic nature of O lines, this is unsurprising. As discussed in Appendix E, Na, Al, Mg, and Si, are all very consistent. The spread in Al dropped to much lower than the *Hypatia* spread for Al in the two higher iron-content stars with a fixed line list, suggesting that Al is sensitive to the lines used. Magnesium has a similar amount of variation to the literature except for the low iron-content HD 10700. Comparison to literature allows us to deduce that Fe is sensitive to the technique, namely a differential line analysis or a bulk solar abundances scaling, which was a factor we do not test. The same may be true to a lesser extent for Na, Al, Si, and Ni, which merits a detailed follow-up. Barium appears to be particularly sensitive to stellar parameters but robust against the line list used.

5. DISCUSSION

It has been the goal of this research to better understand the abundance measuring techniques between groups and attempt to resolve the inherent issues. However, we wished to make it clear that it has not been our objective to try to determine which group determines the most “accurate” stellar abundance, or who is closest to calculating the actual amount of an element within a stellar photosphere. While we agree that this is an important issue, we believe that it is necessary to understand what components of a technique give rise to the observed variations. For now our focus has to be on the precision of the techniques, not the accuracy of their results. This is the first step that needs to be taken such that similar issues don’t arise again down the road. And if nothing else, once made to agree, we know if the stellar abundances do not reflect a true representation of the element within the star, these results can be scaled such that they are accurate without any loss of precision.

5.1. Error Analysis

A major facet of the Investigation was to include participants with a relatively wide variety of abundance determination methods. Not only did we want to see how the techniques compared to each other, but also the ways in which each of the methods were able to adapt to the restrictions placed on the abundance measurements. In this way, we were able to get a more in-depth understanding of the more commonly used techniques, including both their strengths and their limitations. The plots in Figs. 3–4 illustrated the overall abundance variation seen between the groups for all stars and analysis standardizations. However, by employing the metric of data similarity (Table 10) and the respective error bars for each element, we glossed over the details of the individual uncertainties.

In Appendix B, each group described not only their technique for measuring stellar abundances but also the way in which their errors were calculated. Overall, the

four groups who employed the CoG method (ANU, ASU, Carnegie, and Porto) had a similar uncertainty derivation: combining the errors calculated using a standard deviation of the abundances determined by a line-to-line basis and the effect of stellar parameter changes. In comparison, the spectral fitting groups had vastly different techniques for calculating error. For example, Geneva employed a weighted dispersion and Uppsala used a variety of integrated tools to contrast the data with the synthetic spectrum. All of the individually reported errors can be found in Tables 4–9.

To more clearly evaluate the error determinations for the element abundances, we have compiled the error calculations in Table 14 in a variety of different manners. For example, the first set (rows 1-6) shows the average of each group’s uncertainty determinations for all four stars over all four analyses with respect to the 10 elements (columns). The second set (rows 7-10) reports errors for each run, averaging together the error bars from all of the groups’ measurements for all four stars. The last set (rows 11-14) gives errors for each star, taking the mean of all the uncertainties as reported by every group in every run. Finally, the last row shows the average from all 96 calculations, or the four stars across four analyses by six groups. These last values are similar if not the same as the representative error bars, calculated using both medians and means as discussed in §3, given in Figs. 3–4.

We see from the first set of error compilations that ASU has some of the overall lowest uncertainty reports for 9 of 10 elements. While this might imply that ASU’s abundance determinations are more accurate, it may alternatively be the case that their uncertainties are simply underestimated. Porto’s uncertainties tend to be relatively low, but not in all cases. There were few particularly high or low error determinations for ANU, Carnegie, and Uppsala, though Uppsala’s tended to be above average.

Geneva report the highest errors in seven cases, where six of them were by a wide margin. In the cases of O and Eu II, Geneva’s large errors arose because each element only had one line to measure. Therefore, the error did not come from the standard deviation, but directly from the singly fitted line. In these cases, the single-line error is estimated using the covariance matrix by the least square algorithm, and may be overestimated. In addition, the version of iSpec used in this study is not capable of scanning a small range of wavelength-space in order to determine the peak of the absorption line or do small radial velocity corrections to match the line with the synthetic spectra, as is possible in SME. Therefore, it is susceptible to imperfect wavelength calibration, which clearly affects the determination of individual abundances, as was the case for Ni, Eu II, and to a lesser degree Fe. We discuss these issues within the field in general in §5.2. We also noted in §3.2 that the Geneva measurements exhibited opposite trends in their stellar parameter determinations between Runs 1 and 3 as compared with the other groups. It is most likely that the mismatch in wavelength calibration, especially when implementing the standardized list, is responsible for the notably different calculations.

Also discussed within §3.2 were the size of the uncertainties for the stellar parameters calculated by the Uppsala group. These errors were not reflected in the

abundances, as discussed in Appendix B and per Table 14. However, Tables 4–5 demonstrate that they are roughly twice those determined by the other groups. The uncertainties determined by the Uppsala group are consistent with other line-by-line abundance uncertainties and with the parameter uncertainties that were determined for non-solar type stars. Their stellar parameter uncertainties are essentially dominated by the line-to-line scatter which is caused by errors in gf values as well as modeling shortcomings, missing blends, and continuum uncertainties. By adopting astrophysical gf values, some of these errors would cancel and the precision, but not accuracy, would have improved. This would have resulted in error bars more closely aligned with the other groups. As is currently given, however, the values and their uncertainty are more representative of what is produced for the Gaia-ESO survey, which emphasize accuracy over.

In the second set of averages given in Table 14, we find that for the majority of elements, the average stellar abundance error is relatively consistent when cycling from Run 1 through Run 4. There are, however, a few exceptions. For example, the errors for Mg, Al, Si, Ni, and Eu II get worse when implementing the standardized line list, although to varying degrees. However, the opposite was true for C and more predominantly O, where the average errors were halved in Runs 3 and 4 as compared to Runs 1 and 2.

The results for Eu II, O, and to some degree Mg may be related to the method in which errors are calculated for elements with one absorption line by each group. The tables for Runs 3 and 4 (Tables 8 and 9) illustrate how Geneva was not able to calculate the A(O) abundance for any star while ANU and Porto had null results for HD 361 and HD 10700 during Run 4. Also ANU, ANU, and Carnegie had sporadic, if any, results for A(Eu II). Similarly, Porto did not report errors, only abundances, for A(Mg) and A(Eu II). It is clear that many of the groups had difficulty with respect to these single-line elements, since omissions did not occur for any other elements (save that ANU was unable to measure carbon in HD 10700 for any run). However, the uncertainties given in Tables 8, 9, and 14 do not always reflect the lower confidence associated with fewer lines, especially when the lines are weak. The case for the 6156.8 Å oxygen line, which had a EW of 4.1 mÅ, is an excellent example. We therefore make note that special precautions should be made, both when measuring and determining the uncertainties, for elements with only a single absorption line. This is an issue that should be addressed within the community and implemented with more transparency and reproducibility within stellar abundance techniques.

Finally, for the last section in Table 14, with respect to the average errors associated with the individual stars, the most metal-poor star, HD 10700, typically had the largest error bars. This makes sense given the smaller and weaker lines within the spectrum. The other relatively metal-poor star, HD 361, also had slightly larger associated errors. The converse was not always true for HD 202206, which we expected to achieve the lowest uncertainties given that it is metal-rich. However, the average error for A(Fe) was largest for HD 202206.

5.2. Wavelength Calibration

As mentioned previously in the paper, we found a significant mismatch in the provided stellar spectra that resulted in a misalignment between spectral features and wavelength numbers below 5050 Å. Prior to sending the data to the participating groups, the spectra was tested using the ASU methodology and the results were comparable to other data and literature sources. The ASU team has also looked into the typical wavelength calibration from other data/telescopes and found the provided spectra to be similarly, if not better, calibrated than other (published) sources. In addition, per our analysis of the abundances produced here with respect to the literature sources and their uncertainties (§4 and Appendix E), we find that all results are rather standard for the field.

However, while the data provided here was “typical,” the wavelength calibration was not perfect. In general, the EW/CoG methods will find the appropriate line, due to either automatic procedures that have a margin of error in which they can search for the correct spectral feature or because many groups tend to measure the EWs manually. While SME has an option to do small radial velocity corrections, that margin is limited. The version of iSpec used in this study does not implement that kind of correction, so it was more affected by the imperfect wavelength calibration than the rest of techniques.

Rather than see spectral fitting techniques, which have a number of benefits as compared to the CoG techniques, at a disadvantage, it makes sense that proper wavelength calibration should become more of a priority within the field. Offset spectra could affect the shape of the absorption lines, especially when taking into account convective shifts (see Appendix A). In fact, the overall impact that wavelength calibration may have on spectroscopic analysis is not clearly understood and could result in some of the systematic scatter that has been noted here and throughout the field. Therefore, although not specifically tested here, we believe that more precise wavelength calibration could benefit all methodologies for determining stellar abundances.

5.3. Spectral Fitting vs. Curve-of-Growth Techniques

Over the course of our analysis, we compared different levels of standardization throughout the analyses, the absolute abundance results between elements, variations seen in stars of assorted spectral types, and calculations from separate abundance techniques. With respect to the stellar parameters, namely Figure 2 and Tables 4–5, we did not find any correlations between the groups who used spectral fitting (Geneva and Uppsala) and those who used the CoG technique (ANU, ASU, Carnegie, and Porto). In fact, in terms of stellar parameters, the two spectral fitting groups tended to be at the opposite end of the ranges both in terms of values calculated and size of errors reported. No systematic difference was found between groups using the MARCS and ATLAS9 atmosphere models. While EW measurements did affect the results for the CoG techniques, there was no systematic difference between different EW measuring tools.

There were a few instances of similarity for the spectral fitting groups when determining the stellar abundances. For example, both Geneva and Uppsala were often at the extreme ends of the spread, either the highest or lowest, when measuring A(Mg) in general. In addition, both groups had the largest determinations for most A(Al)

calculations compared with the other groups, while they had lowest results in general for A(Fe) and A(Eu II). However, we note that (1) the individual and representative error bars associated with these elements often overlap with the CoG groups, (2) all measurements for Eu II are inconsistent (or unmeasurable) given the weakness of the line, and (3) there are counterexamples prevalent in each of the above elements. Therefore, we are left to conclude that correlations between the spectral fitting and CoG techniques are more likely coincidental and are not strongly related to the differing methods.

5.4. Varying Line Lists

As discussed in §3.4, during both analyses where the groups could choose which lines they measured, a variety of different line lists were used, especially with respect to iron (see Tables F4-F9). However, iron is one of the most important factors when determining stellar abundances, since it influences stellar parameter calculations and the measurements of other elements. With so few overlapping lines between the groups in this study, it was hard to pinpoint areas of variation.

Many line lists used atomic parameters from laboratory or observational sources, such as listed VALD (Kupka et al. 2000). However, we found that the atomic parameters, particularly the value of the oscillator strengths, were correlated with abundance discrepancies. The issue with atomic parameters is well known (e.g. Thévenin & Idiart 1999; Doyle et al. 2013) and often corrected by via a differential analysis technique. This involves using a benchmark star, typically a solar spectrum, to redetermine the $\log(gf)$ values. In this way, an inconsistent atomic parameter can be corrected by reconciling an over- or under-estimated abundance calculation in the solar spectrum, which is then removed from the final result. Differential analysis is a common practice, as seen in Hinkel et al. (2014, Table 3) and Table F1, but can be difficult to compare with results that do not normalize to the same solar abundance scale.

Sousa et al. (2014) tackles the issue of a homogenous line lists specifically with respect to stellar parameter calculations. They found that a consistent line list would improve the accuracy of parameter results, but would require a selection of the “best” iron lines and agreement within the community. With a variation in the number of lines, the particular lines, and the atomic parameters for Runs 1 and 2, we dealt with many free variables in the calculation of stellar parameters. As shown in the last column Table 2, the number of Fe I lines varied from 60–298 between the six groups. Yet, in general, the ranges in stellar parameters became worse when implementing the standardized line list, as compared to the autonomous run and shown in Tables 4–5. However, as discussed in §3.3 and shown in Tables 6–10, the abundances improved when standardizing the stellar parameters and, to a lesser extent, the line list. Therefore, it would appear that perhaps a line list could be chosen such that the stellar parameters are consistent and precise, which would therefore allow the elemental abundances to be more consistent between groups, such as described in Smiljanic et al. (2014). Pagano et al. (2016) test the amount of variation in stellar parameters and final abundance determinations as a function of the number of Fe lines in the linelist using spectra from the same survey used in this work. They

find that above ~ 70 lines parameters and abundances vary by less than the error, with little improvement at higher numbers of lines. For smaller linelists the determinations could change substantially with number of lines and with lines chosen.

5.5. Consistency

In this study, we have attempted to illuminate some of the issues plaguing the stellar abundance community and determine a solution to rectify those differences. We identify quantities that give rise to significant variation and recommend directions for further research. We do not provide specific recommendations of lines, techniques, or parameters to use. Determinations of best practices require a great deal of further investigation.

In a very broad sense, we saw that standardizing either the stellar parameters, the line list, or both typically, but not universally, minimized the discrepancies between groups. Whether a fixed line list or fixed stellar parameters were more beneficial changed on an element-by-element basis. By directly comparing the values for measured EWs on a line-by-line basis, it was found that some discrepancies could be attributed to differences in the EW measurements. However, some lines resulted in discrepant abundances even when the EWs were similar or identical. In such cases the atomic constants, in particular oscillator strength, were often found to be the culprits. Therefore, it is our recommendation that a standard group of benchmark stars (for example Jofré et al. 2014; Blanco-Cuaresma et al. 2014b; Heiter et al. 2015a; Jofré et al. 2015) be established to calibrate abundance finding techniques in order to produce consistency in stellar abundances regardless of measurement technique. Any group could adjust their procedure to reproduce the benchmark EWs (if measured), stellar parameters, and abundances. The community may then directly compare the group’s abundances using the benchmark technique, which should be consistent across all groups, to the group’s preferred method if they believe it to be more accurate. It would also benefit the community to agree upon the best elemental absorption lines and atomic parameters, which would also yield more reliable results. In this way, we may systematically reduce the variation between methods.

While we believe our recommendation is reasonable and consistent with our results, we recognize that this will not solve all of the inherent issues. For example, it was our hypothesis at the beginning of this endeavor that stellar parameters and line lists would account for most of the discrepancies, and increasing standardization of these components would improve the agreement of the results. Namely, if identical stellar parameters and line lists were used, the abundances would be very similar and the results in Run 4 would be best. However, we saw throughout the paper that this was not always the case and particular methods or elements were adversely affected. The overall implication is that there are other aspects of the abundance measurement techniques that need to be addressed or standardized, since the remaining scatter is largely unexplained.

In addition, elements with only one absorption line, blends, non-LTE effects, HFS, et cetera, require special treatment in order to attain even a hint of uniformity, for example O, Mg, and Eu II. We strongly urge the com-

munity to better understand their abundance techniques and the ways in which they may break down, such that these special cases may be properly handled. We also seek to attain error determinations that truly reflect the uncertainties within not only the elements but also the stellar parameters. The error bars may be calculated with respect to benchmark stars, which would ideally provide a basis on which to evaluate abundance variations between groups on a large scale, for example the work conducted by Smiljanic et al. (2014).

To date, the results of multiple analyses of the same targets do not produce the same results. Therefore, we call for transparency in presented results to unravel the systematic offsets that are clearly present in our current stellar abundance data. In other words, it would be beneficial if groups published their full line lists, the EW measurements for their lines, atomic parameters, stellar parameters, error bars, and methods of measurement and error calculation in detail. We also believe that it is important to report absolute abundances unnormalized to solar values wherever possible. While this clearly results in longer papers, as demonstrated here and in the Appendices, we believe that it is an important step towards resolving the issues prevalent in the field.

However, transparency of techniques alone is not sufficient if the community does not come together to increase reproducibility. In this vein, we believe that more rigorous comparisons between data sets should be implemented, specifically those which involve statistics, and an avoidance of purely graphical comparisons. We also encourage members of the field to openly discuss offsets and variations found between techniques in order to discover their fundamental root. Since there is a current lack of “ground-truthing” within astronomy, methodologies are not so much “wrong” as incomparable, which has lead to the current lack of consensus. Once abundance results are accurate and agree between techniques, only then can we focus on determining the true, precise stellar chemical make-up. We are optimistic that stellar abundances can become both precise and accurate, however, it is clear that it requires an effort that spans the entire community.

6. SUMMARY

As a result of the preliminary discussion and tests at ASU’s Stellar Stoichiometry workshop, we have formulated an investigation to understand the causes of variations between stellar abundance measurement techniques. A total of six groups were asked to determine the abundances within four stars, exhibiting a range in iron-content, over a series of multiple tests. Each group was asked to calculate the abundances for each star a total of four times, where Run 1 utilized their own autonomous method, Run 2 employed standardized stellar parameters, Run 3 implemented a standardized line list, and Run 4 had both standardized stellar parameters and element absorption lines. The results for the stellar parameters and the 10 elements, namely C, O, Na, Mg, Al, Si, Fe, Ni, Ba II, and Eu II, can be found in Tables 4–9.

The effect of the standardized line list on the stellar parameters appeared to have a polarizing effect, as summarized in Table 15. In some cases, using the same lines allowed measurements to become more consistent between groups. On the other hand, a number of the

stellar parameter values became more disparate during Run 3. These variations were not due to whether the methodology employed spectral fitting or CoG. However, the cause may be related to the inherent degeneracy between the stellar parameters or the number of Fe lines employed by each of the groups.

It was our expectation at the beginning of the Investigation that Run 4 would yield the most comparable results between groups. While the spread in the abundance determinations did decrease during this run as compared to Run 1, the results were not as consistent as we had expected. We implemented a metric of data similarity (Table 10) in order to quantify the similarity/dispersion of the abundance determinations. In general, we found that Run 2 had consistently better results between the elements and stars, followed by Run 4. As seen in Table 15, out of the 40 possibilities (10 elements within 4 stars), using the standardized parameters (only) achieved the most similar measurements between groups a total of 16 times. Using both the standardized parameters and lines resulted in the most comparable abundances in 12 instances. Given that both Runs 1 and 3 had similar success rates for best abundance similarity for a star between analyses, the implication is that the standardized line list may have adversely affected the abundance techniques for particular elements. This conclusion is mirrored in our line-by-line abundance analysis with respect to iron. Unfortunately, the small number of non-Fe lines measured by all groups for all four analyses made comparisons and broader conclusions difficult. Given that Run 3 generated much larger spreads in stellar parameters than Run 1, it may be that a standardized line list could improve consistency, but the choice of Fe lines used must be optimized. On the whole, elements that had a strong dependence on stellar parameters, as measured by an improvement between Run 1 to Run 2, did not improve or get worse during Run 3.

We saw similar spreads in the data when comparing the values determined here to those found within the literature. Optimistically, this shows that the setup of the Investigation accurately reflected the techniques and measurements found within the community. In addition, it emphasized the point that particular elements, such as C and O, require special attention to determine precise abundances. For elements like Fe and Al, and to a lesser extent Na, Al, Si, and Ni, the overall abundance determinations may be sensitive to either the lines, the technique, or the stellar parameters used in their calculation.

The Investigation that was conducted here is complementary to studies by Smiljanic et al. (2014); Jofré et al. (2014, 2015), all of which are relevant to ongoing and upcoming large stellar surveys, such as the Gaia-ESO survey, the Transiting Exoplanet Survey Satellite (TESS), the Characterizing Exoplanets Satellite (CHEOPS), and the James Webb Space Telescope (JWST). It is important that stars be precisely and consistently measured such that they, and possible orbiting exoplanets, may be well characterized.

It was our hope that either standardized stellar parameters, line list, or both would ameliorate the disparate abundance measurements between different techniques. Instead, we have found a deeper understanding of the problems inherent to the stellar abundance field. The

Investigation has shown that, in order for measurements to be copacetic, 1) the details of the methods and their input parameters need to be directly compared, 2) particular elements require special care, 3) line lists and/or stellar parameters should be standardized, and importantly, 4) all research should be presented with the utmost transparency to ensure reproducibility of the results. Given the huge amount of determination, flexibility, support, and feedback offered by all of the participating groups, we are hopeful that the community can work together to rectify these issues and work towards not only precise but accurate stellar abundances.

ACKNOWLEDGEMENTS

The authors would like to thank Paul Butler for providing the original stellar spectra in addition to Eric Mamajek for his help determining accurate stellar types for our sample. They would also like to thank the anonymous referee for their support and guidance, which has greatly improved the manuscript. N.R.H. would like to thank CHW3. The ASU team (N.R.H., P.A.Y., M.D.P., S.J.D. and A.D.A.) acknowledge that the results reported herein benefitted from collaborations and/or information exchange within NASA's Nexus

for Exoplanet System Science (NExSS) research coordination network sponsored by NASA's Science Mission Directorate. E.D.M. and V.A. acknowledge the support from the Fundação para a Ciência e Tecnologia (FCT, Portugal) in the form of the grants SFRH/BPD/76606/2011 and SFRH/BPD/70574/2010, respectively. J.K.C. acknowledges partial support from an appointment to the NASA Postdoctoral Program at the Goddard Space Flight Center, administered by Universities Space Research Association through a contract with NASA. T.N., A.K., and U.H. acknowledge support by the Swedish National Space Board (SNSB). N.C.S. and S.G.S. acknowledge the support from FCT through Investigador FCT contracts of reference IF/00169/2012 and IF/00028/2014, respectively, and POPH/FSE (EC) by FEDER funding through the program "Programa Operacional de Factores de Competitividade". The Porto group also acknowledges the support from FCT in the form of grant reference PTDC/FIS-AST/7073/2014 (POCI-01-0145-FEDER-007672) and project PTDC/FIS-AST/1526/2014. This research has made use of the SIMBAD database and VizieR catalogue access tools operated at CDS, Strasbourg, France as well as the Exoplanet Orbit Database at exoplanets.org.

REFERENCES

- Adamów, M., Niedzielski, A., Villaver, E., Wolszczan, A., & Nowak, G. 2014, *A&A*, 569, A55
- Adibekyan, V., et al. 2015a, *A&A*, 583, A94
- Adibekyan, V. Z., Sousa, S. G., Santos, N. C., Delgado Mena, E., González Hernández, J. I., Israelian, G., Mayor, M., & Khachatryan, G. 2012, *A&A*, 545, A32
- Adibekyan, V. Z., et al. 2015b, *MNRAS*, 450, 1900
- Allende Prieto, C., Barklem, P. S., Lambert, D. L., & Cunha, K. 2004, *A&A*, 420, 183
- Ammann, M. W., Brodholt, J. P., & Dobson, D. P. 2011, *Earth and Planetary Science Letters*, 302, 393
- Anders, E., & Grevesse, N. 1989, *Geochimica et Cosmochimica Acta*, 53, 197
- Andersen, T., Petersen, P., & Hauge, O. 1976, *Sol. Phys.*, 49, 211, aPH
- Asplund, M. 2005, *ARA&A*, 43, 481
- Asplund, M. 2005, *ARA&A*, 43, 481
- Asplund, M., Grevesse, N., Sauval, A. J., & Scott, P. 2009, *ARA&A*, 47, 481
- Aurière, M. 2003, in *EAS Publications Series*, Vol. 9, EAS Publications Series, ed. J. Arnaud & N. Meunier, 105
- Bard, A., Kock, A., & Kock, M. 1991, *A&A*, 248, 315
- Bard, A., & Kock, M. 1994, *A&A*, 282, 1014
- Barenfeld, S. A., Bubar, E. J., Mamajek, E. E., & Young, P. A. 2013, *ApJ*, 766, 6
- Barklem, P. S., & Asplund-Johansson, J. 2005, *Astron. and Astrophys.*, 435, 373, (BA-J)
- Barklem, P. S., Piskunov, N., & O'Mara, B. J. 2000, *Astron. and Astrophys. Suppl. Ser.*, 142, 467, (BPM)
- Battistini, C., & Bensby, T. 2015, *A&A*, 577, A9
- Bensby, T., Feltzing, S., Lundström, I., & Ilyin, I. 2005, *A&A*, 433, 185
- Bensby, T., Feltzing, S., & Oey, M. S. 2014, *A&A*, 562, A71
- Bernstein, R., Shectman, S. A., Gunnels, S. M., Mochnacki, S., & Athey, A. E. 2003, in *Society of Photo-Optical Instrumentation Engineers (SPIE) Conference Series*, Vol. 4841, Instrument Design and Performance for Optical/Infrared Ground-based Telescopes, ed. M. Iye & A. F. M. Moorwood, 1694–1704
- Bertran de Lis, S., Delgado Mena, E., Adibekyan, V. Z., Santos, N. C., & Sousa, S. G. 2015, *A&A*, 576, A89
- Biazzo, K., D'Orazi, V., Desidera, S., Covino, E., Alcalá, J. M., & Zusi, M. 2012, *MNRAS*, 427, 2905
- Biemont, E., & Godefroid, M. 1980, *A&A*, 84, 361
- Blackwell, D. E., Lynas-Gray, A. E., & Smith, G. 1995, *A&A*, 296, 217
- Blackwell, D. E., Shallis, M. J., & Simmons, G. J. 1980, *Astron. and Astrophys.*, 81, 340, (BSScor)
- Blanco-Cuaresma, S., Soubiran, C., Heiter, U., & Jofré, P. 2014a, *A&A*, 569, A111
- Blanco-Cuaresma, S., Soubiran, C., Jofré, P., & Heiter, U. 2014b, *A&A*, 566, A98
- Blanco-Cuaresma, S., et al. 2015, *A&A*, 577, A47
- Bodaghee, A., Santos, N. C., Israelian, G., & Mayor, M. 2003, *A&A*, 404, 715
- Boesgaard, A. M., Rich, J. A., Levesque, E. M., & Bowler, B. P. 2011, *ApJ*, 743, 140
- Bond, J. C., Lauretta, D. S., Tinney, C. G., Butler, R. P., Marcy, G. W., Jones, H. R. A., Carter, B. D., & Bailey, S. J. O. . J. 2008, *ApJ*, 682, 1234
- Bond, J. C., O'Brien, D. P., & Lauretta, D. S. 2010, *ApJ*, 715, 1050
- Bond, J. C., Tinney, C. G., Butler, R. P., Jones, H. R. A., Marcy, G. W., Penny, A. J., & Carter, B. D. 2006, *MNRAS*, 370, 163
- Brugamyer, E., Dodson-Robinson, S. E., Cochran, W. D., & Sneden, C. 2011, *ApJ*, 738, 97
- Bruntt, H., et al. 2010, *MNRAS*, 405, 1907
- . 2012, *MNRAS*, 423, 122
- Caffau, E., Ludwig, H.-G., Malherbe, J.-M., Bonifacio, P., Steffen, M., & Monaco, L. 2013, *A&A*, 554, A126
- Caffau, E., Ludwig, H.-G., Steffen, M., Freytag, B., & Bonifacio, P. 2011, *Sol. Phys.*, 268, 255
- Carlberg, J. K., Cunha, K., Smith, V. V., & Majewski, S. R. 2012, *ApJ*, 757, 109
- Casagrande, L., Schönrich, R., Asplund, M., Cassisi, S., Ramírez, I., Meléndez, J., Bensby, T., & Feltzing, S. 2011, *A&A*, 530, A138
- Castelli, F., & Kurucz, R. L. 2003, in *IAU Symposium*, Vol. 210, Modelling of Stellar Atmospheres, ed. N. Piskunov, W. W. Weiss, & D. F. Gray, 20P
- Castro, S., de Mello, G. P., & da Silva, L. 1999, *MNRAS*, 305, 693
- Colucci, J. E., Bernstein, R. A., Cameron, S., McWilliam, A., & Cohen, J. G. 2009, *ApJ*, 704, 385
- Cowley, C. R., & Castelli, F. 2002, *A&A*, 387, 595
- Davidson, M. D., Snoek, L. C., Volten, H., & Doenszelmann, A. 1992, *A&A*, 255, 457
- Delgado Mena, E., Israelian, G., González Hernández, J. I., Bond, J. C., Santos, N. C., Udry, S., & Mayor, M. 2010, *ApJ*, 725, 2349
- Doyle, A. P., et al. 2013, *MNRAS*, 428, 3164
- Ecuivillon, A., Israelian, G., Santos, N. C., Mayor, M., & Gilli, G. 2006, *A&A*, 449, 809
- Ecuivillon, A., Israelian, G., Santos, N. C., Mayor, M., Villar, V., & Bihain, G. 2004, *A&A*, 426, 619

- Epstein, C. R., Johnson, J. A., Dong, S., Udalski, A., Gould, A., & Becker, G. 2010, *ApJ*, 709, 447
- Feltzing, S., & Gustafsson, B. 1998, *A&AS*, 129, 237
- Francois, P. 1986, *A&A*, 160, 264
- Frebel, A., & Norris, J. E. 2015, *ARA&A*, 53, 631
- Fuhr, J. R., Martin, G. A., & Wiese, W. L. 1988, *Journal of Physical and Chemical Reference Data*, Volume 17, Suppl. 4. New York: American Institute of Physics (AIP) and American Chemical Society, 1988, 17, (FMW)
- Fuhrmann, K. 2004, *Astronomische Nachrichten*, 325, 3
- Galazutdinov, G. 1992, in *Preprints for the Special Astrophysical Observatory of the Russian Academy of Sciences*, Vol. 92, 96
- Gehren, T., Liang, Y. C., Shi, J. R., Zhang, H. W., & Zhao, G. 2004, *A&A*, 413, 1045
- Gehren, T., Shi, J. R., Zhang, H. W., Zhao, G., & Korn, A. J. 2006, *A&A*, 451, 1065
- Gilli, G., Israelian, G., Ecuivillon, A., Santos, N. C., & Mayor, M. 2006, *A&A*, 449, 723
- Gilmore, G., et al. 2012, *The Messenger*, 147, 25
- Gonzalez, G., & Laws, C. 2007, *MNRAS*, 378, 1141
- Gonzalez, G., Laws, C., Tyagi, S., & Reddy, B. E. 2001, *AJ*, 121, 432
- González Hernández, J. I., Delgado-Mena, E., Sousa, S. G., Israelian, G., Santos, N. C., Adibekyan, V. Z., & Udry, S. 2013, *A&A*, 552, A6
- González Hernández, J. I., Israelian, G., Santos, N. C., Sousa, S., Delgado-Mena, E., Neves, V., & Udry, S. 2010, *ApJ*, 720, 1592
- Gratton, R. G., Carretta, E., Claudi, R., Lucatello, S., & Barbieri, M. 2003, *A&A*, 404, 187
- Gray, D. F. 1975, *ApJ*, 202, 148
- . 1977, *ApJ*, 218, 530
- Gray, R. O., & Corbally, C. J. 1994, *AJ*, 107, 742
- Gray, R. O., Corbally, C. J., Garrison, R. F., McFadden, M. T., Bubar, E. J., McGahee, C. E., O'Donoghue, A. A., & Knox, E. R. 2006, *AJ*, 132, 161
- Grevesse, N., & Sauval, A. J. 1998, *Space Sci Rev*, 85, 161
- Gustafsson, B., Edvardsson, B., Eriksson, K., Jørgensen, U. G., Nordlund, Å., & Plez, B. 2008, *A&A*, 486, 951
- Han, E., Wang, S. X., Wright, J. T., Feng, Y. K., Zhao, M., Fakhouri, O., Brown, J. I., & Hancock, C. 2014, *PASP*, 126, 827
- Hannaford, P., Lowe, R. M., Grevesse, N., Biemont, E., & Whaling, W. 1982, *ApJ*, 261, 736
- Heiter, U., Jofré, P., Gustafsson, B., Korn, A. J., Soubiran, C., & Thévenin, F. 2015a, *A&A*, 582, A49
- Heiter, U., et al. 2015b, *Phys. Scr*, 90, 054010
- Hinkel, N. R., Timmes, F. X., Young, P. A., Pagano, M. D., & Turnbull, M. C. 2014, *AJ*, 148, 54
- Hinkle, K., Wallace, L., Valenti, J., & Harmer, D. 2000, *Visible and Near Infrared Atlas of the Arcturus Spectrum 3727-9300 Å* (Astronomical Society of the Pacific)
- Houk, N., & Cowley, A. P. 1975, *University of Michigan Catalogue of two-dimensional spectral types for the HD stars. Volume I. Declinations -90 to -53* (Dept. of Astronomy, University of Michigan)
- Houk, N., & Smith-Moore, M. 1988, *Michigan Catalogue of Two-dimensional Spectral Types for the HD Stars. Volume 4, Declinations -26 to -12*. (Dept. of Astronomy, University of Michigan)
- Huber, D., et al. 2012, *ApJ*, 760, 32
- Ishigaki, M. N., Aoki, W., & Chiba, M. 2013, *ApJ*, 771, 67
- Ishigaki, M. N., Chiba, M., & Aoki, W. 2012, *ApJ*, 753, 64
- Jofré, P., et al. 2014, *A&A*, 564, A133
- . 2015, *A&A*, 582, A81
- Karinkuzhi, D., & Goswami, A. 2014, *MNRAS*, 440, 1095
- Koleva, M., Prugniel, P., Bouchard, A., & Wu, Y. 2009, *A&A*, 501, 1269
- Korotin, S., Mishenina, T., Gorbaneva, T., & Soubiran, C. 2011, *MNRAS*, 415, 2093
- Kuchner, M. J., & Seager, S. 2005, *ArXiv Astrophysics e-prints*
- Kupka, F. G., Ryabchikova, T. A., Piskunov, N. E., Stempels, H. C., & Weiss, W. W. 2000, *Baltic Astronomy*, 9, 590
- Kurucz, R. 1993a, *ATLAS9 Stellar Atmosphere Programs and 2 km/s grid*. Kurucz CD-ROM No. 13. Cambridge, Mass.: Smithsonian Astrophysical Observatory, 1993, 13
- Kurucz, R. L. 1993b, *SYNTHE spectrum synthesis programs and line data* (Cambridge, MA: Smithsonian Astrophysical Observatory, —c1993)
- . 1998, *Highlights of Astronomy*, 11, 646
- . 2006, Robert L. Kurucz on-line database of observed and predicted atomic transitions
- . 2007, Robert L. Kurucz on-line database of observed and predicted atomic transitions
- . 2008, Robert L. Kurucz on-line database of observed and predicted atomic transitions
- . 2010, Robert L. Kurucz on-line database of observed and predicted atomic transitions
- . 2011, Robert L. Kurucz on-line database of observed and predicted atomic transitions
- . 2013, Robert L. Kurucz on-line database of observed and predicted atomic transitions
- . 2014, Robert L. Kurucz on-line database of observed and predicted atomic transitions
- Kurucz, R. L., & Peytremann, E. 1975, *SAO Special Report*, 362, 1, (KP)
- Laird, J. 1985, *ApJ*, 289, 556
- Lambert, D. L. 1978, *MNRAS*, 182, 249
- Lambert, D. L., Mallia, E. A., & Warner, B. 1969, *MNRAS*, 142, 71, (LMW)
- Lambert, D. L., & Warner, B. 1968, *MNRAS*, 138, 181
- Lawler, J. E., Wickliffe, M. E., den Hartog, E. A., & Sneden, C. 2001, *Astrophys. J.*, 563, 1075, (LWHS)
- Lincke, R., & Ziegenbein, B. 1971, *Zeitschrift fur Physik*, 241, 369, (LZ)
- Liu, F., Chen, Y. Q., Zhao, G., Han, I., Lee, B. C., Kim, K. M., & Zhao, Z. S. 2012, *MNRAS*, 422, 2969
- Lodders, K., Plame, H., & Gail, H.-P. 2009, *Landolt-Börnstein - Group VI Astronomy and Astrophysics Numerical Data and Functional Relationships in Science and Technology Volume 4B: Solar System*. Edited by J.E. Trümper, 4B, 44
- Luck, R. E., & Heiter, U. 2005, *AJ*, 129, 1063
- Magic, Z., Collet, R., Asplund, M., Trampedach, R., Hayek, W., Chiavassa, A., Stein, R. F., & Nordlund, Å. 2013, *A&A*, 557, A26
- Maldonado, J., Villaver, E., & Eiroa, C. 2013, *A&A*, 554, A84
- Mann, A. W., Brewer, J. M., Gaidos, E., Lépine, S., & Hilton, E. J. 2013, *AJ*, 145, 52
- Marcy, G. W., & Butler, R. P. 1992, *PASP*, 104, 270
- Mayor, M., et al. 2003, *The Messenger*, 114, 20
- Meléndez, J., Asplund, M., Gustafsson, B., & Yong, D. 2009, *ApJL*, 704, L66
- Miles, B. M., & Wiese, W. L. 1969, *Atomic Data*, 1, 1, (MW)
- Milford, P. N., O'Mara, B. J., & Ross, J. E. 1994, *A&A*, 292, 276
- Mishenina, T., Gorbaneva, T., Pignatari, M., Thielemann, F.-K., & Korotin, S. A. 2015, *MNRAS*, 454, 1585
- Mishenina, T. V., Kovtyukh, V. V., Korotin, S. A., & Soubiran, C. 2003, *Astronomy Reports*, 47, 422
- Mishenina, T. V., Pignatari, M., Korotin, S. A., Soubiran, C., Charbonnel, C., Thielemann, F.-K., Gorbaneva, T. I., & Basak, N. Y. 2013, *A&A*, 552, A128
- Mitschang, A. W., De Silva, G., Zucker, D. B., Anguiano, B., Bensby, T., & Feltzing, S. 2014, *MNRAS*, 438, 2753
- Morgan, W. W., & Keenan, P. C. 1973, *ARA&A*, 11, 29
- Mortier, A., Santos, N. C., Sousa, S. G., Fernandes, J. M., Adibekyan, V. Z., Delgado Mena, E., Montalto, M., & Israelian, G. 2013, *A&A*, 558, A106
- Neuforge-Verheercke, C., & Magain, P. 1997, *A&A*, 328, 261
- Neves, V., Santos, N. C., Sousa, S. G., Correia, A. C. M., & Israelian, G. 2009, *A&A*, 497, 563
- Nissen, P. E. 2015, *ArXiv e-prints*
- Nissen, P. E., Chen, Y. Q., Carigi, L., Schuster, W. J., & Zhao, G. 2014, *A&A*, 568, A25
- Pagano, M., Truitt, A., Young, P. A., & Shim, S.-H. 2015, *ApJ*, 803, 90
- Pagano, M., Young, P. A., & Challa, P. 2016, *ApJ*, in review
- Peterson, R. C. 2013, *ApJL*, 768, L13
- Petigura, E. A., & Marcy, G. W. 2011, *ApJ*, 735, 41
- Pitts, R. E., & Newsom, G. H. 1986, *J. Quant. Spec. Radiat. Transf.*, 35S, 383, (PN)
- Prochaska, J. X., & McWilliam, A. 2000, *ApJL*, 537, L57
- Ralchenko, Y., Kramida, A., Reader, J., & NIST ASD Team. 2010, *NIST Atomic Spectra Database (ver. 4.0.0)*, [Online].
- Ramírez, I., Allende Prieto, C., & Lambert, D. L. 2013, *ApJ*, 764, 78
- Ramírez, I., Meléndez, J., & Asplund, M. 2014a, *A&A*, 561, A7
- Ramírez, I., Prieto, C. A., & Lambert, D. L. 2007, *A&A*, 465, 271

- Ramírez, I., et al. 2014b, *ApJ*, 787, 154
- Randich, S., Gilmore, G., & Gaia-ESO Consortium. 2013, *The Messenger*, 154, 47
- Recio-Blanco, A., Bijaoui, A., & de Laverny, P. 2006, *MNRAS*, 370, 141
- Reddy, B., Tomkin, J., Lambert, D., & Prieto, C. A. 2003, *MNRAS*, 340, 304
- Reetz, J. K. 1991, PhD thesis, Ludwig-Maximilians-Universität München
- Ryabchikova, T., Piskunov, N., & Shulyak, D. 2015, in *Astronomical Society of the Pacific Conference Series*, Vol. 494, *Physics and Evolution of Magnetic and Related Stars*, ed. Y. Y. Balega, I. I. Romanyuk, & D. O. Kudryavtsev, 308
- Santos, N. C., Israelian, G., & Mayor, M. 2004, *A&A*, 415, 1153
- Santos, N. C., et al. 2015, *A&A*, 580, L13
- Shi, J. R., Takada-Hidai, M., Takeda, Y., Tan, K. F., Hu, S. M., Zhao, G., & Cao, C. 2012, *ApJ*, 755, 36
- Sitnova, T., et al. 2015, *ArXiv e-prints*
- Smiljanic, R., et al. 2014, *A&A*, 570, A122
- Smith, V. V., Cunha, K., & Lazzaro, D. 2001, *AJ*, 121, 3207
- Snedden, C. A. 1973, PhD thesis, THE UNIVERSITY OF TEXAS AT AUSTIN.
- Sobeck, J. S., et al. 2011, *AJ*, 141, 175
- Soubiran, C., & Girard, P. 2005, *A&A*, 438, 139
- Sousa, S. G., Santos, N. C., Adibekyan, V., Delgado-Mena, E., & Israelian, G. 2015, *A&A*, 577, A67
- Sousa, S. G., Santos, N. C., Israelian, G., Lovis, C., Mayor, M., Silva, P. B., & Udry, S. 2011, *A&A*, 526, A99
- Sousa, S. G., Santos, N. C., Israelian, G., Mayor, M., & Monteiro, M. J. P. F. G. 2007, *A&A*, 469, 783
- Sousa, S. G., et al. 2014, *A&A*, 561, A21
- Stonkutė, E., Tautvaišienė, G., Nordström, B., & Ženovienė, R. 2012, *A&A*, 541, A157
- . 2013, *A&A*, 555, A6
- Takeda, Y., Hashimoto, O., Taguchi, H., Yoshioka, K., Takada-Hidai, M., Saito, Y., & Honda, S. 2005, *PASJ*, 57, 751
- Takeda, Y., Taguchi, H., Yoshioka, K., Hashimoto, O., Aikawa, T., & Kawanomoto, S. 2007, *PASJ*, 59, 1127
- Teske, J. K., Cunha, K., Smith, V. V., Schuler, S. C., & Griffith, C. A. 2014, *ApJ*, 788, 39
- Thévenin, F., & Idiart, T. P. 1999, *ApJ*, 521, 753
- Timmes, F. X., Woosley, S. E., & Weaver, T. A. 1995, *ApJS*, 98, 617
- Torres, G., Fischer, D. A., Sozzetti, A., Buchhave, L. A., Winn, J. N., Holman, M. J., & Carter, J. A. 2012, *ApJ*, 757, 161
- Truitt, A., Young, P. A., Spacek, A., Probst, L., & Dietrich, J. 2015, *ApJ*, 804, 145
- Tsymbol, V. 1996, in *Astronomical Society of the Pacific Conference Series*, Vol. 108, *M.A.S.S., Model Atmospheres and Spectrum Synthesis*, ed. S. J. Adelman, F. Kupka, & W. W. Weiss, 198
- Umemoto, K., Wentzcovitch, R. M., & Allen, P. B. 2006, *Science*, 311, 983
- Unsold, A. 1955, *Physik der Sternatmosphären*, MIT besonderer Berücksichtigung der Sonne. (Berlin, Springer, 1955. 2. Aufl.)
- Ženovienė, R., Tautvaišienė, G., Nordström, B., & Stonkutė, E. 2014, *A&A*, 563, A53
- Valenti, J. A., & Fischer, D. A. 2005, *ApJS*, 159, 141
- Valenti, J. A., & Piskunov, N. 1996, *A&AS*, 118, 595
- Venn, K. A., Irwin, M., Shetrone, M. D., Tout, C. A., Hill, V., & Tolstoy, E. 2004, *AJ*, 128, 1177
- Wallace, L., & Hinkle, K. 2009, *ApJ*, 700, 720
- Warner, B. 1968, *MNRAS*, 140, 53, wa
- Wickliffe, M. E., & Lawler, J. E. 1997, *ApJS*, 110, 163
- Wiese, W. L., Fuhr, J. R., & Deters, T. M. 1996, *Atomic transition probabilities of carbon, nitrogen, and oxygen : a critical data compilation* (AIP Press)
- Wiese, W. L., Smith, M. W., & Glennon, B. M. 1966, *Atomic transition probabilities. Vol.: Hydrogen through Neon. A critical data compilation* (US Government Printing Office), (WSG)
- Wiese, W. L., Smith, M. W., & Miles, B. M. 1969, *Atomic transition probabilities. Vol. 2: Sodium through Calcium. A critical data compilation* (US Government Printing Office), (WSM)
- Wright, J. T., et al. 2011, *PASP*, 123, 412
- Wu, X., Wang, L., Shi, J., Zhao, G., & Grupp, F. 2015, *ArXiv e-prints*
- Yan, H. L., Shi, J. R., & Zhao, G. 2015, *ApJ*, 802, 36
- Young, P. A., et al. 2014, *Astrobiology*, 14, 603

TABLE 1
STELLAR PROPERTIES AND STANDARD PARAMETERS

Star	Spectral Type	RA	Dec	T _{eff} (K)	log(g)	ξ (km/s)
HD 361	G1V	00h 08m 16s	-14° 49' 28"	5945	4.69	1.63
HD 10700	G8V	13h 44m 04s	15° 56' 14"	5382	4.57	1.26
HD 121504	G2V	13h 57m 17s	-56° 02' 24"	6048	4.54	1.25
HD 202206	G6V	21h 14m 58s	-20° 47' 21"	5765	4.45	1.43

TABLE 2
ABUNDANCE MODELS FOR INVESTIGATION PARTICIPANTS

Name	Calculations Performed By:	Stellar Atmosphere	EW	CoG or Spectral Fitting	FeI/FeII lines
ANU	Fan Liu	ATLAS9	ARES	CoG (MOOG 2014)	102/13
ASU	Michael Pagano	ATLAS9	ARES/IRAF SPLOT	CoG (MOOG 2014)	69/14
Carnegie	Joleen Carlberg	MARCS	ARES/IRAF SPLOT	CoG (MOOG 2014)	74/13
Geneva	Sergi Blanco-Cuaresma	MARCS	SPECTRUM	SF (SPECTRUM)	298/19
Porto	Vardan Adibekyan,	ATLAS9	ARES/IRAF SPLOT	CoG (MOOG 2014)	210/23
	Elisa Delgado Mena, Sergio Sousa				
Uppsala	Thomas Nordlander	MARCS	SME	SF (SME)	60/12

TABLE 3
REW vs. χ_l (FROM FIGURE 1) SLOPES

Group	HD 361	HD 10700	HD 121504	HD 202206	mean
ANU	-0.043	-0.089	-0.032	-0.027	-0.048
ASU	0.002	-0.054	0.039	-0.002	-0.012
Carnegie	-0.013	-0.059	-0.007	0.004	-0.019
Porto	-0.066	-0.083	-0.058	-0.055	-0.065

TABLE 4
STELLAR PARAMETERS (RUN 1)

Star	Group	T _{eff} (K)	log(g)	ξ (km/s)	[Fe/H] (dex)
HD 361	ANU	5847 ± 47	4.40 ± 0.07	1.08 ± 0.07	-0.12 ± 0.05
	ASU	5970 ± 47	4.73	1.37 ± 0.18	-0.02 ± 0.03
	Carnegie	5980 ± 86	4.61 ± 0.06	1.03 ± 0.13	0.00 ± 0.01
	Geneva	5864 ± 12	4.53 ± 0.02	1.36 ± 0.02	-0.26 ± 0.13
	Porto	5898 ± 31	4.51 ± 0.03	1.07 ± 0.04	-0.09 ± 0.02
	Uppsala	5875 ± 126	4.42 ± 0.28	1.15 ± 0.39	-0.11 ± 0.07
	Avg.	5906	4.53	1.18	-0.10
	Range	133	0.33	0.34	0.26
HD 10700	ANU	5246 ± 54	4.35 ± 0.10	0.60 ± 0.11	-0.52 ± 0.05
	ASU	5404 ± 41	4.59	1.06 ± 0.17	-0.40 ± 0.03
	Carnegie	5360 ± 72	4.55 ± 0.08	0.71 ± 0.14	-0.40 ± 0.09
	Geneva	5339 ± 12	4.55 ± 0.02	1.14 ± 0.05	-0.64 ± 0.13
	Porto	5300 ± 33	4.43 ± 0.06	0.67 ± 0.08	-0.51 ± 0.03
	Uppsala	5291 ± 123	4.37 ± 0.26	0.90 ± 0.57	-0.54 ± 0.07
	Avg.	5323	4.47	0.85	-0.50
	Range	158	0.24	0.54	0.24
HD 121504	ANU	5956 ± 56	4.38 ± 0.09	1.00 ± 0.08	0.17 ± 0.05
	ASU	5999 ± 53	4.48	1.28 ± 0.12	0.20 ± 0.04
	Carnegie	5990 ± 76	4.42 ± 0.08	1.10 ± 0.09	0.20 ± 0.11
	Geneva	5955 ± 9	4.45 ± 0.01	1.36 ± 0.05	-0.03 ± 0.14
	Porto	6065 ± 44	4.48 ± 0.06	1.25 ± 0.05	0.18 ± 0.03
	Uppsala	5869 ± 125	4.23 ± 0.28	1.23 ± 0.38	0.05 ± 0.08
	Avg.	5972	4.41	1.20	0.13
	Range	196	0.25	0.36	0.23
HD 202206	ANU	5707 ± 57	4.38 ± 0.09	1.10 ± 0.09	0.32 ± 0.05
	ASU	5841 ± 57	4.57	1.04 ± 0.10	0.46 ± 0.04
	Carnegie	5830 ± 99	4.65 ± 0.08	1.19 ± 0.11	0.38 ± 0.13
	Geneva	5698 ± 12	4.56 ± 0.02	1.30 ± 0.05	0.12 ± 0.16
	Porto	5785 ± 58	4.47 ± 0.10	1.23 ± 0.07	0.31 ± 0.04
	Uppsala	5734 ± 97	4.48 ± 0.23	1.28 ± 0.28	0.26 ± 0.08
	Avg.	5766	4.52	1.19	0.31
	Range	143	0.27	0.26	0.34

TABLE 5
STELLAR PARAMETERS (RUN 3)

Star	Group	T _{eff} (K)	log(g)	ξ (km/s)	[Fe/H] (dex)
HD 361	ANU	5962 ± 50	4.73 ± 0.08	1.10 ± 0.08	-0.10 ± 0.05
	ASU	5938 ± 81	4.73	1.46 ± 0.21	-0.10 ± 0.06
	Carnegie	5970 ± 70	4.85 ± 0.08	1.02 ± 0.16	-0.06 ± 0.10
	Geneva	5725 ± 29	4.26 ± 0.05	1.46 ± 0.05	-0.28 ± 0.16
	Porto	6015 ± 62	4.91 ± 0.07	1.10 ± 0.07	0.05 ± 0.04
	Uppsala	6026 ± 126	4.86 ± 0.28	0.98 ± 0.39	-0.02 ± 0.1
	Avg.	5939	4.72	1.19	-0.09
	Range	301	0.65	0.48	0.33
HD 10700	ANU	5456 ± 58	4.91 ± 0.10	0.76 ± 0.11	-0.42 ± 0.05
	ASU	5397 ± 40	4.62	0.97 ± 0.12	-0.46 ± 0.03
	Carnegie	5400 ± 71	4.77 ± 0.10	0.74 ± 0.19	-0.43 ± 0.11
	Geneva	5319 ± 21	4.50 ± 0.04	0.95 ± 0.05	-0.47 ± 0.15
	Porto	5477 ± 45	4.88 ± 0.06	0.97 ± 0.04	-0.35 ± 0.03
	Uppsala	5348 ± 123	4.76 ± 0.26	0.67 ± 0.57	-0.48 ± 0.12
	Avg.	5400	4.74	0.84	-0.44
	Range	158	0.41	0.30	0.13
HD 121504	ANU	6111 ± 58	4.78 ± 0.09	1.19 ± 0.08	0.18 ± 0.05
	ASU	6048 ± 88	4.66	1.47 ± 0.18	0.15 ± 0.07
	Carnegie	6050 ± 68	4.79 ± 0.11	1.12 ± 0.13	0.17 ± 0.10
	Geneva	5776 ± 28	4.20 ± 0.04	1.30 ± 0.04	-0.04 ± 0.16
	Porto	6182 ± 61	4.88 ± 0.06	1.36 ± 0.06	0.29 ± 0.04
	Uppsala	6092 ± 125	4.68 ± 0.28	1.13 ± 0.38	0.18 ± 0.10
	Avg.	6043	4.67	1.26	0.16
	Range	406	0.68	0.35	0.33
HD 202206	ANU	5818 ± 58	4.63 ± 0.09	1.05 ± 0.09	0.37 ± 0.05
	ASU	5800 ± 88	4.61	1.27 ± 0.15	0.34 ± 0.07
	Carnegie	5840 ± 70	4.80 ± 0.10	1.07 ± 0.12	0.38 ± 0.10
	Geneva	5546 ± 22	4.26 ± 0.04	1.23 ± 0.03	0.10 ± 0.22
	Porto	5875 ± 46	4.61 ± 0.12	1.28 ± 0.04	0.41 ± 0.03
	Uppsala	5893 ± 97	4.76 ± 0.23	1.20 ± 0.28	0.36 ± 0.09
	Avg.	5795	4.61	1.18	0.33
	Range	347	0.54	0.23	0.31

TABLE 6
ABSOLUTE ABUNDANCES BY INVESTIGATION PARTICIPANTS FOR THE STELLAR
SAMPLE (RUN 1)

Star	Group	A(C)	A(O)	A(Na)	A(Mg)	A(Al)	A(Si)	A(Fe)	A(Ni)	A(BaII)	A(EuII)
HD 361	ANU	8.37 ± 0.09	–	6.03 ± 0.06	7.47 ± 0.05	6.28 ± 0.06	7.35 ± 0.05	7.35 ± 0.05	6.01 ± 0.05	2.20 ± 0.06	–
	ASU	8.28 ± 0.04	–	6.07 ± 0.03	7.48 ± 0.03	6.33 ± 0.02	7.42 ± 0.02	7.44 ± 0.03	6.10 ± 0.04	2.30 ± 0.09	–
	Carnegie	8.21 ± 0.10	8.70 ± 0.09	6.04 ± 0.04	–	6.06 ± 0.04	7.40 ± 0.04	7.46 ± 0.10	6.23 ± 0.18	2.54 ± 0.08	0.55 ± 0.04
	Geneva	8.28 ± 0.04	9.18 ± 0.34	6.14 ± 0.23	7.32 ± 0.08	6.55 ± 0.09	7.35 ± 0.08	7.20 ± 0.13	6.03 ± 0.16	2.40 ± 0.16	0.63 ± 0.28
	Porto	8.32 ± 0.03	8.63 ± 0.10	6.16 ± 0.01	7.53 ± 0.05	6.33 ± 0.01	7.45 ± 0.02	7.38 ± 0.02	6.09 ± 0.03	2.35 ± 0.03	0.57
	Uppsala	8.23 ± 0.08	8.76 ± 0.09	6.15 ± 0.07	7.55 ± 0.07	6.39 ± 0.10	7.39 ± 0.04	7.35 ± 0.07	6.03 ± 0.14	2.34 ± 0.08	0.48 ± 0.10
	Avg. Range	8.28 0.16	8.82 0.55	6.10 0.13	7.47 0.23	6.32 0.49	7.39 0.10	7.36 0.26	6.08 0.22	2.36 0.34	0.56 0.15
HD 10700	ANU	–	–	5.74 ± 0.06	7.37 ± 0.06	6.11 ± 0.06	7.12 ± 0.05	6.94 ± 0.05	5.67 ± 0.05	1.53 ± 0.06	–
	ASU	8.07 ± 0.04	8.57 ± 0.05	5.86 ± 0.05	7.43 ± 0.02	6.27 ± 0.03	7.19 ± 0.02	7.06 ± 0.03	5.78 ± 0.03	1.65 ± 0.07	0.64 ± 0.02
	Carnegie	8.05 ± 0.33	8.70 ± 0.17	5.83 ± 0.11	–	6.00 ± 0.05	7.20 ± 0.02	7.06 ± 0.09	5.87 ± 0.16	1.90 ± 0.09	0.49 ± 0.04
	Geneva	8.18 ± 0.16	8.49 ± 0.42	5.90 ± 0.10	7.15 ± 0.08	6.46 ± 0.07	7.15 ± 0.08	6.82 ± 0.13	5.75 ± 0.14	1.70 ± 0.15	0.37 ± 0.40
	Porto	8.18 ± 0.08	8.67 ± 0.39	5.94 ± 0.10	7.34 ± 0.01	6.22 ± 0.02	7.21 ± 0.06	6.96 ± 0.03	5.76 ± 0.05	1.67 ± 0.05	0.36
	Uppsala	8.05 ± 0.00	8.48 ± 0.10	5.82 ± 0.09	7.66 ± 0.13	6.27 ± 0.14	7.14 ± 0.05	6.92 ± 0.07	5.69 ± 0.13	1.55 ± 0.05	0.23 ± 0.12
	Avg. Range	8.11 0.13	8.58 0.22	5.87 0.12	7.4 0.51	6.24 0.46	7.18 0.07	6.96 0.24	5.77 0.18	1.69 0.35	0.42 0.41
HD 121504	ANU	8.56 ± 0.12	8.59 ± 0.07	6.35 ± 0.06	7.66 ± 0.06	6.51 ± 0.05	7.61 ± 0.05	7.63 ± 0.05	6.31 ± 0.05	2.39 ± 0.05	–
	ASU	8.38 ± 0.03	8.98 ± 0.04	6.34 ± 0.02	7.68 ± 0.06	6.55 ± 0.02	7.64 ± 0.03	7.66 ± 0.04	6.33 ± 0.04	2.41 ± 0.08	0.93 ± 0.02
	Carnegie	8.42 ± 0.07	8.93 ± 0.05	6.30 ± 0.06	–	6.29 ± 0.05	7.63 ± 0.02	7.66 ± 0.11	6.39 ± 0.12	2.61 ± 0.07	0.80 ± 0.05
	Geneva	8.43 ± 0.05	8.92 ± 0.28	6.46 ± 0.14	7.48 ± 0.07	6.80 ± 0.07	7.55 ± 0.07	7.43 ± 0.14	6.29 ± 0.14	2.47 ± 0.19	0.69 ± 0.00
	Porto	8.46 ± 0.01	8.74 ± 0.10	6.49 ± 0.05	7.68 ± 0.04	6.58 ± 0.01	7.69 ± 0.04	7.65 ± 0.03	6.41 ± 0.04	2.45 ± 0.02	0.87
	Uppsala	8.43 ± 0.10	8.74 ± 0.10	6.41 ± 0.06	7.70 ± 0.06	6.56 ± 0.14	7.59 ± 0.08	7.51 ± 0.08	6.25 ± 0.13	2.31 ± 0.04	0.56 ± 0.16
	Avg. Range	8.45 0.18	8.82 0.39	6.39 0.19	7.64 0.22	6.55 0.51	7.62 0.14	7.59 0.23	6.33 0.16	2.44 0.30	0.77 0.37
HD 202206	ANU	8.61 ± 0.06	8.86 ± 0.07	6.55 ± 0.08	7.80 ± 0.06	6.74 ± 0.06	7.81 ± 0.05	7.78 ± 0.05	6.54 ± 0.05	2.39 ± 0.06	–
	ASU	8.53 ± 0.05	9.38 ± 0.05	6.71 ± 0.03	7.88 ± 0.06	6.81 ± 0.04	7.84 ± 0.03	7.92 ± 0.04	6.66 ± 0.04	2.64 ± 0.06	–
	Carnegie	8.64 ± 0.18	9.28 ± 0.09	6.54 ± 0.07	–	6.53 ± 0.04	7.83 ± 0.03	7.84 ± 0.13	6.71 ± 0.14	2.62 ± 0.12	–
	Geneva	8.57 ± 0.06	9.43 ± 0.35	6.45 ± 0.11	7.57 ± 0.08	6.69 ± 0.07	7.73 ± 0.08	7.58 ± 0.16	6.44 ± 0.10	2.44 ± 0.16	0.85 ± 0.35
	Porto	8.63 ± 0.03	9.23 ± 0.10	6.68 ± 0.02	7.81 ± 0.03	6.76 ± 0.05	7.85 ± 0.04	7.78 ± 0.04	6.59 ± 0.04	2.47 ± 0.05	–
	Uppsala	8.61 ± 0.06	9.04 ± 0.16	6.61 ± 0.04	7.91 ± 0.04	6.74 ± 0.00	7.79 ± 0.11	7.72 ± 0.08	6.53 ± 0.16	2.32 ± 0.01	0.39 ± 0.19
	Avg. Range	8.60 0.11	9.20 0.57	6.59 0.26	7.79 0.34	6.71 0.28	7.81 0.12	7.77 0.34	6.58 0.27	2.48 0.32	0.62 0.46

TABLE 7
ABSOLUTE ABUNDANCES BY INVESTIGATION PARTICIPANTS FOR THE STELLAR
SAMPLE (RUN 2)

Star	Group	A(C)	A(O)	A(Na)	A(Mg)	A(Al)	A(Si)	A(Fe)	A(Ni)	A(BaII)	A(EuII)
HD 361	ANU	8.40 ± 0.08	–	6.00 ± 0.06	7.43 ± 0.06	6.30 ± 0.06	7.36 ± 0.05	7.31 ± 0.05	6.02 ± 0.05	2.04 ± 0.05	–
	ASU	8.29 ± 0.03	–	6.05 ± 0.02	7.45 ± 0.01	6.32 ± 0.01	7.40 ± 0.02	7.34 ± 0.11	6.06 ± 0.02	2.14 ± 0.03	–
	Carnegie	8.27 ± 0.08	8.74 ± 0.04	6.01 ± 0.03	–	6.03 ± 0.03	7.38 ± 0.04	7.36 ± 0.12	6.10 ± 0.10	2.20 ± 0.11	0.55 ± 0.03
	Geneva	8.31 ± 0.04	9.24 ± 0.37	6.13 ± 0.19	7.29 ± 0.08	6.57 ± 0.08	7.37 ± 0.07	7.18 ± 0.15	6.05 ± 0.16	2.28 ± 0.14	0.70 ± 0.27
	Porto	8.35 ± 0.03	8.68 ± 0.10	6.16 ± 0.01	7.49 ± 0.09	6.33 ± 0.01	7.44 ± 0.03	7.38 ± 0.10	6.09 ± 0.04	2.14 ± 0.03	0.63
	Uppsala	8.28 ± 0.06	8.86 ± 0.08	6.08 ± 0.08	7.47 ± 0.06	6.34 ± 0.10	7.38 ± 0.03	7.24 ± 0.13	6.06 ± 0.15	2.14 ± 0.12	0.59 ± 0.10
	Avg. Range	8.32 0.13	8.88 0.56	6.07 0.16	7.43 0.20	6.32 0.54	7.39 0.08	7.30 0.20	6.06 0.08	2.16 0.24	0.62 0.15
HD 10700	ANU	–	–	5.77 ± 0.07	7.37 ± 0.07	6.17 ± 0.06	7.13 ± 0.05	6.94 ± 0.05	5.70 ± 0.05	1.40 ± 0.06	–
	ASU	8.07 ± 0.03	8.58 ± 0.08	5.84 ± 0.04	7.41 ± 0.01	6.26 ± 0.02	7.19 ± 0.02	7.07 ± 0.06	5.76 ± 0.02	1.57 ± 0.03	0.63 ± 0.02
	Carnegie	8.04 ± 0.32	8.70 ± 0.17	5.82 ± 0.10	–	5.99 ± 0.04	7.19 ± 0.02	7.01 ± 0.11	5.77 ± 0.11	1.62 ± 0.15	0.50 ± 0.03
	Geneva	8.17 ± 0.16	8.51 ± 0.42	5.91 ± 0.09	7.18 ± 0.08	6.48 ± 0.07	7.15 ± 0.07	6.83 ± 0.13	5.75 ± 0.14	1.65 ± 0.13	0.37 ± 0.40
	Porto	8.17 ± 0.08	8.69 ± 0.32	5.97 ± 0.09	7.33 ± 0.03	6.25 ± 0.02	7.21 ± 0.06	6.95 ± 0.09	5.77 ± 0.06	1.51 ± 0.07	0.41
	Uppsala	8.05 ± 0.05	8.56 ± 0.10	5.80 ± 0.02	7.55 ± 0.12	6.30 ± 0.14	7.16 ± 0.06	6.88 ± 0.09	5.72 ± 0.16	1.47 ± 0.08	0.31 ± 0.11
	Avg. Range	8.10 0.13	8.61 0.19	5.85 0.20	7.37 0.37	6.24 0.49	7.17 0.08	6.95 0.24	5.75 0.07	1.54 0.25	0.44 0.32
HD 121504	ANU	8.54 ± 0.12	8.56 ± 0.07	6.35 ± 0.06	7.66 ± 0.05	6.54 ± 0.05	7.62 ± 0.05	7.62 ± 0.05	6.34 ± 0.05	2.32 ± 0.05	–
	ASU	8.38 ± 0.02	8.96 ± 0.02	6.36 ± 0.05	7.70 ± 0.05	6.57 ± 0.01	7.66 ± 0.03	7.68 ± 0.01	6.37 ± 0.02	2.47 ± 0.03	0.97 ± 0.02
	Carnegie	8.42 ± 0.05	8.96 ± 0.03	6.32 ± 0.05	–	6.30 ± 0.04	7.63 ± 0.01	7.67 ± 0.10	6.41 ± 0.09	2.56 ± 0.08	0.87 ± 0.03
	Geneva	8.40 ± 0.07	8.86 ± 0.27	6.51 ± 0.15	7.54 ± 0.07	6.84 ± 0.07	7.58 ± 0.07	7.52 ± 0.13	6.36 ± 0.15	2.61 ± 0.19	0.74 ± 0.00
	Porto	8.49 ± 0.01	8.77 ± 0.10	6.48 ± 0.05	7.66 ± 0.04	6.57 ± 0.01	7.69 ± 0.04	7.61 ± 0.11	6.40 ± 0.04	2.45 ± 0.02	0.89
	Uppsala	8.43 ± 0.06	8.96 ± 0.08	6.42 ± 0.02	7.75 ± 0.05	6.60 ± 0.03	7.63 ± 0.06	7.59 ± 0.09	6.34 ± 0.13	2.40 ± 0.12	0.72 ± 0.16
	Avg. Range	8.44 0.16	8.85 0.40	6.41 0.19	7.66 0.21	6.57 0.54	7.64 0.11	7.62 0.16	6.37 0.07	2.47 0.29	0.84 0.25
HD 202206	ANU	8.58 ± 0.06	8.83 ± 0.07	6.54 ± 0.08	7.77 ± 0.05	6.75 ± 0.07	7.78 ± 0.05	7.72 ± 0.05	6.51 ± 0.05	2.24 ± 0.07	–
	ASU	8.53 ± 0.03	9.40 ± 0.04	6.65 ± 0.05	7.81 ± 0.04	6.75 ± 0.04	7.79 ± 0.03	7.83 ± 0.09	6.53 ± 0.03	2.34 ± 0.04	–
	Carnegie	8.63 ± 0.17	9.22 ± 0.03	6.50 ± 0.05	–	6.50 ± 0.03	7.80 ± 0.03	7.74 ± 0.13	6.58 ± 0.11	2.40 ± 0.15	–
	Geneva	8.47 ± 0.08	9.36 ± 0.37	6.58 ± 0.09	7.70 ± 0.06	6.73 ± 0.07	7.72 ± 0.07	7.64 ± 0.15	6.46 ± 0.10	2.35 ± 0.16	0.77 ± 0.32
	Porto	8.63 ± 0.03	9.23 ± 0.10	6.65 ± 0.02	7.78 ± 0.01	6.74 ± 0.05	7.82 ± 0.04	7.69 ± 0.12	6.54 ± 0.04	2.35 ± 0.07	–
	Uppsala	8.56 ± 0.04	9.03 ± 0.16	6.62 ± 0.04	7.90 ± 0.05	6.70 ± 0.05	7.77 ± 0.09	7.71 ± 0.11	6.53 ± 0.15	2.25 ± 0.03	0.38 ± 0.22
	Avg. Range	8.57 0.16	9.18 0.57	6.59 0.15	7.79 0.20	6.70 0.25	7.78 0.10	7.72 0.19	6.53 0.12	2.32 0.16	0.58 0.39

TABLE 8
ABSOLUTE ABUNDANCES BY INVESTIGATION PARTICIPANTS FOR THE STELLAR
SAMPLE (RUN 3)

Star	Group	A(C)	A(O)	A(Na)	A(Mg)	A(Al)	A(Si)	A(Fe)	A(Ni)	A(BaII)	A(EuII)
HD 361	ANU	8.31 ± 0.08	–	6.03 ± 0.06	7.39 ± 0.07	6.16 ± 0.14	7.43 ± 0.06	7.37 ± 0.05	6.07 ± 0.05	2.27 ± 0.06	–
	ASU	8.30 ± 0.06	8.68 ± 0.05	6.08 ± 0.05	7.39 ± 0.03	6.16 ± 0.11	7.43 ± 0.03	7.36 ± 0.06	6.01 ± 0.05	2.07 ± 0.08	–
	Carnegie	8.24 ± 0.07	8.69 ± 0.06	6.04 ± 0.05	7.32 ± 0.08	6.17 ± 0.20	7.43 ± 0.10	7.40 ± 0.10	6.05 ± 0.06	2.25 ± 0.10	0.64 ± 0.04
	Geneva	8.29 ± 0.01	–	5.88 ± 0.07	7.52 ± 0.06	6.42 ± 0.07	7.24 ± 0.08	7.18 ± 0.16	5.93 ± 0.33	2.25 ± 0.18	0.52 ± 0.27
	Porto	8.32 ± 0.04	8.78 ± 0.06	6.14 ± 0.03	7.50	6.25 ± 0.13	7.54 ± 0.06	7.52 ± 0.04	6.19 ± 0.06	2.39 ± 0.05	0.78
	Uppsala	8.35 ± 0.00	9.06 ± 0.10	6.28 ± 0.16	7.61 ± 0.15	6.32 ± 0.14	7.44 ± 0.08	7.44 ± 0.10	6.16 ± 0.13	2.71 ± 0.06	0.71 ± 0.10
Avg.		8.30	8.80	6.08	7.46	6.25	7.42	7.38	6.07	2.32	0.66
Range		0.11	0.38	0.40	0.29	0.26	0.30	0.34	0.26	0.64	0.26
HD 10700	ANU	–	–	5.87 ± 0.07	7.34 ± 0.07	6.11 ± 0.13	7.26 ± 0.06	7.04 ± 0.05	5.81 ± 0.05	1.66 ± 0.05	–
	ASU	8.08 ± 0.04	8.74 ± 0.06	5.87 ± 0.04	7.35 ± 0.01	6.10 ± 0.10	7.22 ± 0.02	7.00 ± 0.03	5.71 ± 0.02	1.50 ± 0.03	0.64 ± 0.02
	Carnegie	7.96 ± 0.19	8.82 ± 0.08	5.84 ± 0.08	7.36 ± 0.09	6.11 ± 0.21	7.23 ± 0.08	7.03 ± 0.11	5.75 ± 0.10	1.61 ± 0.07	0.57 ± 0.05
	Geneva	8.14 ± 0.03	–	5.85 ± 0.07	7.64 ± 0.09	6.38 ± 0.13	7.12 ± 0.09	6.99 ± 0.15	5.83 ± 0.32	1.87 ± 0.16	0.38 ± 0.41
	Porto	8.07 ± 0.19	–	5.95 ± 0.07	7.45	6.18 ± 0.12	7.34 ± 0.05	7.12 ± 0.03	5.91 ± 0.07	1.68 ± 0.01	0.60
	Uppsala	8.00 ± 0.05	8.65 ± 0.05	5.96 ± 0.17	7.64 ± 0.02	6.15 ± 0.22	7.23 ± 0.06	6.98 ± 0.12	5.79 ± 0.09	1.80 ± 0.03	0.42 ± 0.07
Avg.		8.05	8.74	5.89	7.46	6.17	7.23	7.03	5.80	1.69	0.52
Range		0.18	0.17	0.12	0.30	0.28	0.22	0.14	0.20	0.37	0.26
HD 121504	ANU	8.50 ± 0.11	8.61 ± 0.07	6.35 ± 0.05	7.56 ± 0.07	6.41 ± 0.13	7.70 ± 0.06	7.64 ± 0.05	6.38 ± 0.05	2.40 ± 0.06	–
	ASU	8.41 ± 0.05	9.03 ± 0.07	6.36 ± 0.04	7.55 ± 0.03	6.39 ± 0.11	7.66 ± 0.04	7.61 ± 0.07	6.26 ± 0.06	2.20 ± 0.08	0.99 ± 0.02
	Carnegie	8.38 ± 0.08	8.98 ± 0.07	6.32 ± 0.04	7.57 ± 0.07	6.42 ± 0.22	7.67 ± 0.10	7.63 ± 0.10	6.32 ± 0.08	2.37 ± 0.09	0.95 ± 0.06
	Geneva	8.47 ± 0.05	–	6.30 ± 0.08	7.76 ± 0.06	6.62 ± 0.13	7.48 ± 0.07	7.42 ± 0.16	6.23 ± 0.36	2.43 ± 0.20	0.58 ± 0.26
	Porto	8.45 ± 0.03	8.98 ± 0.12	6.46 ± 0.03	7.67	6.49 ± 0.12	7.77 ± 0.07	7.76 ± 0.04	6.47 ± 0.07	2.48 ± 0.03	1.07
	Uppsala	8.43 ± 0.02	9.07 ± 0.05	6.57 ± 0.00	7.79 ± 0.01	6.51 ± 0.04	7.65 ± 0.10	7.64 ± 0.10	6.39 ± 0.10	2.73 ± 0.17	0.80 ± 0.20
Avg.		8.44	8.93	6.39	7.65	6.47	7.66	7.62	6.34	2.44	0.88
Range		0.12	0.46	0.27	0.24	0.23	0.29	0.34	0.24	0.53	0.49
HD 202206	ANU	8.52 ± 0.06	8.84 ± 0.07	6.53 ± 0.09	7.68 ± 0.07	6.61 ± 0.11	7.90 ± 0.06	7.83 ± 0.05	6.58 ± 0.05	2.50 ± 0.05	–
	ASU	8.56 ± 0.07	9.45 ± 0.08	6.68 ± 0.05	7.70 ± 0.03	6.60 ± 0.09	7.83 ± 0.03	7.80 ± 0.07	6.47 ± 0.05	2.30 ± 0.07	–
	Carnegie	8.50 ± 0.07	9.21 ± 0.07	6.52 ± 0.07	7.72 ± 0.12	6.64 ± 0.19	7.90 ± 0.12	7.84 ± 0.10	6.54 ± 0.09	2.44 ± 0.08	–
	Geneva	8.61 ± 0.02	–	6.47 ± 0.15	8.06 ± 0.09	6.63 ± 0.01	7.69 ± 0.07	7.56 ± 0.22	6.40 ± 0.34	2.38 ± 0.18	0.40 ± 0.45
	Porto	8.55 ± 0.06	9.21 ± 0.08	6.65 ± 0.04	7.79	6.68 ± 0.09	7.93 ± 0.09	7.88 ± 0.03	6.66 ± 0.08	2.48 ± 0.02	–
	Uppsala	8.64 ± 0.01	9.27 ± 0.14	6.82 ± 0.03	7.98 ± 0.10	6.73 ± 0.11	7.81 ± 0.05	7.82 ± 0.09	6.64 ± 0.15	2.60 ± 0.07	0.45 ± 0.28
Avg.		8.56	9.20	6.61	7.82	6.65	7.84	7.79	6.55	2.45	0.43
Range		0.14	0.61	0.35	0.38	0.13	0.24	0.32	0.26	0.30	0.05

TABLE 9
ABSOLUTE ABUNDANCES BY INVESTIGATION PARTICIPANTS FOR THE STELLAR
SAMPLE (RUN 4)

Star	Group	A(C)	A(O)	A(Na)	A(Mg)	A(Al)	A(Si)	A(Fe)	A(Ni)	A(BaII)	A(EuII)
HD 361	ANU	8.31 ± 0.08	–	6.01 ± 0.06	7.38 ± 0.07	6.15 ± 0.14	7.41 ± 0.06	7.30 ± 0.05	6.01 ± 0.05	2.05 ± 0.06	–
	ASU	8.28 ± 0.03	8.85 ± 0.07	6.08 ± 0.02	7.39 ± 0.05	6.16 ± 0.10	7.43 ± 0.03	7.33 ± 0.02	6.00 ± 0.01	2.01 ± 0.01	–
	Carnegie	8.21 ± 0.06	8.66 ± 0.05	6.03 ± 0.04	7.31 ± 0.07	6.16 ± 0.20	7.40 ± 0.09	7.32 ± 0.13	5.99 ± 0.06	2.01 ± 0.08	0.56 ± 0.03
	Geneva	8.30 ± 0.02	–	5.97 ± 0.06	7.59 ± 0.06	6.50 ± 0.07	7.30 ± 0.09	7.30 ± 0.16	6.02 ± 0.32	2.28 ± 0.14	0.71 ± 0.28
	Porto	8.30 ± 0.03	8.79 ± 0.06	6.10 ± 0.03	7.47	6.21 ± 0.13	7.51 ± 0.05	7.44 ± 0.15	6.09 ± 0.05	2.11 ± 0.03	0.65
	Uppsala	8.29 ± 0.06	8.90 ± 0.08	6.18 ± 0.11	7.48 ± 0.13	6.26 ± 0.12	7.38 ± 0.04	7.26 ± 0.14	6.08 ± 0.10	2.29 ± 0.09	0.60 ± 0.10
	Avg. Range	8.28 0.10	8.80 0.24	6.06 0.21	7.44 0.28	6.24 0.35	7.41 0.21	7.33 0.18	6.03 0.10	2.13 0.28	0.63 0.15
HD 10700	ANU	–	–	5.84 ± 0.07	7.32 ± 0.07	6.08 ± 0.13	7.20 ± 0.06	6.93 ± 0.05	5.72 ± 0.05	1.41 ± 0.05	–
	ASU	8.07 ± 0.03	8.77 ± 0.04	5.86 ± 0.03	7.35 ± 0.05	6.09 ± 0.09	7.21 ± 0.02	7.00 ± 0.07	5.69 ± 0.02	1.41 ± 0.01	0.62 ± 0.02
	Carnegie	7.90 ± 0.19	8.77 ± 0.06	5.83 ± 0.08	7.36 ± 0.04	6.11 ± 0.21	7.20 ± 0.08	6.96 ± 0.13	5.70 ± 0.10	1.43 ± 0.07	0.48 ± 0.03
	Geneva	8.14 ± 0.03	–	5.88 ± 0.07	7.65 ± 0.08	6.41 ± 0.13	7.13 ± 0.09	6.98 ± 0.15	5.82 ± 0.32	1.71 ± 0.13	0.41 ± 0.41
	Porto	8.04 ± 0.19	–	5.91 ± 0.07	7.42	6.14 ± 0.12	7.28 ± 0.05	7.02 ± 0.11	5.80 ± 0.07	1.47 ± 0.01	0.43
	Uppsala	7.89 ± 0.01	8.59 ± 0.05	5.97 ± 0.19	7.60 ± 0.02	6.16 ± 0.22	7.18 ± 0.05	6.92 ± 0.08	5.75 ± 0.10	1.55 ± 0.06	0.33 ± 0.07
	Avg. Range	8.01 0.25	8.71 0.18	5.88 0.14	7.45 0.33	6.17 0.33	7.20 0.15	6.97 0.10	5.75 0.13	1.50 0.30	0.45 0.29
HD 121504	ANU	8.45 ± 0.11	8.56 ± 0.07	6.34 ± 0.05	7.55 ± 0.07	6.39 ± 0.13	7.68 ± 0.06	7.60 ± 0.05	6.34 ± 0.05	2.31 ± 0.06	–
	ASU	8.36 ± 0.02	8.97 ± 0.02	6.39 ± 0.05	7.57 ± 0.05	6.40 ± 0.10	7.67 ± 0.03	7.62 ± 0.01	6.30 ± 0.02	2.30 ± 0.02	0.96 ± 0.02
	Carnegie	8.30 ± 0.07	8.88 ± 0.05	6.33 ± 0.04	7.59 ± 0.10	6.42 ± 0.22	7.66 ± 0.09	7.61 ± 0.11	6.32 ± 0.07	2.32 ± 0.08	0.86 ± 0.03
	Geneva	8.37 ± 0.05	–	6.41 ± 0.07	7.85 ± 0.05	6.73 ± 0.13	7.54 ± 0.07	7.60 ± 0.15	6.37 ± 0.35	2.61 ± 0.19	0.74 ± 0.27
	Porto	8.43 ± 0.02	9.00 ± 0.11	6.42 ± 0.03	7.64	6.45 ± 0.13	7.75 ± 0.07	7.69 ± 0.11	6.41 ± 0.07	2.41 ± 0.04	0.90
	Uppsala	8.39 ± 0.00	8.98 ± 0.07	6.57 ± 0.01	7.77 ± 0.01	6.49 ± 0.05	7.63 ± 0.09	7.61 ± 0.09	6.37 ± 0.10	2.63 ± 0.17	0.73 ± 0.20
	Avg. Range	8.38 0.15	8.88 0.44	6.41 0.24	7.66 0.30	6.48 0.34	7.66 0.21	7.62 0.09	6.35 0.11	2.43 0.33	0.84 0.23
HD 202206	ANU	8.48 ± 0.06	8.83 ± 0.07	6.50 ± 0.09	7.66 ± 0.07	6.58 ± 0.11	7.86 ± 0.06	7.71 ± 0.05	6.48 ± 0.06	2.25 ± 0.06	–
	ASU	8.52 ± 0.03	9.43 ± 0.07	6.66 ± 0.05	7.69 ± 0.05	6.59 ± 0.08	7.81 ± 0.02	7.71 ± 0.02	6.43 ± 0.02	2.17 ± 0.02	–
	Carnegie	8.44 ± 0.05	9.18 ± 0.06	6.50 ± 0.07	7.72 ± 0.12	6.61 ± 0.18	7.86 ± 0.12	7.72 ± 0.12	6.48 ± 0.07	2.20 ± 0.08	–
	Geneva	8.47 ± 0.04	–	6.56 ± 0.15	8.06 ± 0.06	6.73 ± 0.00	7.69 ± 0.08	7.68 ± 0.20	6.48 ± 0.35	2.33 ± 0.16	0.50 ± 0.45
	Porto	8.58 ± 0.05	9.28 ± 0.08	6.59 ± 0.04	7.75	6.63 ± 0.09	7.90 ± 0.08	7.79 ± 0.11	6.56 ± 0.07	2.31 ± 0.04	–
	Uppsala	8.57 ± 0.03	9.04 ± 0.18	6.81 ± 0.13	7.92 ± 0.10	6.66 ± 0.13	7.76 ± 0.08	7.72 ± 0.08	6.53 ± 0.10	2.37 ± 0.13	0.30 ± 0.20
	Avg. Range	8.51 0.14	9.15 0.60	6.60 0.31	7.80 0.40	6.63 0.15	7.81 0.21	7.72 0.11	6.49 0.13	2.27 0.20	0.40 0.20

TABLE 10
METRIC OF DATA SIMILARITY

Element	γ	Star	Run 1		Run 2		Run 3		Run 4	
			Metric	Norm.	Metric	Norm.	Metric	Norm.	Metric	Norm.
C	7.1	HD 361	2.30	<i>0.62</i>	2.74	<i>0.74</i>	3.25	<i>0.88</i>	3.71	<i>1.00</i>
		HD 10700	2.13	<i>0.57</i>	2.05	<i>0.55</i>	1.56	<i>0.42</i>	1.16	<i>0.31</i>
		HD 121504	2.68	<i>0.72</i>	2.35	<i>0.63</i>	2.77	<i>0.75</i>	2.45	<i>0.66</i>
		HD 202206	3.07	<i>0.83</i>	2.24	<i>0.60</i>	2.43	<i>0.65</i>	2.35	<i>0.63</i>
O	3.1	HD 361	1.17	<i>0.44</i>	0.98	<i>0.37</i>	1.48	<i>0.56</i>	1.76	<i>0.67</i>
		HD 10700	2.34	<i>0.89</i>	2.64	<i>1.00</i>	1.39	<i>0.53</i>	1.55	<i>0.59</i>
		HD 121504	2.26	<i>0.86</i>	2.51	<i>0.95</i>	2.22	<i>0.84</i>	2.15	<i>0.81</i>
		HD 202206	1.54	<i>0.58</i>	1.63	<i>0.62</i>	1.57	<i>0.59</i>	0.99	<i>0.38</i>
Na	7.1	HD 361	2.46	<i>0.88</i>	2.08	<i>0.74</i>	1.17	<i>0.42</i>	1.83	<i>0.65</i>
		HD 10700	1.98	<i>0.70</i>	1.93	<i>0.69</i>	2.81	<i>1.00</i>	2.60	<i>0.93</i>
		HD 121504	1.84	<i>0.65</i>	1.85	<i>0.66</i>	1.72	<i>0.61</i>	2.08	<i>0.74</i>
		HD 202206	1.42	<i>0.51</i>	2.24	<i>0.80</i>	1.19	<i>0.42</i>	1.45	<i>0.52</i>
Mg	8.2	HD 361	1.43	<i>0.67</i>	1.75	<i>0.81</i>	1.22	<i>0.57</i>	1.30	<i>0.60</i>
		HD 10700	0.57	<i>0.27</i>	0.69	<i>0.32</i>	1.55	<i>0.72</i>	1.23	<i>0.57</i>
		HD 121504	2.15	<i>1.00</i>	1.48	<i>0.69</i>	1.47	<i>0.68</i>	1.24	<i>0.58</i>
		HD 202206	1.09	<i>0.51</i>	1.44	<i>0.67</i>	1.08	<i>0.50</i>	1.08	<i>0.50</i>
Al	5.5	HD 361	1.47	<i>0.46</i>	1.95	<i>0.61</i>	2.04	<i>0.64</i>	2.30	<i>0.72</i>
		HD 10700	1.28	<i>0.40</i>	1.33	<i>0.42</i>	2.64	<i>0.83</i>	2.49	<i>0.78</i>
		HD 121504	1.69	<i>0.53</i>	1.79	<i>0.56</i>	2.26	<i>0.71</i>	2.31	<i>0.73</i>
		HD 202206	2.38	<i>0.75</i>	3.12	<i>0.98</i>	3.18	<i>1.00</i>	2.99	<i>0.94</i>
Si	8.2	HD 361	2.77	<i>0.78</i>	3.55	<i>1.00</i>	2.45	<i>0.69</i>	1.96	<i>0.55</i>
		HD 10700	2.90	<i>0.82</i>	3.24	<i>0.91</i>	2.13	<i>0.60</i>	2.66	<i>0.75</i>
		HD 121504	2.39	<i>0.67</i>	2.93	<i>0.83</i>	1.81	<i>0.51</i>	2.00	<i>0.56</i>
		HD 202206	2.74	<i>0.77</i>	3.15	<i>0.89</i>	1.68	<i>0.47</i>	1.65	<i>0.46</i>
Fe	5.5	HD 361	2.24	<i>0.53</i>	2.34	<i>0.55</i>	1.89	<i>0.44</i>	3.12	<i>0.73</i>
		HD 10700	2.10	<i>0.49</i>	1.98	<i>0.47</i>	3.24	<i>0.76</i>	3.42	<i>0.80</i>
		HD 121504	2.48	<i>0.58</i>	2.83	<i>0.67</i>	2.39	<i>0.56</i>	4.25	<i>1.00</i>
		HD 202206	1.70	<i>0.40</i>	2.79	<i>0.66</i>	2.69	<i>0.63</i>	3.96	<i>0.93</i>
Ni	4.9	HD 361	2.76	<i>0.65</i>	4.17	<i>0.99</i>	2.03	<i>0.48</i>	3.66	<i>0.87</i>
		HD 10700	2.69	<i>0.64</i>	4.22	<i>1.00</i>	2.67	<i>0.63</i>	3.14	<i>0.74</i>
		HD 121504	2.87	<i>0.68</i>	4.12	<i>0.98</i>	2.16	<i>0.51</i>	3.63	<i>0.86</i>
		HD 202206	2.01	<i>0.48</i>	3.79	<i>0.90</i>	1.94	<i>0.46</i>	3.56	<i>0.84</i>
Ba II	6.2	HD 361	1.57	<i>0.59</i>	2.34	<i>0.88</i>	1.28	<i>0.48</i>	1.69	<i>0.64</i>
		HD 10700	1.49	<i>0.56</i>	1.59	<i>0.60</i>	1.16	<i>0.44</i>	1.95	<i>0.74</i>
		HD 121504	1.75	<i>0.66</i>	1.45	<i>0.55</i>	1.20	<i>0.45</i>	1.65	<i>0.62</i>
		HD 202206	1.32	<i>0.50</i>	2.65	<i>1.00</i>	1.50	<i>0.57</i>	1.95	<i>0.74</i>
Eu II	3.8	HD 361	2.13	<i>0.55</i>	2.07	<i>0.53</i>	1.35	<i>0.35</i>	2.03	<i>0.52</i>
		HD 10700	1.39	<i>0.36</i>	1.65	<i>0.43</i>	1.89	<i>0.49</i>	1.97	<i>0.51</i>
		HD 121504	1.36	<i>0.35</i>	1.96	<i>0.51</i>	1.17	<i>0.30</i>	2.03	<i>0.52</i>
		HD 202206	0.11	<i>0.03</i>	0.20	<i>0.05</i>	3.87	<i>1.00</i>	1.04	<i>0.27</i>

TABLE 11
ABSOLUTE ABUNDANCES FROM HYPATIA SOURCES FOR THE STELLAR SAMPLE

Star	Group	A(C)	A(O)	A(Na)	A(Mg)	A(Al)	A(Si)	A(Fe)	A(Ni)	A(BaII)	A(EuII)
HD 361	Adibekyan et al. (2012)	—	—	6.175	7.467	6.31	7.437	7.35	6.095	—	—
	Bertran de Lis et al. (2015)	—	8.67	—	—	—	—	7.35	—	—	—
	Delgado Mena et al. (2010)	8.36	8.49	—	7.42	—	7.43	7.35	6.09	—	—
	González Hernández et al. (2010)	8.26	8.58	6.085	7.47	6.28	7.387	7.391	6.057	2.345	0.48
	Neves et al. (2009)	—	—	6.15	7.45	6.31	7.43	7.35	6.09	—	—
	Hypatia	8.31	8.58	6.15	7.46	6.31	7.43	7.35	6.09	2.345	0.48
	<i>Range</i>	<i>0.1</i>	<i>0.18</i>	<i>0.09</i>	<i>0.05</i>	<i>0.04</i>	<i>0.05</i>	<i>0.16</i>	<i>0.04</i>	<i>0.0</i>	<i>0.0</i>
HD 10700	Adibekyan et al. (2012)	—	—	5.885	7.297	6.20	7.186	6.95	5.737	—	—
	Allende Prieto et al. (2004)	8.04	8.53	—	7.35	—	7.21	6.98	5.78	1.63	0.50
	Bodaghee et al. (2003)	—	—	—	—	—	7.17	7.17	5.75	—	—
	Bond et al. (2006, 2008)	8.34	—	5.98	—	6.05	7.26	7.07	5.85	—	—
	Castro et al. (1999)	—	—	—	—	—	—	6.96	—	1.65	—
	Delgado Mena et al. (2010)	8.24	8.29	—	7.27	—	7.18	6.95	5.75	—	—
	Ecuivillon et al. (2004)	8.37	—	—	—	—	—	6.95	—	—	—
	Francois (1986)	—	—	5.53	7.19	6.03	7.25	6.9	—	—	—
	Gilli et al. (2006)	—	—	—	—	—	7.12	7.15	5.7	—	—
	Laird (1985)	8.40	—	—	—	—	—	7.09	—	—	—
	Luck & Heiter (2005)	—	—	5.71	—	6.13	7.12	6.92	5.67	1.57	—
	Mishenina et al. (2003)	—	—	5.73	—	—	—	6.94	—	—	—
	Neves et al. (2009)	—	—	5.86	7.31	6.22	7.19	6.95	5.75	—	—
	Petigura & Marcy (2011)	—	8.62	—	—	—	—	6.98	—	—	—
	Ramírez et al. (2007)	—	8.49	—	—	—	—	7.00	—	—	—
	Shi et al. (2012)	—	—	—	—	—	7.17	6.97	—	—	—
	Takeda et al. (2005, 2007)	7.62	8.50	5.88	7.42	6.25	7.26	7.24	5.85	1.38	—
	Thévenin & Idiart (1999)	—	8.39	5.88	7.53	6.18	7.33	7.04	—	—	—
	Valenti & Fischer (2005)	—	—	5.88	—	—	7.24	6.98	5.76	—	—
	Hypatia	8.29	8.50	5.88	7.31	6.18	7.19	6.98	5.75	1.60	0.50
	<i>Range</i>	<i>0.78</i>	<i>0.33</i>	<i>0.45</i>	<i>0.34</i>	<i>0.22</i>	<i>0.21</i>	<i>0.34</i>	<i>0.18</i>	<i>0.27</i>	<i>0.0</i>
HD 202206	Adibekyan et al. (2012)	—	—	6.67	7.83	6.755	7.845	7.76	6.579	—	—
	Bertran de Lis et al. (2015)	—	8.92	—	—	—	—	7.76	—	—	—
	Bodaghee et al. (2003)	—	—	—	—	—	7.85	8.04	6.58	—	—
	Brugamyer et al. (2011)	—	8.84	—	—	—	7.9	7.88	—	—	—
	Delgado Mena et al. (2010)	8.65	8.69	—	7.79	—	7.83	7.76	6.58	—	—
	Ecuivillon et al. (2004)	8.70	—	—	—	—	—	7.82	—	—	—
	Gilli et al. (2006)	—	—	—	—	—	7.77	8.02	6.51	—	—
	Gonzalez et al. (2001)	8.61	8.92	6.57	—	6.80	7.75	7.83	6.48	—	—
	Gonzalez & Laws (2007)	8.51	—	6.51	7.79	6.73	7.82	7.83	6.50	—	0.81
	González Hernández et al. (2010)	8.585	8.800	6.51	7.835	6.685	7.799	7.794	6.543	2.42	0.83
	Neves et al. (2009)	—	8.78	6.61	7.83	6.75	7.85	7.76	6.58	—	—
	Nissen et al. (2014)	8.58	8.78	—	—	—	—	7.79	—	—	—
	Valenti & Fischer (2005)	—	—	6.66	—	—	7.83	7.85	6.60	—	—
	Hypatia	8.60	8.82	6.59	7.83	6.75	7.83	7.82	6.58	2.42	0.82
	<i>Range</i>	<i>0.19</i>	<i>0.23</i>	<i>0.16</i>	<i>0.05</i>	<i>0.12</i>	<i>0.15</i>	<i>0.28</i>	<i>0.12</i>	<i>0.0</i>	<i>0.02</i>

* Errors were not included for the literature due to the varying ways in which they are calculated, for example, on a star-by-star basis or as a representative error per element. In addition, by converting error determinations to an absolute scale may not accurately represent the true error in the abundance calculation.

** Abundances have been normalized to the same solar scale, namely Lodders et al. (2009), per the analysis within the Hypatia Catalog (Hinkel et al. 2014).

TABLE 12
SAMPLE OF LINE-BY-LINE COMPARISONS FOR IRON IN HD 202206 (RUNS 1–4)

Wavelength (Å)	Group	χ_l (eV)	$\log(gf)$	EW (mÅ)	A(Fe) _{Run1} (dex)	A(Fe) _{Run2} (dex)	A(Fe) _{Run3} (dex)	A(Fe) _{Run4} (dex)
5522.45	ANU	4.21	-1.45	60.9	7.76	7.72	7.93	7.83
	ASU	4.21	-1.55	59.7	8.00	7.84	7.97	7.84
	Carnegie	4.21	-1.56	58.4	7.88	7.84	7.87	7.78
	Geneva	4.21	-1.45	–	7.64	7.66	7.57	7.66
	Porto	4.21	-1.42	61.0	7.77	7.71	7.97	7.88
	Avg.				7.81	7.75	7.86	7.80
5778.45	ANU	2.59	-3.44	36.2	7.69	7.70	7.80	7.71
	ASU	2.59	-3.48	35.7	7.87	7.75	7.88	7.75
	Carnegie	2.59	-3.43	36.3	7.76	7.71	7.82	7.71
	Geneva	2.58	-3.43	–	7.65	7.69	7.51	7.69
	Porto	2.59	-3.45	37.9	7.82	7.79	7.88	7.76
	Avg.				7.76	7.72	7.78	7.72
5855.08	ANU	4.61	-1.48	39.1	7.74	7.73	7.80	7.74
	ASU	4.61	-1.48	40.3	7.88	7.79	7.88	7.79
	Carnegie	4.61	-1.48	39.7	7.80	7.77	7.81	7.74
	Geneva	4.61	-1.48	–	7.65	7.68	7.58	7.68
	Porto	4.61	-1.53	39.1	7.83	7.80	7.84	7.76
	Uppsala	4.61	-1.48	–	7.69	7.70	7.78	7.70
	Avg.				7.77	7.75	7.78	7.74
5856.08	ANU	4.29	-1.46	49.6	7.65	7.62	7.82	7.73
	ASU	4.29	-1.56	49.1	7.85	7.72	7.83	7.72
	Carnegie	4.29	-1.64	50.0	7.87	7.83	7.80	7.71
	Geneva	4.29	-1.33	–	7.65	7.68	7.58	7.68
	Porto	4.29	-1.57	49.7	7.77	7.73	7.83	7.74
	Uppsala	4.29	-1.33	–	7.53	7.53	7.84	7.75
	Avg.				7.72	7.69	7.78	7.72
6027.05	ANU	4.08	-1.09	78.9	7.58	7.50	7.72	7.59
	ASU	4.08	-1.09	79.3	7.76	7.56	7.72	7.56
	Carnegie	4.08	-1.09	80.0	7.66	7.63	7.71	7.60
	Geneva	4.08	-1.09	–	7.62	7.64	6.57	7.53
	Porto	4.08	-1.18	79.9	7.71	7.63	7.78	7.67
	Uppsala	4.07	-1.09	–	7.72	7.70	7.89	7.77
	Avg.				7.68	7.61	7.57	7.62
6151.62	ANU	2.18	-3.28	64.5	7.65	7.66	7.77	7.61
	ASU	2.18	-3.30	66.0	7.90	7.65	7.87	7.67
	Carnegie	2.18	-3.30	63.4	7.73	7.65	7.75	7.58
	Geneva	2.17	-3.29	–	7.61	7.65	7.49	7.64
	Porto	2.18	-3.30	67.2	7.77	7.69	7.82	7.67
	Uppsala	2.18	-3.30	–	7.70	7.69	7.86	7.70
	Avg.				7.73	7.67	7.76	7.65
6165.36	ANU	4.14	-1.46	60.2	7.67	7.62	7.74	7.63
	ASU	4.14	-1.47	59.4	7.81	7.65	7.78	7.65
	Carnegie	4.14	-1.55	60.8	7.83	7.79	7.74	7.63
	Geneva	4.14	-1.47	–	7.60	7.62	7.52	7.61
	Porto	4.14	-1.50	60.7	7.61	7.61	7.70	7.59
	Uppsala	4.14	-1.47	–	7.71	7.70	7.77	7.68
	Avg.				7.71	7.67	7.71	7.63
Avg.				Total	7.73	7.69	7.74	7.69

* Geneva and Uppsala do not report abundances from all or some individual lines and Uppsala doesn't report some equivalent widths. The χ_l , $\log(gf)$, and EW values are only applicable to Runs 1 and 2, as indicated by the vertical lines, since Runs 3 and 4 use a standardized line list.

TABLE 13
SAMPLE OF LINE-BY-LINE COMPARISONS FOR ADDITIONAL ELEMENTS IN
HD 202206 (RUNS 1–4)

Element	Wavelength (Å)	Group	χ_l (eV)	$\log(gf)$	EW (mÅ)	A(X) _{Run1} (dex)	A(X) _{Run2} (dex)	A(X) _{Run3} (dex)	A(X) _{Run4} (dex)
C	5052.15	ANU	7.68	-1.3	43.8	8.57	8.55	8.56	8.53
		ASU	7.68	-1.3	42.2	8.63	8.63	8.59	8.60
		Carnegie	—	—	—	—	—	8.46	8.42
		Geneva	7.68	-1.3	—	8.59	8.48	8.62	8.48
		Porto	7.68	-1.303	44.4	8.66	8.66	8.59	8.61
		Uppsala	7.69	-1.3	—	8.57	8.54	8.48	8.47
		Avg.			8.60	8.57	8.55	8.55	8.51
	5380.32	ANU	7.68	-1.6	25.0	8.51	8.50	8.53	8.50
		ASU	7.68	-1.6	22.2	8.52	8.52	8.50	8.50
		Carnegie	—	—	—	—	—	8.52	8.48
		Geneva	—	—	—	—	—	8.61	8.48
		Porto	7.68	-1.616	26.8	8.63	8.63	8.58	8.60
		Uppsala	7.60	-1.6	—	8.61	8.57	8.64	8.57
		Avg.			8.57	8.56	8.56	8.56	8.52
	6587.61	ANU	8.54	-1.0	16.5	8.45	8.44	8.43	8.41
		ASU	8.54	-1.0	16.3	8.47	8.49	8.45	8.47
		Carnegie	8.54	-1.1	17.5	8.57	8.54	8.42	8.39
		Geneva	8.54	-1.0	—	8.50	8.37	8.56	8.37
		Porto	8.54	-1.086	18.2	8.59	8.60	8.49	8.52
		Uppsala	8.54	-1.0	—	8.69	8.66	8.64	8.59
		Avg.			8.55	8.52	8.50	8.50	8.46
	7111.47	Carnegie	8.64	-1.1	13.4	8.53	8.50	—	—
	7113.18	Carnegie	8.65	-0.8	35.2	8.83	8.80	—	—
Mg	5711.09	ANU	4.34	-1.7	126.2	7.74	7.69	—	—
		ASU	4.35	-1.8	126.1	7.99	7.88	—	—
		Geneva	4.35	-1.7	—	7.84	7.87	—	—
		Porto	4.35	-1.777	128.8	7.839	7.792	—	—
		Uppsala	4.35	-1.7	—	7.91	7.90	7.98	7.92
		Avg.			7.86	7.82	7.82	—	—
	6318.72	ANU	5.11	-2.0	54.3	7.68	7.67	7.69	7.66
		ASU	5.11	-2.0	55.7	7.82	7.76	7.75	7.71
		Carnegie	—	—	—	—	—	7.73	7.72
		Geneva	5.10	-1.97	—	—	—	8.06	8.06
		Porto	5.11	-1.97	55.1	—	—	7.789	7.747
		Avg.			7.75	7.83	7.80	7.80	7.71
	6319.24	Porto	5.11	-2.3	35.7	7.777	7.764	—	—
Na	5682.64	ANU	2.10	-0.8	141.8	6.68	6.63	—	—
		Uppsala	2.10	-0.7	—	6.58	6.60	6.80	6.72
	5688.21	Geneva	2.10	-0.4	—	—	6.80	6.86	
		Uppsala	2.10	-0.4	—	6.61	6.63	6.82	6.81
	6154.23	ANU	2.10	-1.6	59.2	6.58	6.57	6.62	6.58
		ASU	2.10	-1.5	65.0	6.74	6.65	6.60	6.53
		Carnegie	2.10	-1.5	57.5	6.57	6.54	6.57	6.55
		Geneva	2.10	-1.5	—	6.63	6.67	6.57	6.67
		Porto	2.10	-1.622	60.0	6.698	6.673	6.691	6.633
		Avg.			6.64	6.62	6.61	6.61	6.59
	6160.75	ANU	2.10	-1.3	71.7	6.45	6.43	6.48	6.44
		ASU	—	—	—	—	—	6.42	6.35
		Carnegie	2.10	-1.2	74.8	6.51	6.48	6.48	6.46
		Geneva	2.10	-1.2	—	6.42	6.40	6.36	6.45
		Porto	2.10	-1.363	76.0	6.657	6.625	6.613	6.553
		Avg.			6.53	6.50	6.48	6.48	6.49
Al	5557.07	ANU	3.14	-2.2	19.1	6.73	6.74	—	—
		Uppsala	3.14	-2.1	—	6.75	6.65	6.73	6.66
		Avg.			6.74	6.70	6.70	—	—
	6696.02	ANU	3.14	-1.5	52.1	6.59	6.58	6.72	6.68
		ASU	3.14	-1.6	51.5	6.77	6.70	6.76	6.69

TABLE 13 — *Continued*

Element	Wavelength (Å)	Group	χ_I (eV)	$\log(gf)$	EW (mÅ)	A(X) _{Run1} (dex)	A(X) _{Run2} (dex)	A(X) _{Run3} (dex)	A(X) _{Run4} (dex)
BaII	6698.67	Carnegie	3.14	-1.3	56.3	6.53	6.50	6.77	6.74
		Geneva	3.14	-1.58	—	—	—	6.63	6.73
		Porto	3.14	-1.571	51.9	6.709	6.687	6.765	6.711
		Uppsala	3.14	-1.6	—	6.75	6.73	6.80	6.74
					Avg.	6.67	6.64	6.74	6.71
		ANU	3.14	-1.8	37.3	6.65	6.65	6.52	6.49
		ASU	3.14	-2.0	35.7	6.87	6.82	6.54	6.48
		Carnegie	3.14	-1.6	37.5	6.53	6.50	6.51	6.49
		Geneva	3.14	-1.4	—	6.69	6.73	6.62	6.72
		Porto	3.14	-1.886	38.1	6.806	6.789	6.594	6.542
		Uppsala	3.14	-1.9	—	6.73	6.70	6.55	6.49
					Avg.	6.71	6.70	6.56	6.54
	5853.69	ANU	0.60	-0.9	73.4	2.31	2.17	2.49	2.21
		ASU	0.60	-1.0	67.9	2.64	2.29	2.35	2.17
		Carnegie	—	—	—	—	—	2.37	2.20
		Geneva	0.60	-0.9	—	2.25	2.16	2.15	2.15
		Porto	0.60	-0.91	75.0	2.50	2.38	2.46	2.28
		Uppsala	0.60	-0.9	—	2.31	2.23	2.56	2.28
					Avg.	2.40	2.25	2.40	2.22
		ANU	0.70	-0.1	133.9	2.46	2.34	2.54	2.34
		ASU	0.70	-0.1	127.6	2.78	2.51	2.47	2.33
		Carnegie	0.70	-0.1	128.2	2.70	2.49	2.33	2.23
		Geneva	0.70	-0.28	—	2.44	2.39	2.40	2.37
		Porto	0.70	-0.03	130.4	2.50	2.39	2.50	2.34
		Uppsala	0.70	0.0	—	2.32	2.33	2.60	2.37
					Avg.	2.53	2.41	2.47	2.33
	6496.91	ANU	0.60	-0.4	111.6	2.35	2.21	2.52	2.28
		ASU	0.60	-0.4	103.0	2.66	2.31	2.40	2.22
		Carnegie	0.60	-0.4	107.1	2.57	2.31	2.42	2.19
		Geneva	0.60	-0.51	—	2.57	2.47	2.51	2.46
		Porto	0.60	-0.41	110.0	2.41	2.27	2.48	2.30
		Uppsala	0.60	-0.4	—	2.67	2.25	2.85	2.54
					Avg.	2.54	2.30	2.53	2.33

* Groups that did not measure particular lines are not listed. Additionally, averages are not given in the cases where only one group measured a line. The χ_I , $\log(gf)$, and EW values are only applicable to Runs 1 and 2, as indicated by the vertical lines, since Runs 3 and 4 use a standardized line list.

TABLE 14
COMPILATION OF ABUNDANCE ERRORS

Averages	A(C)	A(O)	A(Na)	A(Mg)	A(Al)	A(Si)	A(Fe)	A(Ni)	A(BaII)	A(EuII)
ANU	0.09	0.07	0.07	0.06	0.09	0.06	0.05	0.05	0.06	—
ASU	0.04	0.05	0.04	0.04	0.06	0.03	0.05	0.03	0.05	0.02
Carnegie	0.13	0.07	0.06	0.09	0.12	0.06	0.11	0.10	0.09	0.04
Geneva	0.06	0.35	0.11	0.07	0.08	0.08	0.15	0.24	0.16	0.30
Porto	0.06	0.13	0.04	0.04	0.07	0.05	0.07	0.06	0.04	—
Uppsala	0.04	0.10	0.08	0.07	0.11	0.07	0.10	0.13	0.08	0.15
Run 1	0.08	0.16	0.07	0.06	0.05	0.05	0.08	0.10	0.08	0.14
Run 2	0.07	0.14	0.06	0.05	0.05	0.05	0.10	0.08	0.08	0.13
Run 3	0.06	0.08	0.07	0.07	0.13	0.07	0.09	0.12	0.08	0.17
Run 4	0.05	0.07	0.07	0.07	0.13	0.07	0.10	0.11	0.07	0.16
HD 361	0.05	0.11	0.07	0.07	0.09	0.05	0.09	0.10	0.08	0.14
HD 10700	0.11	0.16	0.08	0.06	0.11	0.05	0.08	0.10	0.07	0.14
HD 121504	0.06	0.09	0.05	0.05	0.09	0.06	0.08	0.10	0.09	0.09
HD 202206	0.06	0.11	0.07	0.06	0.07	0.06	0.10	0.10	0.08	0.31
All	0.07	0.11	0.07	0.06	0.09	0.06	0.09	0.10	0.08	0.15

* To determine these numbers, the group/run/star listed in the left-column was kept constant and the errors were averaged across the other two factors. For example, for ‘Run 1 Avg,’ the errors were averaged across all four analyses and all six groups but only for Run 1 determinations. See text for a further explanation.

TABLE 15
SUMMARY OF OPTIMIZED RESULTS

Element	HD 361	HD 10700	HD 121504	HD 202206
C	Std. Params & Lines	Autonomous	Std. Lines	Autonomous
O	Std. Params & Lines	Std. Params	Std. Params	Std. Params
Na	Autonomous	Std. Lines	Std. Params & Lines	Std. Params
Mg	Std. Params	Std. Lines	Autonomous	Std. Params
Al	Std. Params & Lines	Std. Lines	Std. Params & Lines	Std. Lines
Si	Std. Params	Std. Params	Std. Params	Std Params
Fe	Std. Params & Lines	Std. Params & Lines	Std. Params & Lines	Std. Params & Lines
Ni	Std. Params	Std. Params	Std. Params	Std. Params
Ba II	Std. Params	Std. Params & Lines	Autonomous	Std. Params
Eu II	Autonomous	Std. Params & Lines	Std. Params & Lines	Std. Lines

* Here we show a summary table of the results quantified in Table 10, where the run with the most similar element abundances within a star (or the highest metric per row of Table 10) is listed.

APPENDIX

In an effort to follow our own recommendations regarding method transparency, we have provided a variety of detailed explanations and tables in the Appendix.

APPENDIX A: TECHNIQUES IN THE FIELD

Because the stellar abundance field has been evolving for decades, there is a great deal of diversity in terms of the techniques used to quantify the proportions of elements within a star's photosphere. For example, a wide variety of telescopes and spectrographs have been employed in order to acquire stellar spectra: everything from the High Resolution Echelle Spectrometer (HIRES) on the relatively large 10 m Keck telescope (Boesgaard et al. 2011; Gratton et al. 2003) to the CORALIE echelle spectrograph on the comparatively smaller 1.2 m telescopes at the Euler Swiss telescope (Bodaghee et al. 2003; Ecuivillon et al. 2004; Gilli et al. 2006; Mortier et al. 2013).

There is a spectral resolution threshold, typically considered to be $\Delta\lambda/\lambda \approx 50\,000$, which must be attained or exceeded in order to produce respectable error bars for most elements. However, there is quite a variation not only between groups who use single data sources, but also when multiple data sources are employed by one group. For example, Ramírez et al. (2007) incorporated data from four telescopes/spectrographs in order to study iron and oxygen in FGK stars; the resolution of this data varied between $\Delta\lambda/\lambda \approx 45\,000 - 120\,000$. Similarly, Battistini & Bensby (2015) used data from 6 different telescopes/spectrographs where their resolution has a range of $\Delta\lambda/\lambda \approx 42\,000 - 120\,000$. In general, $\sim 35\%$ of groups use spectra from multiple (two or more) instruments that are then homogenized to form one data set (statistics are from the *Hypatia Catalog* per Hinkel et al. 2014, see §4.1). The average spectral resolution for all groups, using single or multiple telescopes, is $R \sim 65\,000$ while the median is $R \sim 60\,000$; the maximum is $R \sim 120\,000$ and the minimum is $R \sim 20\,000$.

While spectral resolution is important for measuring precise stellar abundances, so too is the signal-to-noise (S/N) of the data. In the literature, there are variations from $20 < S/N < 2000$, with the average S/N midpoint (typically defined as a range or a lower-bound) is ~ 280 with a median of 200. Groups that use multiple instruments also have a range of S/N. The most extreme ranges were given by Neves et al. (2009) and Adibekyan et al. (2015b) who both reported $S/N = 70 - 2000$ and Bertran de Lis et al. (2015) with $S/N = 40 - 2000$.

There are two stellar atmosphere models that are very common throughout the literature, namely some flavor of ATLAS (Castelli & Kurucz 2003) or MARCS (Gustafsson et al. 2008). In terms of abundance measuring methods, there are two standard techniques: curve-of-growth (CoG) and spectral fitting. Some of the more common approaches to the CoG method, although certainly not all, utilize IRAF SPLOT and ARES (Sousa et al. 2007) to measure equivalent widths (EWs). However, there are a few groups who use more in-house procedures, such as ABON-TEST8 (via P. Magain) and DECH20 (Galazutdinov 1992), or their own analyses. The CoG groups predominantly use MOOG (Snedden 1973), WIDTH9 (Kurucz 1993b), or Uppsala EQWIDTH for the abundance measurements. In general, 23% of groups use spectral fitting techniques in order to determine stellar abundances, such as Recio-Blanco et al. (2006); Koleva et al. (2009).

There are a number of smaller, less obvious variations that occur while calculating stellar abundances. For example, when implementing a CoG technique the spectral continuum fit may vary between the global and local scales, or when one has zoomed-in to measure a particular line. Continuum placement strongly affects the EW measurement, and may vary depending on the person who is measuring the line. Continuum placement presents a new level of internal uncertainty when more than one person makes these calculations for the same stellar sample. Spectral fitting techniques are limited by the flexibility of their routines to accurately determine the central wavelength of (the correct) absorption features, a process which is often done by-hand for CoG. In addition, the placement of the continuum is also an issue for spectral fitting since it strongly affects the element abundance measurement. The number of lines used to determine the abundance of an element plays an integral role in the total abundance measurement, yet varies widely between groups even for iron (see the penultimate column of Table F1 as well as the discussion in §3.4).

Another aspect to consider when determining stellar abundances is that only the equivalent widths for unblended lines can be estimated by direct integration. For blended spectra, particularly when using synthesis approaches, the *shape* of the line must be taken into account. Physically, line shapes are the result of intrinsic effects of local broadening and velocity fields in the stellar photosphere, rotation, and the extrinsic instrumental profile. If one of these broadening effects is much larger than the others, e.g. in the case of low resolution or very high rotational velocity, the others can be neglected. As no intrinsic line shape is available in CoG methods, a Gaussian profile is usually assumed. In solar-type stars, vertical (radial) and horizontal (tangential) large-scale motions in convective cells on the observed stellar disk result in superimposed line profiles of varying Doppler shift, which result in a broadened but not strengthened line profile (see Asplund 2005, Fig. 3). To-date, this is the method typically employed by spectral fitting techniques.

Additionally, convective velocities are predicted to vary smoothly with stellar parameters. For example, larger velocities are for higher effective temperatures or lower surface gravity, which also varies with metallicity (Fig. 17 in Magic et al. 2013). In one-dimensional radiative transfer, these three-dimensional hydrodynamical effects are usually represented by radial-tangential macroscopic broadening (Gray 1975), where the radial and tangential velocity distributions are typically assumed to be equal. With sufficient data quality, the broadening parameter can be determined simultaneously with rotational velocity. The results in the literature are generally in line with theoretical predictions with very little scatter (e.g. Figs. 4-7 of Fuhrmann 2004). However, the velocity fields vary with depth (Fig. 17 in Magic et al. 2013) such that weak lines form in deep layers where velocities are high and stronger lines form over a range of depths, including where velocities are lower. This pattern is indeed found in the solar spectrum, where

e.g. Gray (1977) determined that the macroturbulent velocity $v_{\text{mac}} = 3.8$ and 3.1 km/s for weak and saturated lines, respectively. A single value of macroturbulent velocity does thus not generally apply to any line of any strength, but should be measured on individual lines if the spectrum quality allows it. Unfortunately, there do not appear to be any studies which test the direct effect of v_{mac} errors on measured abundances.

Finally, once the total absolute abundances have been determined in a star, they are commonly defined as a ratio with respect to the same element abundance within the Sun. This ratio-of-ratios determines whether a star is ‘rich’ or ‘poor’ in that element with respect to the Sun. To date, there are over 40 solar abundance scales, the most popular of which are Anders & Grevesse (1989), Grevesse & Sauval (1998), and Asplund et al. (2009). Note: the total number of solar abundance scales does not include those techniques that use differential analysis to renormalize to the Sun on a line-by-line basis. The majority of solar abundance scales stem from individual determinations usually made from solar spectra reflected off a solar system body during the observation run. Even direct solar observations analyzed for the express purpose of determining solar abundances can vary substantially, for example due to the use of 3D vs. 1D solar atmosphere models (Asplund et al. 2009; Lodders et al. 2009; Caffau et al. 2011). Unfortunately, the choice of solar abundance scale may significantly change the overall abundance determination. For example, the range in solar carbon abundance, $A(\text{C})$, where $A(\text{C}) = \log(\text{atom number})$ of carbon normalized to $A(\text{H})=12$ (described more in §3.3), is 0.28 dex while $A(\text{O})$ varies by 0.33 dex across all scales. The range of $A(\text{Si})$ abundances found within the Sun is 0.28 dex and even $A(\text{Fe})$ may change by 0.26 dex. While it is understandable to measure the solar scale under the same conditions as the other data in order to ensure internal consistency, care must be taken when comparing abundance measurements that use different scales.

APPENDIX B: INVESTIGATION PARTICIPANTS

Australian National University (ANU): The ANU team started their analysis by automatically measuring the EWs of the spectral lines using the ARES code. The line list employed in their analysis was adopted mainly from Asplund et al. (2009) and augmented with additional unblended lines from Bensby et al. (2005); Neves et al. (2009). They performed a 1D, local thermodynamic equilibrium (LTE) abundance analysis using the 2014 version of MOOG (Sneden 1973; Sobeck et al. 2011) with the ODFNEW grid of Kurucz ATLAS9 model atmospheres (Castelli & Kurucz 2003). In order to determine the stellar parameters (effective temperature, surface gravity, microturbulence and metallicity), they force the excitation/ionization balance by minimizing the slopes in $A(\text{Fe I})$ versus excitation potential and reduced the EWs as well as the difference between $A(\text{Fe I})$ and $A(\text{Fe II})$, simultaneously for all of the lines. They also required the derived average $[\text{Fe}/\text{H}]$ to be consistent with the adopted model atmospheric value. They adopted the final results by iterating the whole processes until the balance was exactly achieved. Lines whose abundances departed from the average by $> 2.5\sigma$ were clipped during the analysis. See Table F4 for the ANU line list. They emphasize that their final results do not rely on the initial guess of the stellar parameters. Having established the stellar parameters for the sample stars, they derived chemical abundances for 9 elements: C, O, Na, Mg, Al, Si, Fe, Ni, and Ba. Note that Eu was not measured by the ANU group.

The uncertainties in the stellar parameters were derived with the method described by Epstein et al. (2010) and Bensby et al. (2014), which accounts for the co-variances between changes in the stellar parameters and the chemical abundances. The errors in the abundances were calculated following the manner of Epstein et al. (2010): the standard errors of the mean abundances are added in quadrature to the errors introduced by the uncertainties in the atmospheric parameters. This method is more robust than the simple line-to-line differences and allows for an error calculation when there is only one absorption line.

Arizona State University (ASU): The ASU analysis was done using the CoG method of stellar abundance determination, relying on the 2014 version of the MOOG radiative transfer code. A previously created script was used to run through all of the steps, then edited to meet the requirements and line list for this study (Pagano et al. 2015, 2016). The stellar atmospheres were calculated through ATLAS9 grid model atmospheres (Castelli & Kurucz 2003) via the MSPAWN72 script. These model atmospheres were updated when calculating the stellar parameters for the analyses where they were free variables.

The EWs were measured with the ARES v2 code, such that the output was entered into MOOG with the created model atmosphere. Iron lines that were three standard deviations or greater from the average were automatically removed from further calculations. The stellar parameters were calculated using an iterative script to achieve simultaneous excitation, ionization, and iron abundance balances. The temperature was varied until any trend with Fe I and excitation potential was removed to a Pearson correlation of less than 0.06. The microturbulent velocity was varied to remove any correlation between the Fe I line abundances and the reduced EW of each line. Lastly, the surface gravity and metallicity were varied until the overall abundances of Fe I and Fe II agreed to within 0.005 dex. The iterative process constantly returned to the previous restrictions until all balances were met. The errors on the stellar parameters were calculated after the balances were achieved, derived from varying the stellar parameters until a 1σ correlation was achieved.

After the stellar parameters were calculated, or the parameters were set for Runs 2 and 4, the individual elemental abundances were derived by putting the EW and line information through the ABFIND function in MOOG. See Table F5 for the ASU line list. The final abundance for each element was the average of the abundance calculated for each absorption line. Errors for individual elements were determined by adding in quadrature the variations associated with the parameter errors and the differences between abundances for separate absorption lines. When each abundance for a given element was calculated, the abundance was immediately redone using the same parameters plus and minus their

errors, varying only one parameter at a time. The differences between the calculated abundance and the two plus/minus values were averaged to get error based on the parameters. This was done for temperature and microturbulent velocity, with the error for gravity set at 0.06 dex. Additional error was calculated from the standard deviation between the different element abundance lines divided by the total number of lines used and added in quadrature.

Carnegie Institution of Washington/Department of Terrestrial Magnetism (Carnegie): Runs 1 and 2 use the autonomous line list of 74 Fe I and 13 Fe II lines compiled by Carlberg et al. (2012) for use in red giant stars. This list was tested on the atlas spectra of the Sun and Arcturus (Hinkle et al. 2000) and successfully reproduces the stellar parameters of both. A first pass at measuring the EWs of all of the lines automatically was made with ARES. ARES is run in interactive mode to ensure proper treatment of the continuum. Lines for which the ARES fit was questionable were measured by hand in IRAF using the SPLOT procedure; these are lines that generally require deblending. Gaussian profiles are used for the fitting, and multiple profiles are fit for blended profiles. The high-resolution solar atlas of Hinkle et al. (2000) was used to identify lines in the blend. The stellar parameters were measured by requiring excitation balance of Fe I lines and ionization balance of Fe I and Fe II lines. Abundances were computed with the 2014 version of MOOG using the ABFIND driver and MARCS plane-parallel, standard composition atmosphere models (Gustafsson et al. 2008). An IDL-wrapper code interacts with MOOG and searches through stellar parameter space following the algorithm described in Carlberg et al. (2012). A solution occurs when the input model Fe abundance and output Fe I and Fe II abundances agree better than 0.02 dex. To avoid potential biases, this run was done blinded to the stellar parameters. No SIMBAD² searches to obtain spectral types or looking at the parameters provided for the later analyses was allowed beforehand. The initial guess of the stellar parameters for all stars was $T_{\text{eff}} = 5700$ K, $\log g = 4.0$ dex, $[\text{Fe}/\text{H}] = 0.0$, and $\xi = 1.0$ kms. Abundances of nine additional elemental species were measured using the line list in Smith et al. (2001), given in Table F6. No Mg lines appear in this list and thus were not measured in the autonomous run. Due to the small number of lines, all EWs for these additional elements were measured by hand in IRAF. Abundances were derived using the *abfind* driver in MOOG.

The uncertainties in T_{eff} and microturbulence are calculated as in Neuforge-Verheecke & Magain (1997) using the 1σ uncertainties on the slopes of the line abundances versus excitation potential and reduced EWs, respectively. The T_{eff} uncertainty also includes the contribution from the microturbulence uncertainty. The uncertainty in $A(\text{Fe})$ and $\log(g)$ are given by the standard deviations in the Fe I and Fe II lines, respectively. These errors dominate uncertainties arising from sensitivities to the other stellar parameters. The uncertainties in the non-Fe elemental abundances are the quadrature sum of the standard deviation of the line-by-line abundance measurements (when more than line was measured) plus the error from varying the stellar parameters within their quoted uncertainties.

Observatoire de Genève (Geneva): The iSpec³ program is a spectroscopic framework that implements routines for the determination of chemical abundances by using the spectral fitting technique (Blanco-Cuaresma et al. 2014a). Given a group of spectral regions, iSpec computes synthetic spectra on-the-fly and minimizes the differences with the observed spectra following a Levenberg–Marquardt (least square) algorithm. The spectroscopic analyses were performed using iSpec (Blanco-Cuaresma et al. 2014a) with MARCS model atmospheres (Gustafsson et al. 2008), Gaia-ESO Survey line list (Heiter et al. 2015a) and SPECTRUM (Gray & Corbally 1994) as the radiative transfer code.

Before analyzing the spectra, they were homogenized for a robust analysis, following the same procedure detailed in Blanco-Cuaresma et al. (2015) that globally consists on the following stages:

- Cleaning: Wavelengths below 5050 Å were ignored due to a issues with the wavelength calibration.
- Radial velocity determination and correction: They cross-matched each spectrum with a solar template built from co-adding several NARVAL observations Aurière (2003) and calibrated with HARPS solar spectrum Mayor et al. (2003). The derived velocity corrections were smaller than 2.5 km/s.
- Resampling: Spectra was modified to have a homogeneous sampling with a wavelength step of 0.001 nm using a Bessel interpolator.
- Normalization: A re-normalization was applied to correct observed global trends. Continuum regions were automatically found by applying median/maximum filters and ~ 150 splines were fitted.
- Atmospheric parameter determination: They derived effective temperature, surface gravity, metallicity (i.e. $[\text{M}/\text{H}]$), micro and macroturbulence using a selection of absorption lines and the H- α and magnesium triplet wings. Errors were determined from the covariance matrix reported by the least square algorithm, which is strongly influenced by the spectral flux errors (in our case they considered all spectra to have an average signal-to-noise ratio of 200).
- AP corrections: The atmospheric parameter determination was assessed with the Gaia-ESO FGK benchmark stars (Jofré et al. 2014; Blanco-Cuaresma et al. 2014b; Heiter et al. 2015a; Jofré et al. 2015) and it was determined that a surface gravity correction of 0.15 dex is required, which was applied to the atmospheric parameter derived in the previous step.
- Individual abundances: A line-by-line abundance determination was performed where lines with bad solutions were discarded, see Table F7. The final abundance per element is calculated from a weighted average, while the errors correspond to the weighted dispersion.

Instituto de Astrofísica e Ciências do Espaço, Universidade do Porto (Porto): We derived the stellar atmospheric

² <http://simbad.u-strasbg.fr>

³ <http://www.blancocuaresma.com/s/>

parameters, metallicity and chemical abundances of individual elements using our standard spectroscopic analysis technique, as described in Delgado Mena et al. (e.g. 2010); Adibekyan et al. (e.g. 2012); Sousa et al. (e.g. 2014). To summarize, the EWs of the spectral lines were first automatically measured using the ARES v1⁴ code for a line list of Fe lines, both atomic and ionized. The spectroscopic parameters are derived by imposing both excitation and ionization balance assuming LTE where the iron abundance is used as a proxy for the metallicity. In this process, the 2014 MOOG radiative transfer code was used together with the grid of ATLAS9 plane-parallel model of atmospheres.

To derive the abundance of Na, Mg, Al, Si, and Ni, the EWs of the spectral lines were measured using the ARES v2 (Sousa et al. 2015). Then a standard CoG approach was employed to derive the abundances of iron (as a proxy for the metallicity) and other elements assuming LTE. The initial line-list of these elements were taken from Adibekyan et al. (2012), but several lines (two Si lines at $\lambda 5701.11 \text{ \AA}$, $\lambda 6244.48 \text{ \AA}$, and two Ni lines at $\lambda 5081.11 \text{ \AA}$, $\lambda 6767.78 \text{ \AA}$) were excluded because of large [X/Fe] star-to-star scatter at solar metallicities (Adibekyan et al. 2015a). The final abundance of elements when several spectral lines were available were calculated as a weighted mean of all the abundances, where as a weight the distance from the median abundance was considered. As demonstrated in Adibekyan et al. (2015a), this method can be effectively used without removing suspected outlier lines.

The EWs for C, O, Ba, and Eu were measured manually using the task SPLOT in IRAF. The abundances were derived in the same way as for the rest of elements. For carbon, atomic optical lines from Delgado Mena et al. (2010) was used together with the line at $\lambda 6587.62 \text{ \AA}$, and atomic data from VALD3⁵ database. For oxygen, the lines and atomic data from Bertran de Lis et al. (2015) were used while for Ba data from Prochaska & McWilliam (2000) was employed. For Eu, the line at $\lambda 6587.15 \text{ \AA}$ was analyzed with atomic data from VALD3. See Table F8 for the Porto line list for non-Fe elements. When considering hyper-fine splitting for both Ba and Eu, the same lines as the Geneva and Uppsala groups were used. The 'abfind' driver of MOOG for normal abundances and 'blends' driver for the hyper-fine splitting treatment. The final abundance of these elements is calculated as the mean of all the individual abundances (the maximum number of lines per element is three) and the error is determined by the standard deviation of the abundances given by different lines.

Uppsala University (Uppsala): The spectroscopic analyses were performed using the SME package (Valenti & Piskunov 1996; Valenti & Fischer 2005). The SME pipeline performs on-the-fly spectrum synthesis, explicitly taking into account blends in both lines and (pseudo-)continuum. Stellar parameters are optimized simultaneously using a Levenberg-Marquardt χ^2 minimization technique applied to pixels defined in continuum and line masks. The optimization simply continues until χ^2 is no longer improving, and the gradient search is based on double-sided partial derivatives. The Gaia-ESO Survey line list (Heiter et al. 2015a) was adopted. The line synthesis takes into account radiative, Stark, and van der Waals broadening – the latter using either BPO self-broadening (Cowley & Castelli 2002), Kurucz's calculations (Kurucz 1993a), or the classical Unsöld approximation (Unsöld 1955). Hyperfine structure (HFS) lines were adopted when available. The latest MARCS model atmospheres (Gustafsson et al. 2008) were used, which are interpolated by SME to the stellar parameters of the requested model. Instrumental broadening is taken into account by convolving the synthetic spectrum with a Gaussian kernel, at an assumed resolution of $R = 65\,000$. Additionally, a (fixed) rotational broadening and radial-tangential macroturbulence was applied. The list of lines to analyze was taken from the LUMBA Gaia-ESO survey analysis, and every line was inspected for every star. In regions blueward of 5050 \AA , an essentially linear wavelength drift reaching 50 km/s was identified and corrected. Unfortunately, the drift varies slightly across the spectral orders, such that overlapping regions suffer line doubling. Thus, most lines blueward of 5050 \AA were rejected, where elements were only retained when a few reliable lines were available. Line masks are determined automatically, discarding pixels where more than 1% of absorption is attributed to blends. Continuum normalization likewise automatically selects the pixels with least amount of line absorption.

We determine stellar parameters using the LUMBA Gaia-ESO survey stellar parameter pipeline. Normally, this pipeline determines the stellar parameters of dwarf stars using Balmer lines for T_{eff} , and neutral and singly ionized iron lines of varying strength for [Fe/H] and $\log(g)$. The wings of the Balmer lines turned out to be unreliable in these spectra, and so the pipeline was executed in its iron line mode, normally used only for giant stars. The starting guess is $T_{\text{eff}} = 5700 \text{ K}$, $\log(g) = 4.5$, [Fe/H] = 0.0 and $\xi = 1.0 \text{ km/s}$, while $v \sin(i)$ is kept fixed at 1 km s^{-1} , and the macroturbulence is fitted to the spectrum.

Stellar parameters are determined from a global optimal match of the spectrum taking into account not only line strengths but also their shapes. This means that trends in iron abundance with excitation energy, line strength, or ionization stage are not explicitly balanced. However, additional spectral information carried in the line profiles is taken into account, e.g., the shape of the wings of strong or saturated lines.

Parameter uncertainties are based on a newly implemented technique based on the fit residuals, partial derivatives, and data uncertainties. A cumulative distribution was constructed using all data pixels for a given free parameter p . This distribution describes the fraction of spectral pixels that require a change of δp or less to achieve a “perfect” fit. The change is estimated from the residuals and the partial derivative of the synthetic spectrum. Such distributions typically have very wide wings due to pixels insensitive to the selected parameters or pixels impossible to fit due to erroneous observations or atomic/molecular data, but the central part with the highest gradient is not too far from a Gaussian and can be used to estimate realistic uncertainties of the free parameters. While this method still ignores the cross-talk between different parameters it is a significant improvement over the uncertainties based on the covariance

⁴ The last version of ARES code (ARES v2) can be downloaded at <http://www.astro.up.pt/~simssousasag/ares> - (Sousa et al. 2015).

⁵ [http://vald.astro.univie.ac.at/~sim\\$vald3/php/vald.php](http://vald.astro.univie.ac.at/~sim$vald3/php/vald.php)

matrix (also evaluated by SME). The uncertainties derived from the diagonal of the covariance matrix are effectively a transformation of the observational errors onto the model parameter space using partial derivatives averaged over all data pixels. For high S/N observations the contribution of observational errors is negligible in comparison with model limitations and the resulting uncertainty estimates are unrealistically small. The mathematical background of the new approach can be found in the upcoming paper by Piskunov et al. (2016, in preparation) while practical tests and comparisons with other methods are presented in Ryabchikova et al. (2015). Here, the uncertainties in T_{eff} , $\log(g)$ and $[\text{Fe}/\text{H}]$ are in the range 100–130 K, 0.2–0.3 dex and 0.11–0.15 dex, respectively.

Abundances are determined using the LUMBA Gaia-ESO pipeline, line by line. Only lines that did not converge were rejected. See Table F9 for the Uppsala line list. To lessen the influence of extreme outliers, unweighted medians as averages were adopted, and standard deviations were estimated using the median absolute deviation error statistic. When only a single line has been analyzed, the estimated uncertainty in that measurement is used instead.

APPENDIX C: STANDARDIZED PARAMETERS AND LINE LISTS

During Runs 2 and 4, standardized stellar parameters, namely effective temperature, surface gravity, and microturbulence, were employed by all groups. These are listed in Table 1. We chose to implement a standard set of stellar parameters bearing in mind techniques in astronomy which are able to determine high precision measurements. For example, asteroseismology (e.g. Huber et al. 2012) can measure highly accurate stellar surface gravity which may be applied on a larger scale. While stellar properties must be calculated to measure the element abundances, it follows that stellar abundance techniques should be able to take advantage of high precision parameters offered by other methods while still remaining internally consistent. To this end, the standard parameters were determined using a combination (average) of appropriate literature sources that measured the respective stars (see §4 and Appendix E).

The standardized line list is given in Table F2, used in Runs 3 and 4, and was compiled directly from the respective sources. We focused on predominantly strong lines, although weaker and blended lines were included in order to broaden the scope of our analysis. In addition, the investigated lines span a wide range of ionization potentials, lower excitation energies and line strengths, as well as sampling both the minority and majority state of neutral or ionized species. While the line list included additional elements, we concentrated on C, O, Na, Mg, Al, Si, Fe, Ni, Ba, and Eu, which were consistently measured by most of the groups and included elements with varied nucleosynthetic origins. Namely, C, O, Mg, and Si are all α -elements with varied origins; Na and Al are odd- Z elements; Fe and Ni are iron-peak elements; and Ba and Eu are both neutron-capture elements via the s-process (primarily) and r-process, respectively. We go into a more detailed analysis of the individual lines in §3.4.

Due to the nature of the spectral fitting techniques used by the Geneva and Uppsala groups, namely iSpec and SME respectively, they required a complete line list including background features blending into targeted lines as well as the continuum. They isolated the lines that were used by the other groups in Table F2 and added the appropriate broadening parameters per Heiter et al. (2015b). In other words, the standardized $\log(gf)$ values were maintained across all groups to be as consistent as possible. In addition, Geneva and Uppsala added lines that were part of the Gaia-ESO line list (Heiter et al. 2015b), including HFS lines for both Ba and Eu, while molecules were ignored. High ionization stages were also removed from the Gaia-ESO line list, retaining only neutrals and singly ionized species. The full line list used by the spectral fitting groups can be found in Table F3.

The individual line lists used by the respective groups during Runs 1 and 2 are given in Tables F4-F9, in alphabetical order by group name. The groups who used the CoG method, namely ANU, ASU, Carnegie, and Porto, all had the option to include the Ba and Eu HFS lines given in Table F3, however only Porto opted to use them. We will discuss the comparison of groups who used HFS lines for Ba and Eu in §3.3.

APPENDIX D: INVESTIGATION RESULTS

In this appendix, we go into more detail regarding the trends that were found within the data output of the Investigation. While the key results were summarized in the corresponding sections of the main paper, namely those sections with the same name, we wanted to include a more thorough discussion for those interested.

Appendix D.1: Stellar Parameters

This section continues discussion from §3.2 with respect to Figure 2. To begin, we consider how parameter balance is achieved, specifically with respect to the CoG method. Stellar effective temperature is determined by adjusting the temperature solution until the correlation between the abundances and excitation potential are identically zero. To determine temperature errors, the effective temperature of the solution was varied above and below the optimal solution until the square of the sample correlation coefficient, r^2 , was equal to the 1σ variance of the sample. A typical value of $|r|$ that agreed with the 1σ variance was around 0.05-0.06, as mentioned in the ASU section of Appendix B. Therefore, there is no additional error term from stopping the regression before $r = 0$, since it did not stop at an arbitrary limit.

The top-left figure in Figure 2 shows $\log(g)$ versus T_{eff} for Run 1. While the groups' determinations do not completely overlap to within average-median error (± 52 K and ± 0.08 , respectively), they do produce results for each star that follow a consistent internal stellar trend such that as T_{eff} is increased for each star, $\log(g)$ also increases in a monotonic fashion. In general and within the average-median error for each star, the ANU and Uppsala groups calculated the lowest T_{eff} and $\log(g)$ values for the stellar sample. While the measurements for both parameters in HD 121504 by Uppsala appear rather low, both are within individual error of other data points for the sample. Although, it should

be noted that the Uppsala error estimates are at least double the average-median errors for T_{eff} , $\log(g)$, and ξ , which will be discussed more in §5.1. Both Carnegie and the ASU teams determined consistently higher values for T_{eff} and $\log(g)$ for all four stars during Run 1. Of note, the ANU and Porto groups calculated nearly identical $\log(g)$ values, to within individual error, for all stars regardless of temperature or spectral type. All methods measured HD 10700 to have the lowest T_{eff} , while the other three stars do not show any general trends that aren’t blurred by the error determinations (see Table 4).

Compared to Run 1, the $\log(g)$ and T_{eff} parameters in Figure 2 (top-right) were both consistently increased when using a standard line list (Run 3), where the errors are ± 62 K and ± 0.09 , respectively. The exception to this trend was seen in the Geneva group, which saw a decrease in both parameters for HD 361, HD 121504, and HD 202206; the $\log(g)$ and T_{eff} determinations for HD 10700 were the same between Runs 1 and 3 to within individual error. Despite the overall increase in the parameter values, the general internal stellar trend between the groups for each star was maintained, as compared to Run 1. We find that only the Carnegie group maintains consistent $\log(g)$ values between stars, similar to Run 1. Geneva determines significantly lower T_{eff} and $\log(g)$ values for all stars, which may be reconciled with the other groups via their large error bars, which we discuss more thoroughly in §5.1. On the other hand, if we were to temporarily ignore the ‘outlier’ stellar parameters from Geneva in both T_{eff} and $\log(g)$ for all but HD 10700, since the results from ASU were similar to within error for the metal-poorest star, we would find a significant improvement in the range for both parameters in all three stars. Namely, the updated ranges for HD 361, HD 121504, and HD 202206 (without the respective Geneva outliers) in T_{eff} would be 88 K, 134 K, and 93 K while $\log(g)$ would be 0.18, 0.22, and 0.19, which are smaller than the ranges in Run 1.

In the middle-left panel of Figure 2 is a plot showing ξ with respect to T_{eff} for Run 1, where the average-median errors are ± 0.10 km/s and ± 52 K, respectively. Similar to the graphs in the top panel of the figure, HD 361, HD 121504, and HD 202206 are clustered together, while HD 10700 is at the lower end of both parameters. The Geneva group tends to have consistently higher ξ values for all stars while the ANU group has consistently lower, although all are within the error of each other. In addition, beyond a certain temperature, the ANU, Carnegie, Geneva, and Uppsala measurements have ξ values for HD 361, HD 121504, and HD 202206 that are all similar per group to within individual error.

The ξ versus T_{eff} plot in Figure 2 (middle-right) for Run 3 has average-median errors of ± 0.11 km/s and ± 62 K, respectively. The dispersion between the groups for the “clustered” HD 361, HD 121504, and HD 202206 measurements is relatively similar to Run 1, per Table 5. Again, Geneva has consistently lower T_{eff} as compared to the other groups, but their ξ values are all the same to within error, which we discuss in §5.1. Also, ANU, ASU, Carnegie, and Uppsala all measure similar ξ values for the three higher-metallicity stars, showing that their methods do not have a sensitive relationship between ξ and T_{eff} .

Given that we have already discussed the trends between stars and groups for both ξ and $\log(g)$, we will now examine the relationship between these two parameters with respect to Run 1 (Figure 2, bottom-left) and Run 3 (bottom-right). Unlike any of the other plots in Figure 2, there is less segregation between stars for ξ with respect to $\log(g)$, namely that HD 10700 is no longer occupying an entirely separate parameter space. Instead, the HD 10700 measurements are relatively lower in ξ , but similar with $\log(g)$. A noticeable variation between Runs 1 and 3 is the shift in $\log(g)$ while ξ remains roughly the same. The outlying measurements follow a similar pattern, such that they are similar to within error for Run 1 but vary dramatically for Run 3.

Appendix D.2: C, O, Mg, & Si

Here we go into more detail from §3.3.1. Figure 3 (top-left) shows the absolute carbon abundances, $A(\text{C})$, in dex for our stellar sample along the y-axis with respect to all four analyses. In general, we find that $A(\text{C})$ measurements were relatively consistent between groups to within representative error, with an average range of 0.15 dex. There was no clear indication that standardizing the stellar parameters or line list consistently improved the $A(\text{C})$ measurements within all stars. However, standardization of some kind did generally improve the group’s results, since all stars but HD 202206 had optimized results in Runs 2–4 (see Table 10). The measurements for HD 202206 have a relatively consistent range across all four analyses, varying from 0.11–0.16 dex, per Tables 6–9. Yet the metric values in Table 10 show that the autonomous Run 1 yielded more uniform results. HD 121504 also had a small variation in abundance ranges between analyses, varying from 0.12–0.18 dex, except in this case Run 3 had the highest metric. For HD 361, the combination of standardized parameters and line list produced the best results in Run 4. Finally, HD 10700 had bimodal measurement groupings for Runs 1 and 2. Despite this, Run 2 exhibited a slightly smaller range (0.13 dex) and larger metric than the other analyses.

Oxygen was not easily accessible in these spectra, since the wavelength cutoff was after the near-UV OH lines and before the O I triplet at 7700 Å. While the forbidden [O I] lines at 6300.3 Å and 6360 Å were considered for the standardized line list, the blending from the Ni I line and CN lines, respectively, would have created significant issues (e.g. Ecuivillon et al. 2006; Caffau et al. 2013; Nissen et al. 2014, and references therein). Rather than test how each groups’ method responded to heavily blended lines, we opted to use the 6156.8 Å line. This line does not suffer from blending and is stronger than the 6158.2 Å line, which was thoroughly discussed in Bertran de Lis et al. (2015). We found that most groups chose not to use the [O I] lines when implementing their own line lists (see Tables F4-F9). The lack of discussion in the literature regarding the 6156.8 Å oxygen line also made its use more interesting, especially when considering a metal-poor star such as HD 10700.

Figure 3 (top-right) shows the $A(\text{O})$ values for all groups, analyses, and stars. Measuring the oxygen values with the

given spectra was difficult. In fact, not all groups were able to measure A(O) in all of the stars (Tables 6–9), especially for the two more metal-poor stars, HD 361 and HD 10700. Despite the large representative error, ± 0.13 dex which was the largest of the 10 elements, the A(O) measurements have a number of outliers. Overall though, standardizing stellar parameters gave the best results for A(O), where Run 2 produced the best results in three stars (HD 10700, HD 121504, and HD 202206). Run 4 was best for HD 361 which benefited from a lack of outliers. Interestingly, the groups were most inhomogeneous when measuring the metal-rich star, HD 202206.

With regard to the ANU oxygen measurements for HD 121504 and HD 202206, they believe the cause for their deviation from the other groups has to do with their inability to differentially adjust the oxygen determinations to match measured solar values (see Appendix B). Since the original data set from which the four target stars were selected did not include a solar spectrum, ANU could not adjust to solar values when using the standard line list, which affected their oxygen measurements very strongly. This deviation serves as an excellent consideration when implementing standardized line lists in the future.

Figure 3 (middle-left) shows A(Mg) for all analyses with a representative error of ± 0.06 dex. No clear pattern emerged for Mg. For example, the standard stellar parameters gives the best results for two stars (HD 361 and HD 202206), the standardized line list for one (HD 10700), and the autonomous analysis for one (HD 121504). Given the prevalence of outliers, is hard to ignore them and gauge the range, since that means that a significant fraction of the data is ignored. Fortunately, the metric weighs the outliers less and instead emphasizes the total grouping of the remaining data. The case of two outliers puts more onus on the total spread between groups’ measurements and therefore isn’t as strongly rated on the metric scale. For HD 121504 Run 1 yielded the most consistent results between groups. In this case, ignoring Geneva, the four groups have a range of 0.04 dex. Both HD 361 and HD 202206 had the highest metric value per Table 10 during Run 2 while HD 10700 was best during Run 3.

Figure 3 (middle-right) shows A(Si) abundances. Of all the elements shown in Figures 3 and 4, silicon has the most consistent measurements, overall lowest ranges, and similar metric values for all stars across all analyses. The ranges had an average of 0.16 dex, where the maximum was 0.29 dex and the minimum was 0.07 dex. The representative error is ± 0.06 dex, the lowest among the elements (along with magnesium). This shows that Si is overall a robustly useful element. The similarity of A(Si) abundances between the groups is not surprising given the number of silicon lines typically used for measurements and overall agreement currently seen between literature sources (Hinkel et al. 2014). For the Investigation, we found that the standardized stellar parameters produced the most uniform measurements and the smallest ranges between stars: 0.08–0.11 dex. Notably, the A(Si) measurements were not improved by the standardized line list in Runs 3 and 4. The ranges and metrics were considerably worse for both of these analyses, for example, the average ranges for these two runs was 0.23 dex. .

Appendix D.3: Na & Al

We continue the discussion from §3.3.2. Figure 3 (bottom-left) shows A(Na) for our stellar sample across the four analyses. Similar to the A(Mg) abundances, we find that there was no method that reliably refined the measurement homogeneity for all stars. Per Table 10, HD 361 has the best results in Run 1, HD 10700 in Run 3, HD 121504 in Run 4, and HD 202206 in Run 2. Both the plot and Table 9 reveal that there is an outlier for both HD 121504 and HD 202206 during Run 4, namely Uppsala. However, despite the outlier, HD 121504 had the highest metric in Run 4 due to the very tight clustering of the other five groups. HD 361 has an outlier during Run 3, although the large spread in group measurements dominated the metric calculation in this case. The representative error for A(Na) is ± 0.07 dex.

The A(Al) results are shown in Figure 3, bottom-right, where the representative error is ± 0.09 dex. In the majority of cases, a standardized line list – even one employing a weaker line – is beneficial for determining similar abundance measurements with different techniques. HD 10700 and HD 202206 are the most homogeneous in Run 3 while HD 361 and HD 121504 are better in Run 4, as is shown in Table 10.

Both Runs 1 and 2 resulted in substantially different A(Al) determinations between groups for all stars. In many cases, Carnegie was a lower outlier, for example HD 361 and HD 121504 in Run 1; HD 361, HD 121504, and HD 202206 in Run 2. However, Geneva was oftentimes an upper outlier, namely for HD 10700 and HD 121504 in Run 1; HD 361 and HD 121504 in Run 2. The other four groups were typically clustered in the middle having measured more similar A(Al) abundances. While the removal of these outliers drastically reduced the ranges, it is at the loss of one third of data. Beyond a certain extremity, the metric is no longer affected by the presence of an outlier. However two outliers dramatically reduces the quality and robustness of the metric.

Appendix D.4: Fe & Ni

Now we go into more detail from §3.3.3. Iron is the most commonly measured elemental abundance since there are hundreds of iron lines in the optical wavelength range. A large number of iron lines were employed by all of the groups in this study (see column 6 in Table 2), such that no group measured less than 60 Fe lines. We note that 70 Fe lines were used in the standard line list, see Table F2. Iron is used as a proxy to indicate the overall metallicity within a star (to the extent that people will often say ‘metallicity’ when in fact they are discussing iron-content), which affects stellar lifetime, color, structure, and a multitude of other properties. Nickel is also an iron-peak element and shares a number of characteristics with iron, for example, similar atomic structures and ionization potentials as well as a large number of optical lines. In Figure 4, top-left and -right, we show the A(Fe) and A(Ni) abundance results, respectively.

It clear from both Figure 4 (top-left) and Tables 6–10 that the A(Fe) measurements for all stars are the most comparable during Run 4. The ranges for Run 4, 0.11–0.18 dex, are significantly smaller compared to the other

runs, which vary from 0.14–0.34 dex with an average of 0.25 dex. This clear trend indicates that both standard stellar parameters and line list are beneficial for determining similar $A(\text{Fe})$ abundance measurements between methods. There are only two outliers for the $A(\text{Fe})$ determinations, occurring during Run 3, which indicates that the standardized line list may have polarizing effects on the participants’ methods. Note, the representative error bar is ± 0.09 dex.

Despite similar nucleosynthetic origins and atomic structure between iron and nickel, the $A(\text{Ni})$ abundance measurements in Figure 4 top-right show better agreement across all analyses as compared to the $A(\text{Fe})$ determinations. The average $A(\text{Ni})$ range from all four analyses is 0.16 dex, while the average $A(\text{Fe})$ range was 0.21 dex. The groups have the strongest overlap and highest metric for the $A(\text{Ni})$ measurements during Run 2, where the ranges vary from 0.07–0.12 dex. It is worth noting that, while Ni lines are the most predominant in our wavelength band compared to any other non-Fe element, the number of lines are only a fraction of the total Fe lines. Namely, ANU measured 48 Ni lines, ASU had 20 Ni lines, Carnegie used 15 Ni lines, Geneva had 32 Ni Lines, Porto measured 43 Ni lines, and Uppsala had 14 Ni lines. A total of 15 Ni lines were used in the Standard Line List, as compared to 70 Fe I and 14 Fe II lines, where only four had an EW below 30 mÅ.

Appendix D.5: Ba & Eu

We continue the analysis from §3.3.4. The $A(\text{Ba II})$ metric values in Table 10 for the different analyses vary depending on the star: HD 121504 is the most uniform during Run 1, HD 361 peaks during Run 4, and both HD 361 and HD 202206 are the most consistent during Run 2. The $A(\text{Ba II})$ absolute abundance measurements in Fig. 4 (bottom-left) have some of the largest group spreads for all of the stars across the four analyses (see Tables 6–9). Namely, the average range is 0.33 dex, where the maximum is 0.64 dex and the minimum is 0.16 dex. However, this may be biased by the outlier for HD 10700 in Run 1 as well as the outliers in HD 361 and HD 121504 in Run 3. In addition, we note the similar stellar abundance clustering in Runs 1 and 3, which shows the average $A(\text{Ba II})$ measurement linearly increasing from HD 361 to HD 121504 and then to HD 202206. The pattern changes when compared to Runs 2 and 4, which shows the abundances for HD 361 again at a lower value, then HD 121504 is maximum, finally HD 202206 falls between the other two stars. The conclusion is that the implementation of the standardized stellar parameters has a marked effect on the overall abundances for this element.

As discussed in Appendix B, three groups utilized the HFS lines for Ba II within the standardized line list (as given in Table F3). Namely, the two spectral fitting groups, Geneva and Uppsala, used HFS lines in addition to one CoG group (Porto). In general, the three groups measure higher abundances values for all three stars during Run 3, though most are within error.

There are three very strong BaII lines in our stellar spectra, see Table F2. In comparison, there is only one weak Eu II line, which made the measurement of this element so difficult that ANU was not able to determine any measurements. Additionally, ASU, Carnegie, and Porto did not report values for all stars (see in Figure 4 bottom-right). In the case with so few measurements, in addition to the relatively large ± 0.13 dex representative error, it makes determining outliers questionable.

For $A(\text{EuII})$, Table 10 shows that HD 361 is most uniform during Run 1 while HD 10700 and HD 121504 were best during Run 4. Since HD 202206 was only measured by two groups, we are unable to accurately determine the best run. We discuss the errors associated for an element with a single absorption line in §5.1. Geneva, Porto, and Uppsala utilized the HFS lines for Eu II in a similar way as for Ba II. As is shown in Fig. 4 (bottom-right), both Geneva and Uppsala determine smaller $A(\text{Eu II})$ abundances during Run 3 for HD 10700 and HD 121504, while Porto had some of the larger values (when measured). On the other hand, Run 4 did not have any discernible pattern between these three groups. It is interesting to note that only the spectral fitting groups, Geneva and Uppsala, were able to measure $A(\text{Eu II})$ in HD 202206 for any of the four analyses.

Appendix D.6: Iron Line Analysis

This appendix gives a detailed discussion of the iron lines found in Table 12, which were summarized in §3.4.1. Of all the iron lines used for HD 202206, only 5 lines were used by all 6 groups: 5855.08 Å, 5856.08 Å, 6027.05 Å, 6151.62 Å, and 6156.36 Å. A total of 16 lines were commonly measured by 5 groups and 27 lines were measured by 4 groups. These numbers are only a small percentage of the total discrete lines used when adding all of the groups’ lines for HD 202206. Along with the varying atomic parameters for the same lines, the inconsistent lines used between groups will be discussed in §5.

For the 5522.45 Å iron line, the three CoG groups that used both MOOG and ATLAS9, namely ANU, ASU, and Porto, have the same excitation potential but different oscillator strengths. Additionally, their measured EWs are within 1.3 mÅ of each other. When the stellar parameters are standardized in Run 2, the abundances determined for this line are 7.72 dex for ANU and 7.71 dex for Porto. While the ASU group measured 7.84 dex, their oscillator strength is smaller compared to ANU and Porto yet consistent with the Carnegie group. The Carnegie group also used MOOG but a different model atmosphere (MARCS). Carnegie’s EW measurement was different by 1.3 mÅ from ASU but the abundance is also 7.84 dex. Interestingly, while the Geneva group measured the same atomic parameters as ANU, their abundances (7.66 dex) were lower than ANU (7.72 dex). In Run 4, when the line list and atomic parameters are the same between all groups, the two sets of CoG groups (ANU and Porto; ASU and Carnegie) diverge from each other even though the total Fe abundances become more uniform. This may be an indication of how the differing methods and models effect the abundances on a line-by-line basis. Still, Run 4 is an improvement for almost every line, which is reflected in the overall agreement of most groups in Fig. 4 (top-left) and discussed §3.3.3.

For line 5778.45 Å, the ASU and Porto groups use slightly different atomic parameters as compared with the other groups, namely lower $\log(gf)$ values. While this generated expectedly larger iron abundances, the results were still within representative error. Geneva utilizes similar ξ_i and $\log(gf)$ as the other groups for all runs, but their determination of $A(\text{Fe})$ during Run 3 was much lower. For line 5855.08 Å, where again Porto has a $\log(gf)$ value that is 0.05 lower than the other groups, there is still good agreement among the abundance measurements. In comparison, the Geneva and Uppsala determinations are on the lower side for all analyses by ~ 0.1 dex, despite the similar atomic parameters. Unlike the other selected lines, there is a large variation in the oscillator strengths for line 5856.08 Å. The abundance results are diverse during Run 1, but become more copacetic through the implementation of standardized parameters and the line list. As expected, the results of all groups scale inversely with the oscillator strength, where Geneva and Uppsala have the largest $\log(gf)$ and the smallest abundances. On the other hand, Carnegie has the smallest $\log(gf)$ and largest abundance measurement. The range between these abundances is ~ 0.3 dex for Runs 1 and 2, which is much larger than the ± 0.09 representative iron error. When the same line list is used in Run 3, the spread between groups decreases somewhat, with the most similar results occurring during Run 4. In this case it appears as though the adopted standardized line parameters are influencing the measured abundances more so than, for example, stellar atmospheric parameters or EWs.

Most groups use the same atomic parameters for line 6027.05 Å, except Porto whose oscillator strength is relatively lower (4.07 eV) than the other groups (4.08 eV). However, this does not appear to have an impact on the abundances for Runs 1 and 2. Despite having similar atomic parameters, the Uppsala abundance determinations are notably larger than the other groups (+0.07 dex) for Runs 2–4, yet within representative error. Their overall iron abundances in Figure 4 (top-left) is very similar to the other groups, so this pattern may not be expressed within all of their lines. Line 6151.62 Å has the best agreement between groups for Run 2, with a range of only 0.04 dex. The atomic parameters are all similar and the EWs vary by a few mÅ. This is one of the few lines where Run 2 has better agreement than Run 4. Line 6165.36 Å shows varying oscillator strengths among the methods. However, the methods converge in Runs 3 and 4 for this line where the ranges are 0.08 dex and 0.06 dex, respectively.

Appendix D.7: Other Elements Line Analysis

This appendix offers a more a detailed discussion of the line-by-line analysis summarized in §3.4.2 for carbon, magnesium, sodium, aluminum, and barium and examines the trends seen in Table 13.

Carbon: For carbon, three lines were readily used between all groups, shown in Table 13. Additionally, Carnegie had two extra lines in the 7100 Å range. While all of the ξ_i and $\log(gf)$ values were nearly identical, Porto tended to have larger abundance values ($\gtrsim 0.1$ dex) during Runs 1 and 2 which may be due to their larger EW measurements. Both ASU and Uppsala had comparable values for 5052.15 Å during Runs 1 and 2, but that similarity was not seen for either Runs 3 and 4. The same was true for line 5380.32 Å. The 5052.15 Å line showed the best agreement between groups during Run 1, while 6587.61 Å had a slight improvement during Runs 3 and 4. In comparison, the abundance determinations by each group for line 5380.32 Å were relatively similar for all of the analyses. The difference between Carnegie's 7111.47 Å and 7113.18 Å abundance determinations is noticeable, varying by ~ 0.3 dex which is much higher than the carbon ± 0.07 dex representative error.

Magnesium: For line 5711.09 Å, both ASU and Uppsala determined abundances that were on the higher end of the scale by ~ 0.1 dex. Interestingly, Uppsala was the only group who was able to measure this line in Runs 3 and 4. The contrary is true for the 6318.72 Å magnesium line, where all groups produced results for Runs 3 and 4 and they agreed well, with the exception of Geneva. Despite having the same atomic parameters, the abundances by ASU and ANU were rather different during Runs 1 and 2. Namely, ANU found significantly lower magnesium values for Runs 1 and 2: 7.68 Å and 7.67 Å, respectively, as compared to ASU: 7.82 Å and 7.76 Å, respectively. This difference can be seen on the magnesium plot in Figure 3 (middle-left), where ASU tends to yield higher $A(\text{Mg})$ results while ANU determines lower ones. We discuss the errors associated for an element with a single absorption line in §5.1.

Sodium: For the two commonly measured sodium lines, namely 6154.23 Å and 6160.75 Å, the atomic parameters between groups are very similar. However, there are some variations in the oscillator strength, which varied from -1.622– -1.5 and -1.363– -1.2, respectively. ASU measured a larger EW and used a higher $\log(gf)$ for 6154.23 Å, which yielded larger abundances in Runs 1 and 2. Porto continued to determine higher abundances for both Runs 1–4, which can be seen in Fig. 3 (middle-left), although the spread decreased during Run 4. The results for the 6160.75 Å are interesting in that the oscillator strengths are measured in decreasing order: Carnegie/Geneva, ANU, then Porto, while the EWs are Porto, Carnegie, then ANU. The abundance determinations for Runs 1–4 are Porto, Carnegie, and then ANU, in descending order. This implies that the EW measurement is more significant than the oscillator strength, although perhaps only for this line. Geneva produced abundances at the lower end of the range for all runs except Run 4.

Aluminum: For aluminum, three total lines were measured by the groups, where 5557.07 Å was only measured by ANU and Uppsala and was not part of the set line list. The measurements of the 6696.02 Å line used the same excitation potential but with oscillator strengths that varied by 0.3. Carnegie had both the highest $\log(gf)$ value and EW, which resulted in the lowest abundance values for Runs 1 and 2, as expected. ASU's low oscillator strength produced relatively higher abundance measurements for Runs 1 and 2, while the Runs 3 and 4 determinations were about average. The same was true for ASU, Porto, and Uppsala when measuring the 6698.67 Å line: relatively low $\log(gf)$ values produced large abundances for Runs 1 and 2, but more average determinations for Runs 3 and 4. Geneva measured the highest $A(\text{Al})$ abundances for Runs 3 and 4.

It may be the case that the chosen $\log(gf)$ values are strongly affecting the overall Al abundance results. In Runs 1 and 2, the abundances for the two Al lines are consistent (< 0.1 dex) with each other for all groups. However, for Runs 3 and 4, all of the groups get similar *average* abundances for Al (and quite similar EWs) but much higher errors because the two lines give discrepant results. For example, the bluer line gives significantly larger abundances.

Barium: As discussed in Appendix D.5, singly ionized barium has three strong lines in our spectra which were measured by nearly all of our groups. In general, the atomic parameters are relatively similar between the groups for each line such that the small discrepancies do not always account for the varying results, see Table 13. For example, a larger oscillator strength does not always produce a smaller abundance measurement. Therefore, we examine the EW measurements. For the 5853.69 Å line, Porto measured the largest EW, followed by ANU and then ASU. In Run 1, ASU measures the largest abundance, along with the smallest $\log(gf)$. Porto determines the next largest abundance and then ANU. For Run 2, the descending order is Porto, ASU, and then ANU. Everything changes in Runs 3 and 4 where Uppsala and Porto measure the highest A(Ba II) content. For the 6141.73 Å line, the ASU and Carnegie abundances are all much larger than the ANU and Uppsala determinations for Runs 1 and 2, although their EWs are not consistently smaller or larger. That pattern changes for the latter two analyses, where the measurements converge better during Run 4. The final Ba II line, 6496.91 Å, has identical atomic parameters for all groups and a variety of EWs. Unfortunately, there does not appear to be any obvious pattern across the analyses.

APPENDIX E: COMPARISON TO LITERATURE ABUNDANCES

Expanding upon the discussion in §4 and relating to Table 11, the abundance of Na is consistent across all analyses for HD 361, with average $A(\text{Na}) = 6.06 - 6.10$ dex, compared to a literature value of 6.15 dex. We find that HD 10700 is similarly consistent at 5.85 - 5.89 dex, compared to 5.88 dex in *Hypatia*. The HD 202206 range of 6.59 - 6.61 dex is in good agreement with the literature 6.59 dex. Spreads for HD 10700 are substantially lower than in the literature; in other stars spreads were larger for the Investigation, especially for Runs 3 and 4.

Again for Mg, the values are quite consistent across all analyses and with the literature for all three stars. The largest difference between the Investigation and a literature results was for HD 10700 with a range of 0.15 dex, which is less than the spread. Spreads are larger in the Investigation than the literature for HD 361 and HD 20226. For HD 10700 the spreads are comparable to *Hypatia*.

The abundances measured for Al are consistent with *Hypatia* for all stars. The exception was found in Runs 3 and 4 for HD 202206, where the values for the Investigation (6.65 dex and 6.63 dex, respectively) were lower by slightly more than the spread (*Hypatia* value of 6.75 dex with a range 0.12 dex). Differences were generally much smaller than this instance and were well within the spread. Spreads improved markedly with the introduction of the fixed line list in Runs 3 and 4 for all three stars, where the average spreads were 0.41, 0.43, 0.22, and 0.28 dex, respectively. HD 361 has an extremely small *Hypatia* spread and only three measurements in the literature. Otherwise literature spreads were somewhat smaller than the Investigation values.

Silicon was extremely consistent both across analyses and with the literature for all stars. In every case the literature values fell within the range spanned by the different analyses, and the largest difference between analyses was 0.06 dex, for HD 10700 Runs 2 and 3. The largest difference with the *Hypatia* A(Si) was 0.09 dex for HD10700 Run 3. Investigation ranges were always smaller than the *Hypatia* spreads.

Nickel behaves similarly to Fe, except that the systematically lower values in the Investigation are not seen. The Investigation spread are small and comparable to the literature for Runs 2 and 4, with averages of 0.09 and 0.12 dex, respectively. However, ranges are larger for Runs 1 and 3, which had averages of 0.22 and 0.24 dex, respectively. The *Hypatia* spread is smallest for HD 361 at 0.04 dex, but that can be attributed to the effect of all the literature values for HD 361 coming from groups with very similar observations and methodology.

Barium is measured by only one group for HD 361 and HD 202206 and by four groups for HD 10700. For HD 361 A(Ba II) differs from the value in González Hernández et al. (2010) by 0.015 dex and 0.025 dex in Runs 1 and 3, respectively. The abundance for A(Ba II) is much lower, 2.16 dex and 2.13 dex in Runs 2 and 4, when the stellar parameters are fixed. HD 10700 behaves similarly, save that the literature average, 1.56 dex, lies roughly between the two extremes of fixed (1.50 dex) vs. free stellar parameters (1.69 dex). The spreads are large for HD 10700, with an average of 0.32 dex, and the low value reported by Takeda et al. (2005, 2007) brings the *Hypatia* average down. The single value available for HD 202206 is 2.42 dex (González Hernández et al. 2010) which falls between the higher values for the analyses that do not have fixed stellar parameters (average 2.47 dex) and the lower values for Runs 2 and 4 (average 2.30 dex).

Europium has a single value in the literature for HD 361 and HD 10700 and two for HD 202206, which differ by only 0.02 dex. The single measurement for HD 361 is lower than the Investigation values, which has an average of 0.62 dex, but falls within the average 0.18 dex spread. HD 10700 matches well. The Investigation averages, 0.50 dex, are much lower than *Hypatia* for HD 202206, but only two groups in the Investigation returned abundances. While it is difficult to draw conclusions from so few points, we can at least say that values in this study are broadly consistent with those in the literature.

APPENDIX F: SUPPLEMENTAL TABLES

The first is the updated *Hypatia Catalog*, similar to the one seen in Hinkel et al. (2014), shown in Table F1 including the specifics of the added data sets: such as the telescope(s) used, data resolution, S/N, wavelength range, model stellar atmosphere, EW technique (when applicable), whether spectral fitting or the CoG method was used, the solar

normalization scale, the number of Fe I and Fe II lines implemented, and the total number of stars that were added into the *Hyppatia Catalog*, respectively. We present the standard line lists used during Runs 3 and 4 for both the CoG methods (Table F2) and the spectral fitting techniques (Table F3), with the appropriate references. The line lists used by the individual groups for Runs 1 and 2, as given to the lead author, are shown in Tables F4-F9. It is our hope that providing all of this information will not only encourage others to share the details of their analysis but will help other groups/methods determine consistent results for future abundance determinations.

TABLE F1
HYPATIA 2.0 UPDATE

Catalog	Telescope	Resolution ($\Delta\lambda/\lambda$)	S/N	λ Range (\AA)	Stellar Atmo	Eq. Width	CoG or SF	Solar Scale	Num. of FeI/II lines	Stars in Hypatia
Adamów et al. (2014)	Hobby-Eberly Telescope (HET) at McDonald Observatory using High Resolution Spectrograph (HRS)	60000	>200-250	407-592 and 602-784	ATLAS9 per Kurucz (1993b)	spectral fitting	SME	their own	269 / 27	8
Adibekyan et al. (2012)	3.6m telescope at ESO equipped with High Accuracy Radial Velocity Planet Searcher (HARPS) using CORALIE	110000	70-2000	3800-6900	ATLAS9	ARES	MOOG	Anders & Grevesse (1989)	263 / 36	996
Adibekyan et al. (2015b)	La Silla Observatory using CORALIE and Ultraviolet and Visual Echelle Spectrograph (UVES)	110000	150	4780-6805	ATLAS9	ARES	MOOG	Anders & Grevesse (1989)	420 / 17	223
Battistini & Bensby (2015)	Fibre Fed Extended Range Optical Spectrograph (FEROS) on the ESO 1.5-m and 2.2-m telescopes; Soviet-Finnish Spectrograph (SOFIN) and Fibre-fed Echelle Spectrograph (FIES) on the Nordic Optical Telescope; HARPS on the ESO 3.6-m telescope; and Magellan Inamori Kyocera Echelle Spectrograph (MIKE) on the Magellan Clay telescope; UVES on the ESO Very Large Telescope (VLT)	48000 / 80000 / 67000 / 120000 / 42000- 80000 / 110000	150-300	3800-9200 / 4500-8800 / 3650-7300 / 3780-6910 / 3600-9300 / 5500-7500	MARCS	IRAF SPLOT	Uppsala EQWIDTH	Asplund et al. (2009)	226 / 36	637
Bensby et al. (2014)	FEROS on the ESO 1.5-m and 2.2-m telescopes; SOFIN and FIES on the Nordic Optical Telescope; HARPS on the ESO 3.6-m telescope; and MIKE on the Magellan Clay telescope; UVES on the ESO Very Large Telescope	48000 / 80000 / 67000 / 120000 / 42000- 80000 / 110000	150-300	3800-9200 / 4500-8800 / 3650-7300 / 3780-6910 / 3600-9300 / 5500-7500	MARCS	IRAF SPLOT	Uppsala EQWIDTH	Asplund et al. (2009)	226 / 36	689
Bertran de Lis et al. (2015)	3.6 m telescope at ESO using HARPS spectrograph; 8.2 m telescope at VLT / UT2 with UVES; and the 4.2m telescope at WHT using UES	115000	40-2000	3800-6900	ATLAS9	IRAF SPLOT	MOOG	their own	263 / 36	524
Biazzo et al. (2012)	FEROS on the ESO/MPG 2.2m telescope	48000	80-250	3600-9200	ATLAS9	ARES	MOOG	their own	126 / 11	9
Bruntt et al. (2012)	ESPaDONs spectrograph at the 3.6-m Canada-France-Hawaii Telescope (CFHT) and with the NARVAL spectrograph mounted on the 2-m Bernard Lyot Telescope at the Pic du Midi Observatory	80000 (both)	200-300	N/A	MARCS	Spectral fitting using VWA (Bruntt et al. 2010)	Spectral fitting using VWA (Bruntt et al. 2010)	differential analysis	variable	9

TABLE F1 — *Continued*

Catalog	Telescope	Resolution ($\Delta\lambda/\lambda$)	S/N	λ Range (\AA)	Stellar Atmo	Eq. Width	CoG or SF	Solar Scale	Num. of FeI/II lines	Stars in Hypatia
Gehren et al. (2004)	FOCES echelle spectrograph on the 2.2 m telescope of the DSAZ at Calar Alto Observatory and UVES echelle spectrograph mounted at the ESO VLT2	40000 / 60000	200 / 300	3700-9800 and 3300-6650	N/A	spectral fitting (IDL/ Fortran-based SIU software package)	spectral fitting (IDL/ Fortran-based SIU software package)	their own	0 / 8	30
Gehren et al. (2006)	FOCES echelle spectrograph on the 2.2 m telescope of the DSAZ at Calar Alto Observatory	40000-65000	100-200	3900-9000	N/A	spectral fitting (IDL/ Fortran-based SIU software package)	spectral fitting (IDL/ Fortran-based SIU software package)	their own	0 / 8	41
González Hernández et al. (2013)	3.6 m telescope at ESO using HARPS spectrograph; 8.2 m telescope at VLT / UT2 with UVES; and the 4.2m telescope at WHT using UES	110000 / 85000 / 65000	265-2015 / 510-940 / 520-850	3800-6900 / 4800-6800 / 4150-7950	ATLAS9	ARES	MOOG	differential analysis	263 / 36	61
Ishigaki et al. (2012)	High Dispersion Spectrograph (HDS) mounted on the Subaru Telescope	50000-90000	140-390	4000-6800	ATLAS9	spectral fitting	spectral fitting	Asplund et al. (2009)	N/A	7
Ishigaki et al. (2013)	HDS mounted on the Subaru Telescope	50000-90000	140-390	4000-6800	ATLAS9	spectral fitting	spectral fitting	Asplund et al. (2009)	N/A	1
Jofré et al. (2015)	HARPS (3.6 m ESO telescope; La Silla; Chile); FEROS (2.2 m ESO/MPI telescope; La Silla; Chile); ELODIE (1.93 m telescope; Observatoire de Haute Provence (OHP); France); and SOPHIE (1.93 m telescope; OHP; France); EBASIM (2.15m telescope; CASLEO; San Juan; Argentina)	120000 / 48000 / 40000 / 75000 / 30000	> 150	3780 - 6910 / 3500 - 9200 / 3850 - 6800 / 3872 - 6943 / 5000-7000	ATLAS9	ARES	MOOG	Anders & Grevesse (1989)	52 / 12	212
Karinkuzhi & Goswami (2014)	ELODIE echelle spectrograph at the 1.93 m telescope of OHP	42000	> 20	3900-6800	ATLAS	N/A	MOOG	Asplund (2005)	185 / 13	10
Liu et al. (2012)	BOES on the 1.8 m telescope at Bohyunsan Optical Astronomy Observatory (BOAO)	45000	100-200	3700-9250	ATLAS	ABON-TEST8	ABONTEST8	differential analysis	64 / 11	4
Maldonado et al. (2013)	HERMES spectrograph at the MERCATOR (1.2 m) telescope at La Palma observatory and FIES at the Nordic Optical Telescope (2.56 m)	85000 / 67000	90-340 / 75-480	3800-9000 / 3640-7360	ATLAS9	WIDTH9	WIDTH9	Asplund et al. (2009)	263 / 36	130
Mann et al. (2013)	ESPaDOnS spectrograph on the Canada-France-Hawaii Telescope on Mauna Kea	65000	>100	3700-10500	ATLAS9	spectral fitting	SME	Anders & Grevesse (1989)	N/A	38
Mishenina et al. (2013)	1.93 m telescope at the OHP equipped with the echelle-spectrograph ELODIE	42000	100-350	4400 / 6800	ATLAS9	WIDTH9	WIDTH9	their own	N/A	274

TABLE F1 — *Continued*

Catalog	Telescope	Resolution ($\Delta\lambda/\lambda$)	S/N	λ Range (\AA)	Stellar Atmo	Eq. Width	CoG or SF	Solar Scale	Num. of FeI/II lines	Stars in Hypatia
Mishenina et al. (2015)	1.93 m OHP telescope equipped with two echelle-spectrograph SOPHIE and ELODIE	75000 / 42000	100-300	4400–6800	STARSP LTE software (Tsymbal 1996)	spectral fitting	spectral fitting	differential analysis	N/A	244
Mortier et al. (2013)	UVES (VLT Kueyen telescope); FEROS (2.2 m ESO/MPI telescope); HARPS (3.6 m ESO telescope); CORALIE (1.2 m Swiss telescope); SOPHIE (1.93 m telescope; OHP); SARG (TNG Telescope); FIES (Nordic Optical Telescope); NARVAL (2 m Telescope Bernard Lyot); High Resolution Echelle Spectrometer or HIRES (Keck-I) and UES (William Herschel Telescope)	48000-110000	100-300	3000-10500	ATLAS9	ARES	MOOG	Anders & Grevesse (1989)	263 / 36	5
Nissen et al. (2014)	HARPS (3.6 m ESO telescope); FEROS (2.2 m ESO/MPI telescope); UVES (VLT Kueyen telescope); FIES (Nordic Optical Telescope)	115000 / 48000 / 55000 / 40000	> 300 / 200 / 250-500 / 140-200	N/A	MARCS	EQWIDTH	EQWIDTH	differential analysis		101
Nissen (2015)	HARPS (3.6 m ESO telescope; La Silla; Chile)	115000	> 600	3800-6900	MARCS	EQWIDTH	EQWIDTH	differential analysis	47 / 9	61
Peterson (2013)	10m telescope at Keck using the HIRES	42000	Median 106	3440-3950	MOOG (SYNTHÉ)	spectral fitting	spectral fitting	differential analysis	N/A	15
Ramírez et al. (2013)	2.7m telescope at McDonald using the Tull coude spectrograph; HIRES spectrograph at the Keck I Telescope; MIKE spectrograph on the 6.5 m Magellan/Clay Telescope	60000 / 50000 - 100000 / 65000	~200	4500-7800 / N/A / 3350-9500	MARCS	IRAF SPLOT	MOOG	differential analysis	N/A	34
Ramírez et al. (2014a)	UVES on the Unit Telescope 2 (UT2) on the VLT array	65000 (blue) and 100000 (red)	400	3260 and -4450 5650-9460	Kurucz odnew model atmosphere grid	IRAF SPLOT	MOOG	differential analysis	59 / 8	111
Ramírez et al. (2014b)	Tull coud spectrograph on the 2.7m Harlan J. Smith Telescope at McDonald Observatory; MIKE spectrograph on the 6.5m telescope at Las Campanas Observatory	60000 (both)	>200	N/A	MARCS	IRAF SPLOT	MOOG	differential analysis	N/A	18
Shi et al. (2012)	Infrared Camera and Spectrograph (IRCS) on the 8.2 m Subaru Telescope on Mauna Kea	20000	100-300	10100 - 11900	MAFAGS code	spectral fitting	spectral fitting	differential analysis		12
Sitnova et al. (2015)	Hamilton Echelle Spectrograph mounted on the Shane 3-m telescope of the Lick observatory	60000	100	3700-9300	MARCS	their own analysis	their own analysis	differential analysis	31 / 18	34

TABLE F1 — *Continued*

Catalog	Telescope	Resolution ($\Delta\lambda/\lambda$)	S/N	λ Range (Å)	Stellar Atmo	Eq. Width	CoG or SF	Solar Scale	Num. of FeI/II lines	Stars in Hypatia
Stonkutė et al. (2012)	FIES on the Nordic Optical 2.5 m telescope	68000	> 100	3680-7270	MARCS	spectral fitting (EQWIDTH)	spectral fitting (Spectrum)	differential analysis	N/A	23
Stonkutė et al. (2013)	FIES on the Nordic Optical 2.5 m telescope	68000	> 100	3680-7270	MARCS	spectral fitting	spectral fitting	their own	N/A	21
Wu et al. (2015)	HIRES spectrograph at the Keck I Telescope	48000	> 100	3200-3500	MAFAGS	spectral fitting using IDL/ Fortran SIU (Reetz 1991)	spectral fitting using IDL/ Fortran SIU (Reetz 1991)	their own	N/A	70
Yan et al. (2015)	FOCES echelle spectrograph on the 2.2 m telescope at Calar Alto Observatory	> 40000	> 100	3700-9800	MAFAGS	spectral fitting	spectral fitting	their own	0 / 8	52
Ženovienė et al. (2014)	FIES on the Nordic Optical 2.5 m telescope	68000	> 100	3680-7270	MARCS	spectral fitting (EQWIDTH)	spectral fitting (BSYN)	differential analysis	N/A	32

* Telescope/spectrograph information and the methods for determining abundances as given by the recently added literature sources into *Hypatia* 2.0. Please see Hinkel et al. (2014) for more details.

TABLE F2
STANDARD LINE LIST

Ion	Wavelength (Å)	χ_I (eV)	$\log(gf)$	$\delta\Gamma_6^{5/2}$	EW_\odot (mÅ)	Reference
Cl	5052.15	7.68	-1.30	9.9	37.8	Wiese et al. (1996)
	5380.32	7.68	-1.61	9.9	21.9	Wiese et al. (1996)
	6587.62	8.54	-1.00	9.9	14.0	Wiese et al. (1996)
OI	6156.80	10.74	-0.43	2.5	4.1	Feltzing & Gustafsson (1998)
NaI	6154.23	2.10	-1.57	6.4	39.8	Lambert & Warner (1968)
	6160.75	2.10	-1.27	6.4	58.4	Lambert & Warner (1968)
MgI	6318.71	5.11	-1.97	9.9	39.8	Lambert (1978)
AlI	6696.03	3.14	-1.58	2.5	38.1	Feltzing & Gustafsson (1998)
	6698.67	3.14	-1.63	9.9	21.9	Lambert (1978)
SiI	5793.08	4.93	-2.06	1.9	44.9	Reddy et al. (2003)
	6125.03	5.61	-1.51	1.9	33.8	Reddy et al. (2003)
	6142.49	5.62	-1.54	1.9	36.8	Reddy et al. (2003)
	6145.02	5.61	-1.48	1.9	40.3	Reddy et al. (2003)
	6244.48	5.61	-1.36	1.9	48.4	Reddy et al. (2003)
CrI	6721.84	5.86	-1.06	1.9	49.1	Reddy et al. (2003)
	5300.75	0.98	-2.13	9.9	62.2	Blackwell et al. (1995)
	5783.87	3.32	-0.29	9.9	45.8	Blackwell et al. (1995)
	5787.93	3.32	-0.08	9.9	48.3	Blackwell et al. (1995)
	6330.10	0.94	-2.90	9.9	27.1	Reddy et al. (2003)
CrII	5305.87	3.83	-1.97	9.9	26.7	Reddy et al. (2003)
FeI	5141.75	2.42	-2.18	2.3	89.4	Reddy et al. (2003)
	5247.06	0.09	-4.94	2.3	67.6	Blackwell et al. (1995)
	5358.12	3.30	-3.16	2.3	10.2	Reddy et al. (2003)
	5412.79	4.44	-1.71	2.3	20.1	Bard et al. (1991); Bard & Kock (1994)
	5522.45	4.21	-1.55	2.2	39.9	Kupka et al. (2000)
	5543.94	4.22	-1.14	2.2	63.9	Kupka et al. (2000)
	5560.21	4.43	-1.19	2.2	49.5	Feltzing & Gustafsson (1998)
	5577.03	5.03	-1.55	2.2	11.7	Feltzing & Gustafsson (1998)
	5651.47	4.47	-2.00	2.2	20.4	Kupka et al. (2000)
	5653.87	4.39	-1.64	2.2	35.8	Kupka et al. (2000)
	5661.35	4.28	-1.75	2.3	24.2	Bard et al. (1991); Bard & Kock (1994)
	5741.85	4.26	-1.85	2.2	31.4	Kupka et al. (2000)
	5752.03	4.55	-1.18	2.2	53.2	Kupka et al. (2000)
	5778.46	2.59	-3.45	2.3	22.6	meanofBard et al. (1991)
						Bard & Kock (1994); Blackwell et al. (1995)
	5784.66	3.40	-2.53	2.3	27.8	Bard et al. (1991); Bard & Kock (1994)
	5809.22	3.88	-1.61	2.3	50.8	Milford et al. (1994)
	5849.69	3.70	-2.93	2.3	7.6	Blackwell et al. (1995)
	5852.23	4.55	-1.17	2.3	41.1	Reddy et al. (2003)
	5855.09	4.61	-1.48	2.3	22.2	Bard et al. (1991); Bard & Kock (1994)
	5856.10	4.29	-1.56	2.3	33.7	Reddy et al. (2003)
	5858.79	4.22	-2.18	2.3	13.0	Reddy et al. (2003)
	5859.60	4.55	-0.61	2.3	73.0	Reddy et al. (2003)
	5862.37	4.55	-0.25	2.3	97.3	Reddy et al. (2003)
	5956.70	0.86	-4.60	2.3	52.9	Blackwell et al. (1995)
	6005.54	2.59	-3.60	2.2	22.1	Kupka et al. (2000)
	6027.06	4.07	-1.17	2.3	66.2	Reddy et al. (2003)
	6085.26	2.76	-3.10	2.2	41.5	Kupka et al. (2000)
	6105.13	4.55	-2.05	2.2	11.6	Kupka et al. (2000)
	6151.62	2.18	-3.28	2.3	51.1	meanofBard et al. (1991)
						Bard & Kock (1994); Blackwell et al. (1995)
	6157.73	4.08	-1.26	2.2	59.2	Kupka et al. (2000)
	6159.38	4.61	-1.83	2.3	12.7	Reddy et al. (2003)
	6165.36	4.14	-1.46	2.3	46.6	Reddy et al. (2003)
	6173.34	2.22	-2.88	2.3	69.4	Blackwell et al. (1995)
	6200.32	2.61	-2.44	2.3	79.4	Blackwell et al. (1995)
	6213.44	2.22	-2.56	2.3	88.0	Reddy et al. (2003)
	6220.78	3.88	-2.46	2.2	19.5	Kupka et al. (2000)
	6226.73	3.88	-2.22	2.2	29.2	Kupka et al. (2000)
	6240.65	2.22	-3.23	2.3	49.9	Bard et al. (1991); Bard & Kock (1994)
	6265.14	2.18	-2.55	2.3	90.7	Blackwell et al. (1995)
	6271.28	3.33	-2.70	2.3	24.6	Bard et al. (1991); Bard & Kock (1994)
	6297.80	2.22	-2.73	2.3	75.1	meanofBard et al. (1991)
						Bard & Kock (1994); Blackwell et al. (1995)
	6322.69	2.59	-2.43	2.3	74.2	Blackwell et al. (1995)
	6358.69	0.86	-4.00	2.3	85.0	Reddy et al. (2003)
	6380.74	4.19	-1.27	2.2	56.9	Feltzing & Gustafsson (1998)
	6436.41	4.19	-2.36	2.3	10.1	Reddy et al. (2003)
	6481.88	2.28	-2.97	2.3	65.4	Blackwell et al. (1995)
	6494.50	4.73	-1.46	2.2	35.1	Kupka et al. (2000)
	6498.95	0.96	-4.69	2.3	48.3	Blackwell et al. (1995)
	6518.37	2.83	-2.45	2.3	58.9	Bard et al. (1991); Bard & Kock (1994)
	6574.23	0.99	-5.00	2.3	28.9	Blackwell et al. (1995)
	6581.21	1.48	-4.68	2.3	19.6	Bard et al. (1991); Bard & Kock (1994)

TABLE F2 — *Continued*

Ion	Wavelength (Å)	χ_1 (eV)	$\log(gf)$	$\delta\Gamma_6^{5/2}$	EW_\odot (mÅ)	Reference
	6591.33	4.59	-1.95	2.3	10.7	Reddy et al. (2003)
	6608.04	2.28	-3.91	2.3	18.8	Reddy et al. (2003)
	6625.03	1.01	-5.34	2.3	16.6	Blackwell et al. (1995)
	6627.54	4.55	-1.68	2.2	25.4	Kupka et al. (2000)
	6699.14	4.59	-2.10	2.3	8.4	Bard et al. (1991); Bard & Kock (1994)
	6703.57	2.76	-3.01	2.2	38.1	Feltzing & Gustafsson (1998)
	6705.10	4.61	-1.39	2.2	47.0	Kupka et al. (2000)
	6710.32	1.49	-4.81	2.2	16.6	Feltzing & Gustafsson (1998)
	6713.75	4.80	-1.39	2.3	21.7	Reddy et al. (2003)
	6715.38	4.61	-1.64	2.2	28.7	Kupka et al. (2000)
	6716.22	4.58	-1.92	2.2	15.5	Kupka et al. (2000)
	6725.36	4.10	-2.17	2.3	17.9	Reddy et al. (2003)
	6733.15	4.64	-1.40	2.3	27.5	Bard et al. (1991); Bard & Kock (1994)
	6739.52	1.56	-4.79	2.3	11.9	Bard et al. (1991); Bard & Kock (1994)
	6750.16	2.42	-2.62	2.3	76.1	meanofBard et al. (1991)
						Bard & Kock (1994); Blackwell et al. (1995)
	6752.71	4.64	-1.20	2.3	37.5	Bard et al. (1991); Bard & Kock (1994)
	6837.01	4.59	-1.69	2.3	18.3	Bard et al. (1991); Bard & Kock (1994)
	6857.25	4.08	-2.04	2.3	23.4	Reddy et al. (2003)
	6971.94	3.02	-3.34	2.3	13.4	Bard et al. (1991); Bard & Kock (1994)
FeII	5234.62	3.22	-2.18	9.9	85.0	Meléndez et al. (2009)
	5425.26	3.20	-3.22	9.9	42.5	Meléndez et al. (2009)
	5991.38	3.15	-3.54	2.2	29.0	Meléndez et al. (2009)
	6084.11	3.20	-3.79	2.2	20.2	Meléndez et al. (2009)
	6147.74	3.89	-2.69	2.2	72.0	Meléndez et al. (2009)
	6149.25	3.89	-2.69	9.9	37.4	Meléndez et al. (2009)
	6238.39	3.89	-2.60	2.2	47.7	Meléndez et al. (2009)
	6247.56	3.89	-2.30	9.9	54.4	Meléndez et al. (2009)
	6369.46	2.89	-4.11	9.9	19.8	Meléndez et al. (2009)
	6416.92	3.89	-2.64	2.2	37.6	Meléndez et al. (2009)
	6432.68	2.89	-3.57	9.9	41.7	Meléndez et al. (2009)
	6442.95	5.55	-2.44	2.2	6.0	Meléndez et al. (2009)
	6446.40	6.22	-1.97	2.2	3.7	Meléndez et al. (2009)
	6456.39	3.90	-2.05	9.9	65.2	Meléndez et al. (2009)
NiII	5082.35	3.66	-0.59	9.9	69.1	Reddy et al. (2003)
	5088.54	3.85	-1.04	9.9	33.6	Reddy et al. (2003)
	5088.96	3.68	-1.24	9.9	31.3	Reddy et al. (2003)
	5094.42	3.83	-1.07	9.9	32.6	Reddy et al. (2003)
	5115.40	3.83	-0.28	9.9	79.2	Reddy et al. (2003)
	5847.01	1.68	-3.41	9.9	23.2	Reddy et al. (2003)
	6111.08	4.09	-0.81	9.9	35.8	Reddy et al. (2003)
	6130.14	4.27	-0.94	9.9	22.4	Reddy et al. (2003)
	6175.37	4.09	-0.55	9.9	50.5	Reddy et al. (2003)
	6176.82	4.09	-0.26	9.9	67.3	Wickliffe & Lawler (1997)
	6177.25	1.83	-3.51	9.9	15.2	Reddy et al. (2003)
	6204.61	4.09	-1.11	9.9	22.8	Wickliffe & Lawler (1997)
	6378.26	4.15	-0.83	9.9	33.1	Wickliffe & Lawler (1997)
	6643.64	1.68	-2.03	9.9	101.4	Reddy et al. (2003)
	6772.32	3.66	-0.97	9.9	50.9	Reddy et al. (2003)
ZnI	6362.35	5.79	0.14	9.9	20.6	Biemont & Godefroid (1980)
YI	6687.50	0.00	-0.67	2.5	4.3	Feltzing & Gustafsson (1998)
YII	5087.43	1.08	-0.16	9.9	48.6	Hannaford et al. (1982)
	5200.42	0.99	-0.57	9.9	39.0	Hannaford et al. (1982)
	5402.78	1.84	-0.44	9.9	12.6	Hannaford et al. (1982)
BaII	5853.69	0.60	-0.91	9.9	66.7	Davidson et al. (1992)
	6141.73	0.70	-0.03	9.9	132.8	Davidson et al. (1992)
	6496.91	0.60	-0.41	9.9	112.2	Davidson et al. (1992)
EuII	6645.13	1.38	0.20	9.9	5.6	Kurucz (1998)

TABLE F3
SPECTRAL FITTING STANDARD LINE LIST

Wavelength (Å)	Elem.	Lower χ_I (cm ⁻¹)	Upper χ_I (cm ⁻¹)	log(gf)	Rad. Damp.	Stark	Waals	Wavelength Ref	Lande Ref	Damp. Ref	Stark Ref	VDW Ref
5052.1443	C	61983	81768	-1.3	8.69	-4.69	-7.31	Kurucz (2010)	Kurucz (2010)	Kurucz (2010)	Kurucz (2010)	Kurucz (2010)
5082.3441	Ni	29503	49175	-0.59	8.35	-4.03	811.278	Kurucz (2008)	Kurucz (2008)	Kurucz (2008)	Kurucz (2008)	Barklem & Aspelund-Johansson (2005); Barklem et al. (2000)
5087.416	Y II	8743	28390	-0.16	0	0	0	Hannaford et al. (1982)	Hannaford et al. (1982)	Hannaford et al. (1982)	Hannaford et al. (1982)	Kurucz (2011)
5088.5377	Ni	31028	50675	-1.04	8.31	-5.58	-7.51	Kurucz (2008)	Kurucz (2008)	Kurucz (2008)	Kurucz (2008)	Kurucz (2008)
5088.9557	Ni	29673	49312	-1.24	8.09	-4.64	829.278	Kurucz (2008)	Kurucz (2008)	Kurucz (2008)	Kurucz (2008)	Barklem & Aspelund-Johansson (2005); Barklem et al. (2000)
5094.4107	Ni	30915	50538	-1.07	8.18	-4.51	788.277	Kurucz (2008)	Kurucz (2008)	Kurucz (2008)	Kurucz (2008)	Barklem & Aspelund-Johansson (2005); Barklem et al. (2000)
5115.3922	Ni	30923	50466	-0.28	7.9	-5.42	769.235	Kurucz (2008)	Kurucz (2008)	Kurucz (2008)	Kurucz (2008)	Barklem et al. (2000)
5141.7389	Fe	19550	38996	-2.18	8.2	-5.88	367.251	Kurucz (2007)	Kurucz (2007)	Kurucz (2007)	Kurucz (2007)	Barklem & Aspelund-Johansson (2005); Barklem et al. (2000)
5200.406	Y II	8001	27229	-0.57	0	0	0	Hannaford et al. (1982)	Hannaford et al. (1982)	Hannaford et al. (1982)	Hannaford et al. (1982)	Kurucz (2011)
5234.6226	Fe II	25979	45078	-2.18	8.46	-6.53	180.249	Kurucz (2013)	Kurucz (2013)	Kurucz (2013)	Kurucz (2013)	Barklem & Aspelund-Johansson (2005); Barklem et al. (2000)
5247.0501	Fe	701	19760	-4.94	3.63	-6.28	206.253	Kurucz (2007)	Kurucz (2007)	Kurucz (2007)	Kurucz (2007)	Barklem & Aspelund-Johansson (2005); Barklem et al. (2000)
5305.8526	Cr II	30866	49707	-1.97	8.36	-6.49	187.218	Kurucz (2010)	Kurucz (2010)	Kurucz (2010)	Kurucz (2010)	Barklem & Aspelund-Johansson (2005); Barklem et al. (2000)
5380.3252	C	61983	80566	-1.61	8.69	-5.65	0	Kurucz (2010)	Kurucz (2014)	Kurucz (2010)	Kurucz (2010)	Ralchenko et al. (2010)
5402.774	Y II	14832	33334	-0.44	0	0	0	Pitts & Newsom (1986)	Pitts & Newsom (1986)	Pitts & Newsom (1986)	Pitts & Newsom (1986)	Kurucz (2011)
5412.7838	Fe	35770	54240	-1.71	8.29	-4.54	971.28	Kurucz (2007)	Kurucz (2007)	Kurucz (2007)	Kurucz (2007)	Barklem & Aspelund-Johansson (2005); Barklem et al. (2000)
5425.2485	Fe II	25801	44231	-3.22	8.46	-6.53	178.255	Kurucz (2013)	Kurucz (2013)	Kurucz (2013)	Kurucz (2013)	Barklem & Aspelund-Johansson (2005); Barklem et al. (2000)
5522.4461	Fe	33947	52046	-1.55	8.02	-5.57	744.215	Kurucz (2007)	Kurucz (2007)	Kurucz (2007)	Kurucz (2007)	Barklem & Aspelund-Johansson (2005); Barklem et al. (2000)

TABLE F3 — *Continued*

Wavelength (Å)	Elem.	Lower χ_I (cm ⁻¹)	Upper χ_I (cm ⁻¹)	log(gf)	Rad. Damp.	Stark	Waals	Wavelength Ref	Lande Ref	Damp. Ref	Stark Ref	VDW Ref
5543.9356	Fe	34020	52046	-1.14	8.48	-5.57	742.238	Kurucz (2007)	Kurucz (2007)	Kurucz (2007)	Kurucz (2007)	Barklem & Aspelund-Johansson (2005); Barklem et al. (2000)
5560.2115	Fe	35770	53748	-1.19	8.28	-4.24	895.278	Kurucz (2007)	Kurucz (2007)	Kurucz (2007)	Kurucz (2007)	Barklem & Aspelund-Johansson (2005); Barklem et al. (2000)
5577.0247	Fe	40593	58523	-1.55	8.88	-5.29	-7.39	Kurucz (2007)	Kurucz (2007)	Kurucz (2007)	Kurucz (2007)	Kurucz (2007)
5651.4689	Fe	36077	53772	-2	8.27	-5.41	898.278	Kurucz (2007)	Kurucz (2007)	Kurucz (2007)	Kurucz (2007)	Barklem & Aspelund-Johansson (2005); Barklem et al. (2000)
5653.8651	Fe	35383	53063	-1.64	8.31	-3.96	792.277	Kurucz (2007)	Kurucz (2007)	Kurucz (2007)	Kurucz (2007)	Barklem & Aspelund-Johansson (2005); Barklem et al. (2000)
5661.3447	Fe	34552	52216	-1.75	8	-5.47	765.209	Kurucz (2007)	Kurucz (2007)	Kurucz (2007)	Kurucz (2007)	Barklem & Aspelund-Johansson (2005); Barklem et al. (2000)
5741.8477	Fe	34326	51740	-1.85	8.47	-5.57	725.232	Kurucz (2007)	Kurucz (2007)	Kurucz (2007)	Kurucz (2007)	Barklem & Aspelund-Johansson (2005); Barklem et al. (2000)
5752.0319	Fe	36690	54063	-1.18	8.33	-4.69	-7.51	Kurucz (2007)	Kurucz (2007)	Kurucz (2007)	Kurucz (2007)	Kurucz (2007)
5783.85	Cr	26793	44078	-0.29	7.99	-4.34	1098.29	Wallace & Hinkle (2009)	Kurucz (2010)	Kurucz (2010)	Kurucz (2010)	Barklem & Aspelund-Johansson (2005); Barklem et al. (2000)
5784.658	Fe	27398	44675	-2.53	8.05	-5.41	796.244	Kurucz (2007)	Kurucz (2007)	Kurucz (2007)	Kurucz (2007)	Barklem & Aspelund-Johansson (2005); Barklem et al. (2000)
5787.919	Cr	26793	44070	-0.08	8.03	-4.43	1097.29	Wallace & Hinkle (2009)	Kurucz (2010)	Kurucz (2010)	Kurucz (2010)	Barklem & Aspelund-Johansson (2005); Barklem et al. (2000)
5793.0726	Si	39763	57015	-2.06	8.53	-4.37	1700.23	Kurucz (2007)	Kurucz (2007)	Kurucz (2007)	Kurucz (2007)	Barklem & Aspelund-Johansson (2005); Barklem et al. (2000)
5809.2174	Fe	31326	48530	-1.61	7.78	-5.29	956.244	Kurucz (2007)	Kurucz (2007)	Kurucz (2007)	Kurucz (2007)	Barklem & Aspelund-Johansson (2005); Barklem et al. (2000)
5846.9935	Ni	13517	30616	-3.41	7.97	-6.13	284.296	Kurucz (2008)	Kurucz (2008)	Kurucz (2008)	Kurucz (2008)	Barklem & Aspelund-Johansson (2005); Barklem et al. (2000)
5849.6833	Fe	29802	46893	-2.93	7.78	-5.88	379.305	Kurucz (2007)	Kurucz (2007)	Kurucz (2007)	Kurucz (2007)	Barklem & Aspelund-Johansson (2005); Barklem et al. (2000)

TABLE F3 — *Continued*

Wavelength (Å)	Elem.	Lower χ_I (cm ⁻¹)	Upper χ_I (cm ⁻¹)	log(gf)	Rad. Damp.	Stark	Waals	Wavelength Ref	Lande Ref	Damp. Ref	Stark Ref	VDW Ref
5853.6663	Ba II	4871	21954	-0.907	0	0	0	Miles & Wiese (1969)	Miles & Wiese (1969)	Miles & Wiese (1969)	Miles & Wiese (1969)	Barklem & Aspelund-Johansson (2005); Barklem et al. (2000)
5853.6666	Ba II	4871	21954	-0.947	0	0	0	Miles & Wiese (1969)	Miles & Wiese (1969)	Miles & Wiese (1969)	Miles & Wiese (1969)	Barklem & Aspelund-Johansson (2005); Barklem et al. (2000)
5853.668	Ba II	4871	21954	-0.907	0	0	0	Miles & Wiese (1969)	Miles & Wiese (1969)	Miles & Wiese (1969)	Miles & Wiese (1969)	Barklem & Aspelund-Johansson (2005); Barklem et al. (2000)
5853.6686	Ba II	4871	21954	-0.907	0	0	0	Miles & Wiese (1969)	Miles & Wiese (1969)	Miles & Wiese (1969)	Miles & Wiese (1969)	Barklem & Aspelund-Johansson (2005); Barklem et al. (2000)
5853.6695	Ba II	4871	21954	-0.907	0	0	0	Miles & Wiese (1969)	Miles & Wiese (1969)	Miles & Wiese (1969)	Miles & Wiese (1969)	Barklem & Aspelund-Johansson (2005); Barklem et al. (2000)
5853.6756	Ba II	4871	21954	-1.965	0	0	0	Miles & Wiese (1969)	Miles & Wiese (1969)	Miles & Wiese (1969)	Miles & Wiese (1969)	Barklem & Aspelund-Johansson (2005); Barklem et al. (2000)
5855.0758	Fe	37166	54240	-1.48	8.33	-4.54	962.279	Kurucz (2007)	Kurucz (2007)	Kurucz (2007)	Kurucz (2007)	Barklem & Aspelund-Johansson (2005); Barklem et al. (2000)
5856.0879	Fe	34633	51708	-1.56	7.99	-5.26	404.264	Kurucz (2007)	Kurucz (2007)	Kurucz (2007)	Kurucz (2007)	Barklem & Aspelund-Johansson (2005); Barklem et al. (2000)
5858.778	Fe	34036	51103	-2.18	8.48	-4.38	786.278	Fuhr et al. (1988)	Kurucz (2007)	Kurucz (2007)	Kurucz (2007)	Barklem & Aspelund-Johansson (2005); Barklem et al. (2000)
5859.5863	Fe	36690	53748	-0.61	8.33	-4.24	-7.51	Kurucz (2007)	Kurucz (2007)	Kurucz (2007)	Kurucz (2007)	Kurucz (2007)
5862.3564	Fe	36690	53740	-0.25	8.33	-4.63	-7.52	Kurucz (2007)	Kurucz (2007)	Kurucz (2007)	Kurucz (2007)	Kurucz (2007)
5956.694	Fe	6928	23712	-4.6	4	-6.17	227.252	Kurucz (2007)	Kurucz (2007)	Kurucz (2007)	Kurucz (2007)	Barklem & Aspelund-Johansson (2005); Barklem et al. (2000)
5991.3709	Fe II	25430	42118	-3.54	8.54	-6.53	172.221	Kurucz (2013)	Kurucz (2013)	Kurucz (2013)	Kurucz (2013)	Barklem & Aspelund-Johansson (2005); Barklem et al. (2000)
6027.0508	Fe	32875	49457	-1.17	8.01	-6.03	380.25	Kurucz (2007)	Kurucz (2007)	Kurucz (2007)	Kurucz (2007)	Barklem & Aspelund-Johansson (2005); Barklem et al. (2000)
6084.1017	Fe II	25801	42239	-3.79	8.54	-6.53	173.223	Kurucz (2013)	Kurucz (2013)	Kurucz (2013)	Kurucz (2013)	Barklem & Aspelund-Johansson (2005); Barklem et al. (2000)

TABLE F3 — *Continued*

Wavelength (Å)	Elem.	Lower χ_I (cm ⁻¹)	Upper χ_I (cm ⁻¹)	log(gf)	Rad. Damp.	Stark	Waals	Wavelength Ref	Lande Ref	Damp. Ref	Stark Ref	VDW Ref
6085.2582	Fe	22252	38682	-3.1	8.2	-5.89	344.26	Kurucz (2007)	Kurucz (2007)	Kurucz (2007)	Kurucz (2007)	Barklem et al. (2000)
6105.1279	Fe	36690	53063	-2.05	8.33	-3.96	788.274	Kurucz (2007)	Kurucz (2007)	Kurucz (2007)	Kurucz (2007)	Barklem & Aspelund-Johansson (2005); Barklem et al. (2000)
6111.0703	Ni	32971	49336	-0.81	8.2	-3.6	845.28	Kurucz (2008)	Kurucz (2008)	Kurucz (2008)	Kurucz (2008)	Barklem & Aspelund-Johansson (2005); Barklem et al. (2000)
6125.0209	Si	45279	61596	-1.51	7.91	-5.56	-7.13	Kurucz (2007)	Kurucz (2007)	Kurucz (2007)	Kurucz (2007)	Kurucz (2007)
6130.1348	Ni	34407	50716	-0.94	8.45	-6	825.281	Kurucz (2008)	Kurucz (2008)	Kurucz (2008)	Kurucz (2008)	Barklem & Aspelund-Johansson (2005); Barklem et al. (2000)
6141.7096	Ba II	5678	21954	-0.395	0	0	0	Miles & Wiese (1969)	Miles & Wiese (1969)	Miles & Wiese (1969)	Miles & Wiese (1969)	Barklem & Aspelund-Johansson (2005); Barklem et al. (2000)
6141.713	Ba II	5678	21954	-0.032	0	0	0	Miles & Wiese (1969)	Miles & Wiese (1969)	Miles & Wiese (1969)	Miles & Wiese (1969)	Barklem & Aspelund-Johansson (2005); Barklem et al. (2000)
6141.7137	Ba II	5678	21954	-0.032	0	0	0	Miles & Wiese (1969)	Miles & Wiese (1969)	Miles & Wiese (1969)	Miles & Wiese (1969)	Barklem & Aspelund-Johansson (2005); Barklem et al. (2000)
6141.7146	Ba II	5678	21954	-0.032	0	0	0	Miles & Wiese (1969)	Miles & Wiese (1969)	Miles & Wiese (1969)	Miles & Wiese (1969)	Barklem & Aspelund-Johansson (2005); Barklem et al. (2000)
6141.7157	Ba II	5678	21954	-0.032	0	0	0	Miles & Wiese (1969)	Miles & Wiese (1969)	Miles & Wiese (1969)	Miles & Wiese (1969)	Barklem & Aspelund-Johansson (2005); Barklem et al. (2000)
6141.7183	Ba II	5678	21954	-0.279	0	0	0	Miles & Wiese (1969)	Miles & Wiese (1969)	Miles & Wiese (1969)	Miles & Wiese (1969)	Barklem & Aspelund-Johansson (2005); Barklem et al. (2000)
6142.4832	Si	45320	61596	-1.54	7.9	-3.57	-7.13	Kurucz (2007)	Kurucz (2007)	Kurucz (2007)	Kurucz (2007)	Kurucz (2007)
6145.0159	Si	45296	61564	-1.48	7.92	-3.63	-7.13	Kurucz (2007)	Kurucz (2007)	Kurucz (2007)	Kurucz (2007)	Kurucz (2007)
6147.7341	Fe II	31366	47627	-2.69	8.5	-6.53	186.269	Kurucz (2013)	Kurucz (2013)	Kurucz (2013)	Kurucz (2013)	Barklem & Aspelund-Johansson (2005)
6151.6173	Fe	17550	33802	-3.28	8.29	-6.16	277.263	Kurucz (2007)	Kurucz (2007)	Kurucz (2007)	Kurucz (2007)	Barklem & Aspelund-Johansson (2005); Barklem et al. (2000)
6154.2255	Na	16953	33197	-1.57	7.85	-4.39	0	Ralchenko et al. (2010)	Kurucz & Peytremann (1975)	Kurucz & Peytremann (1975)	Kurucz & Peytremann (1975)	Kurucz & Peytremann (1975)
6156.778	O	86632	102867	-0.43	7.62	-3.96	1915.32	Ralchenko et al. (2010)	Wiese et al. (1966)	Wiese et al. (1966)	Wiese et al. (1966)	Barklem et al. (2000)
6159.3737	Fe	37166	53393	-1.83	8.33	-4.71	840.273	Kurucz (2007)	Kurucz (2007)	Kurucz (2007)	Kurucz (2007)	Barklem & Aspelund-Johansson (2005); Barklem et al. (2000)

TABLE F3 — *Continued*

Wavelength (Å)	Elem.	Lower χ_I (cm ⁻¹)	Upper χ_I (cm ⁻¹)	log(gf)	Rad. Damp.	Stark	Waals	Wavelength Ref	Lande Ref	Damp. Ref	Stark Ref	VDW Ref
6160.7471	Na	16969	33197	-1.27	7.85	-4.39	0	Ralchenko et al. (2010)	Kurucz & Peytremann (1975)	Kurucz & Peytremann (1975)	Kurucz & Peytremann (1975)	Kurucz & Peytremann (1975)
6165.3598	Fe	33415	49627	-1.46	8	-6.02	380.25	Kurucz (2007)	Kurucz (2007)	Kurucz (2007)	Kurucz (2007)	Barklem & Aspelund-Johansson (2005); Barklem et al. (2000)
6173.3343	Fe	17929	34125	-2.88	8.31	-6.16	281.266	Kurucz (2007)	Kurucz (2007)	Kurucz (2007)	Kurucz (2007)	Barklem & Aspelund-Johansson (2005); Barklem et al. (2000)
6175.3665	Ni	32980	49175	-0.55	8.44	-4.03	804.274	Kurucz (2008)	Kurucz (2008)	Kurucz (2008)	Kurucz (2008)	Barklem & Aspelund-Johansson (2005); Barklem et al. (2000)
6176.807	Ni	32971	49159	-0.26	8.21	-4.84	826.284	Wickliffe & Lawler (1997)	Kurucz (2008)	Kurucz (2008)	Kurucz (2008)	Barklem & Aspelund-Johansson (2005); Barklem et al. (2000)
6177.2415	Ni	14727	30915	-3.51	7.72	-6.12	-7.76	Kurucz (2008)	Kurucz (2008)	Kurucz (2008)	Kurucz (2008)	Kurucz (2008)
6200.3125	Fe	21043	37166	-2.44	8.08	-6.29	350.235	Kurucz (2007)	Kurucz (2007)	Kurucz (2007)	Kurucz (2007)	Barklem & Aspelund-Johansson (2005); Barklem et al. (2000)
6204.6	Ni	32971	49086	-1.11	8.28	-5.46	719.247	Wickliffe & Lawler (1997)	Kurucz (2008)	Kurucz (2008)	Kurucz (2008)	Barklem & Aspelund-Johansson (2005); Barklem et al. (2000)
6213.4294	Fe	17929	34020	-2.56	8.31	-6.16	280.265	Kurucz (2007)	Kurucz (2007)	Kurucz (2007)	Kurucz (2007)	Barklem & Aspelund-Johansson (2005); Barklem et al. (2000)
6220.7797	Fe	31310	47377	-2.46	7.8	-5.27	845.244	Kurucz (2007)	Kurucz (2007)	Kurucz (2007)	Kurucz (2007)	Barklem & Aspelund-Johansson (2005); Barklem et al. (2000)
6226.7342	Fe	31326	47377	-2.22	7.83	-5.27	845.244	Kurucz (2007)	Kurucz (2007)	Kurucz (2007)	Kurucz (2007)	Barklem & Aspelund-Johansson (2005); Barklem et al. (2000)
6238.3859	Fe II	31366	47393	-2.6	8.5	-6.53	186.271	Kurucz (2013)	Kurucz (2013)	Kurucz (2013)	Kurucz (2013)	Barklem & Aspelund-Johansson (2005); Barklem et al. (2000)
6240.6462	Fe	17929	33947	-3.23	6.81	-6.13	301.272	Kurucz (2007)	Kurucz (2007)	Kurucz (2007)	Kurucz (2007)	Barklem & Aspelund-Johansson (2005); Barklem et al. (2000)
6244.4655	Si	45296	61306	-1.36	7.91	-3.49	-7.13	Kurucz (2007)	Kurucz (2007)	Kurucz (2007)	Kurucz (2007)	Kurucz (2007)
6265.1323	Fe	17550	33504	-2.55	8.3	-6.16	274.261	Kurucz (2007)	Kurucz (2007)	Kurucz (2007)	Kurucz (2007)	Barklem & Aspelund-Johansson (2005); Barklem et al. (2000)

TABLE F3 — *Continued*

Wavelength (Å)	Elem.	Lower χ_I (cm ⁻¹)	Upper χ_I (cm ⁻¹)	log(gf)	Rad. Damp.	Stark	Waals	Wavelength Ref	Lande Ref	Damp. Ref	Stark Ref	VDW Ref
6271.2779	Fe	26874	42819	-2.7	8.22	-5.41	720.247	Kurucz (2007)	Kurucz (2007)	Kurucz (2007)	Kurucz (2007)	Barklem & Aspelund-Johansson (2005); Barklem et al. (2000)
6297.7926	Fe	17929	33802	-2.73	8.29	-6.16	278.264	Kurucz (2007)	Kurucz (2007)	Kurucz (2007)	Kurucz (2007)	Barklem & Aspelund-Johansson (2005); Barklem et al. (2000)
6318.717	Mg	41198	57023	-1.97	0	0	0	Ralchenko et al. (2010)	Kurucz & Peytremann (1975)	Kurucz & Peytremann (1975)	Kurucz & Peytremann (1975)	Kurucz & Peytremann (1975)
6322.685	Fe	20873	36690	-2.43	8.07	-6.09	345.238	Kurucz (2007)	Kurucz (2007)	Kurucz (2007)	Kurucz (2007)	Barklem & Aspelund-Johansson (2005); Barklem et al. (2000)
6330.091	Cr	7589	23390	-2.9	7.54	-6.12	308.241	Wallace & Hinkle (2009)	Kurucz (2010)	Kurucz (2010)	Kurucz (2010)	Barklem & Aspelund-Johansson (2005); Barklem et al. (2000)
6358.6967	Fe	6928	22648	-4	2.39	-6.2	223.253	Kurucz (2007)	Kurucz (2007)	Kurucz (2007)	Kurucz (2007)	Barklem & Aspelund-Johansson (2005); Barklem et al. (2000)
6362.338	Zn	46747	62459	0.14	0	0	0	Lambert et al. (1969)	Lambert et al. (1969)	Lambert et al. (1969)	Lambert et al. (1969)	Lambert et al. (1969)
6369.459	Fe II	23317	39013	-4.11	8.47	-6.53	169.204	Kurucz (2013)	Kurucz (2013)	Kurucz (2013)	Kurucz (2013)	Barklem & Aspelund-Johansson (2005); Barklem et al. (2000)
6378.247	Ni	33504	49175	-0.83	8.39	-4.87	825.283	Wickliffe & Lawler (1997)	Kurucz (2008)	Kurucz (2008)	Kurucz (2008)	Barklem & Aspelund-Johansson (2005); Barklem et al. (2000)
6380.7432	Fe	33762	49433	-1.27	7.88	-6.03	380.25	Kurucz (2007)	Kurucz (2007)	Kurucz (2007)	Kurucz (2007)	Barklem & Aspelund-Johansson (2005); Barklem et al. (2000)
6416.919	Fe II	31391	46965	-2.64	8.5	-6.53	185.276	Blackwell et al. (1980)	Kurucz (2013)	Kurucz (2013)	Kurucz (2013)	Barklem & Aspelund-Johansson (2005); Barklem et al. (2000)
6436.4059	Fe	33762	49296	-2.36	7.48	-6.03	-7.81	Kurucz (2007)	Kurucz (2007)	Kurucz (2007)	Kurucz (2007)	Kurucz (2007)
6446.407	Fe II	50191	65693	-1.97	8.64	-6.53	181.214	Kurucz (2013)	Kurucz (2013)	Kurucz (2013)	Kurucz (2013)	Barklem & Aspelund-Johansson (2005)
6456.3796	Fe II	31479	46965	-2.05	8.5	-6.53	185.276	Kurucz (2013)	Kurucz (2013)	Kurucz (2013)	Kurucz (2013)	Barklem & Aspelund-Johansson (2005); Barklem et al. (2000)
6494.4981	Fe	38174	53571	-1.46	8.41	-4.57	-7.51	Kurucz (2007)	Kurucz (2007)	Kurucz (2007)	Kurucz (2007)	Kurucz (2007)
6496.8848	Ba II	4871	20260	-1.143	0	0	0	Miles & Wiese (1969)	Miles & Wiese (1969)	Miles & Wiese (1969)	Miles & Wiese (1969)	Barklem & Aspelund-Johansson (2005); Barklem et al. (2000)

TABLE F3 — *Continued*

Wavelength (Å)	Elem.	Lower χ_I (cm ⁻¹)	Upper χ_I (cm ⁻¹)	log(gf)	Rad. Damp.	Stark	Waals	Wavelength Ref	Lande Ref	Damp. Ref	Stark Ref	VDW Ref
6496.8856	Ba II	4871	20260	-1.14	0	0	0	Miles & Wiese (1969)	Miles & Wiese (1969)	Miles & Wiese (1969)	Miles & Wiese (1969)	Barklem & Aspelund-Johansson (2005); Barklem et al. (2000)
6496.897	Ba II	4871	20260	-0.407	0	0	0	Miles & Wiese (1969)	Miles & Wiese (1969)	Miles & Wiese (1969)	Miles & Wiese (1969)	Barklem & Aspelund-Johansson (2005); Barklem et al. (2000)
6496.8976	Ba II	4871	20260	-0.407	0	0	0	Miles & Wiese (1969)	Miles & Wiese (1969)	Miles & Wiese (1969)	Miles & Wiese (1969)	Barklem & Aspelund-Johansson (2005); Barklem et al. (2000)
6496.8984	Ba II	4871	20260	-0.407	0	0	0	Miles & Wiese (1969)	Miles & Wiese (1969)	Miles & Wiese (1969)	Miles & Wiese (1969)	Barklem & Aspelund-Johansson (2005); Barklem et al. (2000)
6496.8999	Ba II	4871	20260	-0.503	0	0	0	Miles & Wiese (1969)	Miles & Wiese (1969)	Miles & Wiese (1969)	Miles & Wiese (1969)	Barklem & Aspelund-Johansson (2005); Barklem et al. (2000)
6496.9009	Ba II	4871	20260	-0.507	0	0	0	Miles & Wiese (1969)	Miles & Wiese (1969)	Miles & Wiese (1969)	Miles & Wiese (1969)	Barklem & Aspelund-Johansson (2005); Barklem et al. (2000)
6518.3657	Fe	22841	38174	-2.45	8.21	-5.91	336.251	Kurucz (2007)	Kurucz (2007)	Kurucz (2007)	Kurucz (2007)	Barklem & Aspelund-Johansson (2005); Barklem et al. (2000)
6574.2266	Fe	7984	23196	-5	4.22	-6.21	227.254	Kurucz (2007)	Kurucz (2007)	Kurucz (2007)	Kurucz (2007)	Barklem & Aspelund-Johansson (2005); Barklem et al. (2000)
6581.2092	Fe	11977	27164	-4.68	7.25	-6.15	254.245	Kurucz (2007)	Kurucz (2007)	Kurucz (2007)	Kurucz (2007)	Barklem & Aspelund-Johansson (2005); Barklem et al. (2000)
6587.61	C	68855	84034	-1	8.1	-3.44	1953.32	Ralchenko et al. (2010)	Kurucz (2010)	Kurucz (2010)	Kurucz (2010)	Barklem & Aspelund-Johansson (2005); Barklem et al. (2000)
6591.3128	Fe	37045	52216	-1.95	8.22	-5.75	276.262	Kurucz (2007)	Kurucz (2007)	Kurucz (2007)	Kurucz (2007)	Barklem & Aspelund-Johansson (2005); Barklem et al. (2000)
6608.025	Fe	18381	33504	-3.91	8.3	-6.16	306.242	Kurucz (2007)	Kurucz (2007)	Kurucz (2007)	Kurucz (2007)	Barklem & Aspelund-Johansson (2005); Barklem et al. (2000)
6625.0215	Fe	8154	23244	-5.34	4.06	-6.21	-7.83	Kurucz (2007)	Kurucz (2007)	Kurucz (2007)	Kurucz (2007)	Kurucz (2007)
6627.5438	Fe	36690	51772	-1.68	8.33	-5.34	754.209	Kurucz (2007)	Kurucz (2007)	Kurucz (2007)	Kurucz (2007)	Barklem & Aspelund-Johansson (2005); Barklem et al. (2000)

TABLE F3 — *Continued*

Wavelength (Å)	Elem.	Lower χ_I (cm ⁻¹)	Upper χ_I (cm ⁻¹)	log(gf)	Rad. Damp.	Stark	Waals	Wavelength Ref	Lande Ref	Damp. Ref	Stark Ref	VDW Ref
6643.6303	Ni	13517	28568	-2.03	8.1	-6.14	258.274	Kurucz (2008)	Kurucz (2008)	Kurucz (2008)	Kurucz (2008)	Barklem & Aspelund-Johansson (2005); Barklem et al. (2000)
6645.1006	Eu II	11130	26172	-0.625	0	0	0	Lawler et al. (2001)	Lawler et al. (2001)	Lawler et al. (2001)	Lawler et al. (2001)	Lawler et al. (2001)
6645.1205	Eu II	11130	26172	-0.693	0	0	0	Lawler et al. (2001)	Lawler et al. (2001)	Lawler et al. (2001)	Lawler et al. (2001)	Lawler et al. (2001)
6645.1366	Eu II	11130	26172	-0.773	0	0	0	Lawler et al. (2001)	Lawler et al. (2001)	Lawler et al. (2001)	Lawler et al. (2001)	Lawler et al. (2001)
6645.149	Eu II	11130	26172	-0.871	0	0	0	Lawler et al. (2001)	Lawler et al. (2001)	Lawler et al. (2001)	Lawler et al. (2001)	Lawler et al. (2001)
6687.5664	Y	0	14945	-0.67	6.05	-6.02	-7.74	Kurucz (2006)	Kurucz (2006)	Kurucz (2006)	Kurucz (2006)	Kurucz (2006)
6696.023	Al	25350	40279	-1.58	0	0	0	Wiese et al. (1969)	Wiese et al. (1969)	Wiese et al. (1969)	Wiese et al. (1969)	Wiese et al. (1969)
6698.673	Al	25350	40271	-1.63	0	0	0	Wiese et al. (1969)	Wiese et al. (1969)	Wiese et al. (1969)	Wiese et al. (1969)	Wiese et al. (1969)
6699.1413	Fe	37045	51966	-2.1	8.09	-5.63	297.273	Kurucz (2007)	Kurucz (2007)	Kurucz (2007)	Kurucz (2007)	Barklem & Aspelund-Johansson (2005); Barklem et al. (2000)
6703.566	Fe	22252	37166	-3.01	8.08	-6.28	320.264	Kurucz (2007)	Kurucz (2007)	Kurucz (2007)	Kurucz (2007)	Barklem & Aspelund-Johansson (2005); Barklem et al. (2000)
6705.1009	Fe	37157	52071	-1.39	8.4	-4.47	-7.48	Kurucz (2007)	Kurucz (2007)	Kurucz (2007)	Kurucz (2007)	Kurucz (2007)
6710.3181	Fe	11977	26874	-4.81	7.27	-6.15	252.246	Kurucz (2007)	Kurucz (2007)	Kurucz (2007)	Kurucz (2007)	Barklem & Aspelund-Johansson (2005); Barklem et al. (2000)
6713.7425	Fe	38682	53571	-1.39	8.41	-4.57	857.272	Kurucz (2007)	Kurucz (2007)	Kurucz (2007)	Kurucz (2007)	Barklem & Aspelund-Johansson (2005); Barklem et al. (2000)
6715.3818	Fe	37166	52046	-1.64	8.33	-5.57	777.208	Kurucz (2007)	Kurucz (2007)	Kurucz (2007)	Kurucz (2007)	Barklem et al. (2000)
6716.2363	Fe	36940	51829	-1.92	7.82	-5.37	274.26	Kurucz (2007)	Kurucz (2007)	Kurucz (2007)	Kurucz (2007)	Barklem & Aspelund-Johansson (2005); Barklem et al. (2000)
6721.8481	Si	47288	62161	-1.06	7.39	-3.1	-7.02	Kurucz (2007)	Kurucz (2007)	Kurucz (2007)	Kurucz (2007)	Kurucz (2007)
6725.3558	Fe	33092	47957	-2.17	8.4	-5.38	897.241	Kurucz (2007)	Kurucz (2007)	Kurucz (2007)	Kurucz (2007)	Barklem & Aspelund-Johansson (2005); Barklem et al. (2000)
6739.5204	Fe	12558	27398	-4.79	7.24	-6.15	256.244	Kurucz (2007)	Kurucz (2007)	Kurucz (2007)	Kurucz (2007)	Barklem & Aspelund-Johansson (2005); Barklem et al. (2000)
6750.1515	Fe	19550	34359	-2.62	6.69	-6.13	335.241	Kurucz (2007)	Kurucz (2007)	Kurucz (2007)	Kurucz (2007)	Barklem & Aspelund-Johansson (2005); Barklem et al. (2000)

TABLE F3 — *Continued*

Wavelength (Å)	Elem.	Lower χ_I (cm ⁻¹)	Upper χ_I (cm ⁻¹)	log(gf)	Rad. Damp.	Stark	Waals	Wavelength Ref	Lande Ref	Damp. Ref	Stark Ref	VDW Ref
6752.7066	Fe	37407	52216	-1.2	8.42	-5.47	778.274	Kurucz (2007)	Kurucz (2007)	Kurucz (2007)	Kurucz (2007)	Barklem & Aspelund-Johansson (2005); Barklem et al. (2000)
6772.3149	Ni	29503	44263	-0.97	8.28	-5.33	795.245	Kurucz (2008)	Kurucz (2008)	Kurucz (2008)	Kurucz (2008)	Barklem & Aspelund-Johansson (2005); Barklem et al. (2000)
6837.0056	Fe	37045	51667	-1.69	7.85	-6.12	273.258	Kurucz (2007)	Kurucz (2007)	Kurucz (2007)	Kurucz (2007)	Barklem & Aspelund-Johansson (2005); Barklem et al. (2000)
6857.2493	Fe	32875	47449	-2.04	7.23	-6.03	-7.82	Kurucz (2007)	Kurucz (2007)	Kurucz (2007)	Kurucz (2007)	Kurucz (2007)
6971.9322	Fe	24341	38682	-3.34	8.2	-5.89	381.239	Kurucz (2007)	Kurucz (2007)	Kurucz (2007)	Kurucz (2007)	Barklem et al. (2000)

TABLE F4
ANU LINE LIST

Wavelength (Å)	Species	χ_1 (eV)	$\log(gf)$
5067.14	26	4.22	-0.86
5090.77	26	4.26	-0.49
5109.65	26	4.3	-0.73
5127.36	26	0.91	-3.33
5132.66	26.1	2.81	-4.17
5141.74	26	2.42	-2.23
5145.09	26	2.2	-3.08
5187.91	26	4.14	-1.26
5197.58	26.1	3.23	-2.22
5198.71	26	2.22	-2.14
5234.62	26.1	3.22	-2.18
5242.49	26	3.63	-0.99
5243.77	26	4.26	-0.99
5253.46	26	3.28	-1.57
5264.8	26.1	3.23	-3.13
5288.52	26	3.69	-1.51
5386.33	26	4.15	-1.67
5389.48	26	4.41	-0.45
5409.13	26	4.37	-1.06
5414.07	26.1	3.22	-3.58
5425.26	26.1	3.2	-3.22
5432.95	26	4.45	-0.94
5441.34	26	4.31	-1.63
5464.28	26	4.14	-1.58
5472.71	26	4.21	-1.52
5491.83	26	4.18	-2.19
5522.45	26	4.21	-1.45
5525.54	26	4.23	-1.12
5543.94	26	4.22	-1.04
5546.51	26	4.37	-1.21
5554.89	26	4.55	-0.36
5560.21	26	4.43	-1.09
5584.76	26	3.57	-2.22
5618.63	26	4.21	-1.27
5633.95	26	4.99	-0.23
5635.82	26	4.26	-1.79
5638.26	26	4.22	-0.77
5650.71	26	5.09	-0.86
5651.47	26	4.47	-1.75
5653.87	26	4.39	-1.54
5661.35	26	4.28	-1.76
5679.02	26	4.65	-0.75
5696.09	26	4.55	-1.72
5701.54	26	2.56	-2.16
5705.46	26	4.3	-1.35
5731.76	26	4.26	-1.2
5775.08	26	4.22	-1.3
5778.45	26	2.59	-3.44
5793.91	26	4.22	-1.62
5806.73	26	4.61	-0.95
5809.22	26	3.88	-1.71
5852.22	26	4.55	-1.23
5855.08	26	4.61	-1.48
5856.09	26	4.29	-1.46
5859.59	26	4.55	-0.58
5905.67	26	4.65	-0.69
5916.25	26	2.45	-2.99
5927.79	26	4.65	-0.99
5929.68	26	4.55	-1.31
5930.18	26	4.65	-0.17
5934.65	26	3.93	-1.07
5956.69	26	0.86	-4.55
6003.01	26	3.88	-1.06
6027.05	26	4.08	-1.09
6056	26	4.73	-0.4
6079.01	26	4.65	-1.02
6084.09	26.1	3.2	-3.83
6085.26	26	2.76	-3.05
6093.64	26	4.61	-1.3
6127.91	26	4.14	-1.4
6149.24	26.1	3.89	-2.75
6151.62	26	2.18	-3.28
6157.72	26	4.07	-1.2

TABLE F4 — *Continued*

Wavelength (Å)	Species	χ_I (eV)	$\log(gf)$
6165.36	26	4.14	-1.46
6170.51	26	4.8	-0.38
6173.34	26	2.22	-2.88
6180.2	26	2.73	-2.63
6187.99	26	3.94	-1.62
6200.31	26	2.61	-2.42
6213.43	26	2.22	-2.52
6219.28	26	2.2	-2.43
6229.23	26	2.85	-2.83
6232.64	26	3.65	-1.22
6238.38	26.1	3.89	-2.63
6240.65	26	2.22	-3.29
6247.55	26.1	3.89	-2.38
6265.13	26	2.18	-2.55
6297.79	26	2.22	-2.71
6322.69	26	2.59	-2.43
6335.33	26	2.2	-2.26
6336.82	26	3.69	-0.93
6344.15	26	2.43	-2.92
6358.68	26	0.86	-4.24
6369.46	26.1	2.89	-4.11
6380.74	26	4.19	-1.32
6416.92	26.1	3.89	-2.75
6419.95	26	4.73	-0.24
6432.68	26.1	2.89	-3.57
6481.87	26	2.28	-2.98
6498.94	26	0.96	-4.7
6516.08	26.1	2.89	-3.31
6518.37	26	2.83	-2.45
6574.23	26	0.99	-5.01
6593.87	26	2.43	-2.39
6597.56	26	4.8	-0.97
6609.11	26	2.56	-2.68
6703.57	26	2.76	-3.02
6705.1	26	4.61	-0.98
6713.74	26	4.8	-1.4
6726.67	26	4.61	-1.03
6750.15	26	2.42	-2.62
6752.71	26	4.64	-1.22
6810.26	26	4.61	-0.99
6828.59	26	4.64	-0.82
6837.01	26	4.59	-1.69
6842.69	26	4.64	-1.22
6843.66	26	4.55	-0.83
6858.15	26	4.61	-0.94
7022.95	26	4.19	-1.15
7038.22	26	4.22	-1.2
7090.38	26	4.23	-1.11
—	—	—	—
5052.17	6	7.68	-1.3
5380.32	6	7.68	-1.61
6587.61	6	8.54	-1.02
6156.8	8	10.74	-0.43
5682.64	11	2.1	-0.77
5688.21	11	2.1	-0.48
6154.23	11	2.1	-1.55
6160.75	11	2.1	-1.25
5711.09	12	4.34	-1.73
6318.72	12	5.11	-1.95
5557.07	13	3.14	-2.21
6696.02	13	3.14	-1.48
6698.67	13	3.14	-1.78
5517.54	14	5.08	-2.5
5645.61	14	4.93	-2.04
5665.55	14	4.92	-1.94
5684.48	14	4.95	-1.55
5690.42	14	4.93	-1.77
5701.1	14	4.93	-1.95
5753.64	14	5.62	-1.33
5772.15	14	5.08	-1.65
5793.07	14	4.93	-1.96
5948.54	14	5.08	-1.21
6125.03	14	5.61	-1.51
6142.49	14	5.62	-1.54

TABLE F4 — *Continued*

Wavelength (Å)	Species	χ_i (eV)	$\log(gf)$
6145.02	14	5.61	-1.48
6237.33	14	5.61	-1.12
6243.82	14	5.62	-1.31
6244.48	14	5.61	-1.36
6527.21	14	5.87	-1.23
6721.84	14	5.86	-1.06
6741.64	14	5.98	-1.65
7034.9	14	5.87	-0.78
4633.26	24	3.12	-1.11
4708.02	24	3.17	0.09
4767.86	24	3.56	-0.6
5214.14	24	3.37	-0.78
5238.96	24	2.71	-1.43
5241.45	24	2.71	-1.92
5247.57	24	0.96	-1.62
5272.01	24	3.45	-0.42
5304.18	24	3.46	-0.68
5628.62	24	3.42	-0.76
5719.81	24	3.01	-1.62
5781.16	24	3.01	-1
5783.07	24	3.23	-0.48
5783.87	24	3.32	-0.29
5787.93	24	3.32	-0.08
6330.1	24	0.94	-2.9
6882.48	24	3.44	-0.38
6883	24	3.44	-0.42
5237.33	24.1	4.07	-1.09
5305.87	24.1	3.83	-1.97
5502.07	24.1	4.17	-2.05
5082.35	28	3.66	-0.59
5084.11	28	3.68	-0.06
5088.54	28	3.85	-1.04
5088.96	28	3.68	-1.29
5094.42	28	3.83	-1.07
5102.97	28	1.68	-2.66
5157.98	28	3.61	-1.51
5392.33	28	4.15	-1.32
5578.73	28	1.68	-2.57
5587.87	28	1.93	-2.44
5589.36	28	3.9	-1.15
5593.75	28	3.9	-0.78
5625.32	28	4.09	-0.73
5628.35	28	4.09	-1.32
5638.75	28	3.9	-1.7
5641.88	28	4.11	-1.02
5643.08	28	4.16	-1.23
5694.99	28	4.09	-0.63
5748.36	28	1.68	-3.24
5749.3	28	3.94	-2.11
5754.67	28	1.93	-1.85
5805.22	28	4.17	-0.62
5847.01	28	1.68	-3.41
5996.74	28	4.24	-1.01
6007.32	28	1.68	-3.41
6086.29	28	4.27	-0.46
6108.12	28	1.68	-2.43
6111.08	28	4.09	-0.81
6119.76	28	4.27	-1.32
6128.98	28	1.68	-3.36
6130.14	28	4.27	-0.94
6133.98	28	4.09	-1.91
6175.37	28	4.09	-0.55
6176.8	28	4.09	-0.26
6177.25	28	1.83	-3.51
6186.72	28	4.11	-0.88
6204.6	28	4.09	-1.1
6223.99	28	4.11	-1.05
6230.1	28	4.11	-1.13
6314.67	28	1.94	-2
6322.17	28	4.15	-1.21
6327.6	28	1.68	-3.06
6360.81	28	4.17	-1.15
6378.26	28	4.15	-0.97
6414.59	28	4.15	-1.18

TABLE F4 — *Continued*

Wavelength (Å)	Species	χ_I (eV)	$\log(gf)$
6482.81	28	1.93	-2.76
6598.61	28	4.24	-0.91
6635.13	28	4.42	-0.72
6643.64	28	1.68	-2.03
6767.78	28	1.83	-2.1
6772.32	28	3.66	-0.97
6842.04	28	3.66	-1.5
6362.35	30	5.8	0.14
4900.11	39.1	1.03	-0.09
5087.42	39.1	1.08	-0.17
5119.11	39.1	0.99	-1.36
5200.41	39.1	0.99	-0.57
5402.78	39.1	1.84	-0.63
5853.7	56.1	0.6	-0.91
6141.69	56.1	0.7	-0.08
6496.9	56.1	0.6	-0.38

* Break in the table (–) indicates the distinction between the iron and the non-iron lines.

TABLE F5
ASU LINE LIST

Wavelength (Å)	Species	χ_l (eV)	$\log(gf)$	$\delta\Gamma_6^{5/2}$
5380.34	6	7.68	-1.61	9.9
6587.62	6	8.54	-1	9.9
6156.8	8	10.7	-0.43	2.5
6154.23	11	2.1	-1.57	6.4
6318.72	12	5.11	-1.97	9.9
6696.03	13	3.14	-1.58	2.5
6698.67	13	3.14	-1.63	9.9
5793.08	14	4.93	-2.06	1.9
6125.03	14	5.61	-1.51	1.9
6142.48	14	5.62	-1.54	1.9
6145.01	14	5.61	-1.48	1.9
6244.48	14	5.61	-1.36	1.9
6721.84	14	5.86	-1.06	1.9
5300.75	24	0.98	-2.13	9.9
5783.89	24	3.32	-0.29	9.9
5787.93	24	3.32	-0.08	9.9
5305.87	24.1	3.83	-1.97	9.9
5141.75	26	2.42	-2.18	2.3
5247.06	26	0.09	-4.94	2.3
5358.12	26	3.3	-3.16	2.3
5412.79	26	4.44	-1.71	2.3
5522.45	26	4.21	-1.55	2.2
5543.94	26	4.22	-1.14	2.2
5560.21	26	4.43	-1.19	2.2
5577.03	26	5.03	-1.55	2.2
5651.47	26	4.47	-2	2.2
5653.87	26	4.39	-1.64	2.2
5661.35	26	4.28	-1.75	2.3
5741.85	26	4.26	-1.85	2.2
5752.03	26	4.55	-1.18	2.2
5778.45	26	2.59	-3.48	2.2
5784.66	26	3.4	-2.53	2.3
5809.22	26	3.88	-1.61	2.3
5849.69	26	3.7	-2.93	2.3
5852.23	26	4.55	-1.17	2.3
5855.09	26	4.61	-1.48	2.3
5856.1	26	4.29	-1.56	2.3
5858.79	26	4.22	-2.18	2.3
5859.6	26	4.55	-0.61	2.3
5862.37	26	4.55	-0.25	2.3
5956.7	26	0.86	-4.6	2.3
6005.54	26	2.59	-3.6	2.2
6027.05	26	4.07	-1.17	2.2
6085.26	26	2.76	-3.1	2.2
6105.13	26	4.55	-2.05	2.2
6151.62	26	2.18	-3.28	2.2
6157.73	26	4.08	-1.26	2.2
6159.37	26	4.61	-1.83	2.2
6165.36	26	4.14	-1.46	2.2
6173.34	26	2.22	-2.88	2.3
6200.32	26	2.61	-2.44	2.3
6213.44	26	2.22	-2.56	2.3
6220.78	26	3.88	-2.46	2.2
6226.73	26	3.88	-2.22	2.2
6240.65	26	2.22	-3.23	2.2
6265.14	26	2.18	-2.55	2.3
6271.28	26	3.33	-2.72	2.2
6297.8	26	2.22	-2.73	2.3
6322.69	26	2.59	-2.43	2.3
6358.69	26	0.86	-4	2.3
6380.74	26	4.19	-1.27	2.3
6436.41	26	4.19	-2.36	2.3
6481.88	26	2.28	-2.97	2.3
6494.5	26	4.73	-1.46	2.2
6498.95	26	0.96	-4.7	2.2
6581.21	26	1.48	-4.68	2.3
6591.33	26	4.59	-1.95	2.3
5234.62	26.1	3.22	-2.18	9.9
5425.26	26.1	3.2	-3.22	9.9
5991.38	26.1	3.15	-3.54	2.2
6084.11	26.1	3.2	-3.79	2.2
6149.25	26.1	3.89	-2.69	2.2
6238.39	26.1	3.89	-2.6	2.2

TABLE F5 — *Continued*

Wavelength (Å)	Species	χ_l (eV)	$\log(gf)$	$\delta\Gamma_6^{5/2}$
6247.56	26.1	3.89	-2.3	2.2
6369.46	26.1	2.89	-4.11	2.2
6416.92	26.1	3.89	-2.64	2.2
6432.68	26.1	2.89	-3.57	9.9
6442.95	26.1	5.55	-2.44	2.2
6446.4	26.1	6.22	-1.97	2.2
5082.35	28	3.66	-0.59	9.9
5088.54	28	3.85	-1.04	9.9
5088.96	28	3.68	-1.24	9.9
5094.42	28	3.83	-1.07	9.9
5115.4	28	3.83	-0.28	9.9
5847.01	28	1.68	-3.41	9.9
6111.08	28	4.09	-0.81	9.9
6130.14	28	4.27	-0.94	9.9
6175.37	28	4.09	-0.55	9.9
6176.8	28	4.09	-0.26	9.9
6177.25	28	1.82	-3.51	9.9
6204.61	28	4.09	-1.11	9.9
6378.26	28	4.15	-0.83	9.9
6643.64	28	1.68	-2.03	9.9
6772.32	28	3.66	-0.97	9.9
6687.5	39	0	-0.67	2.5
5087.43	39.1	1.08	-0.16	9.9
5200.42	39.1	0.99	-0.57	9.9
5402.78	39.1	1.84	-0.44	9.9
5853.69	56.1	0.6	-0.91	9.9
6141.73	56.1	0.7	-0.03	9.9
6496.91	56.1	0.6	-0.41	9.9

TABLE F6
CARNEGIE LINE LIST

Wavelength (Å)	Species	χ_i (eV)	$\log(gf)$
5234.625	26.1	3.221	-2.23
5284.098	26.1	2.891	-3.195
5307.361	26	1.608	-2.987
5322.041	26	2.279	-2.803
5325.559	26.1	3.221	-3.324
5412.784	26	4.435	-1.89
5414.046	26.1	3.221	-3.645
5425.247	26.1	3.199	-3.39
5466.988	26	3.573	-2.233
5491.829	26	4.186	-2.188
5522.447	26	4.209	-1.557
5536.583	26	2.832	-3.81
5539.284	26	3.642	-2.66
5560.207	26	4.435	-1.19
5577.031	26	5.033	-1.55
5607.664	26	4.154	-2.27
5611.361	26	3.635	-2.99
5618.633	26	4.209	-1.276
5633.947	26	4.991	-0.27
5635.823	26	4.256	-1.89
5636.696	26	3.64	-2.61
5638.262	26	4.22	-0.87
5661.363	26	4.284	-1.736
5691.497	26	4.301	-1.52
5698.023	26	3.64	-2.68
5705.476	26	4.301	-1.6
5712.134	26	3.417	-2.06
5753.122	26	4.26	-0.76
5760.345	26	3.642	-2.49
5778.453	26	2.588	-3.43
5784.66	26	3.397	-2.67
5793.913	26	4.22	-1.829
5807.782	26	3.292	-3.41
5809.217	26	3.884	-1.69
5811.917	26	4.143	-2.43
5814.805	26	4.283	-1.97
5837.7	26	4.294	-2.34
5838.37	26	3.943	-2.337
5849.682	26	3.695	-2.99
5853.149	26	1.485	-5.28
5855.076	26	4.608	-1.478
5856.084	26	4.294	-1.64
5861.107	26	4.283	-2.45
5916.246	26	2.453	-2.832
5991.368	26.1	3.153	-3.56
6024.058	26	4.548	-0.12
6027.051	26	4.076	-1.089
6056.005	26	4.733	-0.46
6079.009	26	4.652	-1.12
6084.099	26.1	3.199	-3.881
6120.25	26	0.915	-5.95
6127.904	26	4.143	-1.399
6149.246	26.1	3.889	-2.841
6151.617	26	2.176	-3.299
6165.36	26	4.142	-1.55
6173.334	26	2.223	-2.858
6180.203	26	2.728	-2.591
6200.312	26	2.609	-2.437
6232.64	26	3.654	-1.223
6247.577	26.1	3.892	-2.31
6271.282	26	3.332	-2.95
6311.5	26	2.832	-3.23
6322.685	26	2.588	-2.426
6393.601	26	2.433	-1.62
6416.921	26.1	3.891	-2.68
6432.682	26.1	2.891	-3.687
6456.383	26.1	3.903	-2.185
6481.87	26	2.279	-3.113
6518.366	26	2.832	-2.75
6593.871	26	2.437	-2.422
6597.561	26	4.795	-0.92
6609.11	26	2.559	-2.692
6699.153	26	4.593	-2.19

TABLE F6 — *Continued*

Wavelength (Å)	Species	χ_I (eV)	$\log(gf)$
6733.151	26	4.637	-1.349
6750.152	26	2.424	-2.621
6820.372	26	4.638	-1.17
6837.02	26	4.593	-1.81
6855.161	26	4.559	-0.741
6858.15	26	4.607	-1.046
7112.172	26	2.99	-3.09
—	—	—	—
6587.61	6	8.537	-1.12
7111.472	6	8.64	-1.13
7113.178	6	8.647	-0.81
7115.172	6	8.642	-0.71
6156.76	8	10.741	-0.477
6300.311	8	0	-9.77
6154.2	11	2.102	-1.53
6160.8	11	2.104	-1.23
6696.023	13	3.143	-1.32
6698.673	13	3.143	-1.62
6125.021	14	5.614	-1.54
6125.021	14	5.614	-1.54
6145.016	14	5.616	-1.42
6721.84	14	5.86	-1.14
6327.6	28	1.676	-3.113
6532.89	28	1.935	-3.39
6586.33	28	1.951	-2.81
6643.64	28	1.676	-2.3
6767.77	28	1.826	-2.17
6772.36	28	3.658	-0.98
6435.004	39	0.066	-0.82
6795.414	39.1	1.738	-1.14
6141.73	56.1	0.704	-0.077
6496.9	56.1	0.604	-0.38
6645.11	63.1	1.37	0.199

* Break in the table (—) indicates the distinction between the iron and the non-iron lines.

TABLE F7
GENEVA LINE LIST

Wavelength (Å)	Species	Lower χ_l (cm ⁻¹)	Upper χ_l (cm ⁻¹)	log(<i>gf</i>)
5052.1443	6	61985	81779	-1.304
6587.61	6	68857	84037	-1.021
6411.648	7	94796	110393	-2.014
5577.3386	8	15865	33795	-8.241
6158.1858	8	86634	102872	-0.296
6300.3038	8	0	15872	-9.715
6363.776	8	161	15875	-10.19
5688.205	11	16970	34550	-0.404
5688.205	11	16970	34550	-0.404
6154.2255	11	16954	33203	-1.547
6160.7471	11	16970	33202	-1.246
5528.4047	12	35053	53142	-0.498
5711.088	12	35053	52563	-1.724
6698.673	13	25350	40279	-1.87
5645.6128	14	39764	57477	-2.043
5665.5545	14	39683	57334	-1.94
5684.484	14	39957	57549	-1.553
5701.104	14	39764	57304	-1.953
5708.3995	14	39957	57476	-1.37
5772.146	14	40990	58315	-1.653
5780.3838	14	39683	56983	-2.25
5793.0726	14	39764	57026	-1.963
5797.8559	14	39957	57205	-1.95
5948.541	14	40990	57801	-1.13
6131.5729	14	45297	61606	-1.556
6131.8516	14	45297	61605	-1.615
6142.4832	14	45321	61601	-1.295
6155.6933	14	45321	61566	-2.252
6237.3191	14	45281	61313	-0.975
6244.4655	14	45297	61311	-1.093
6347.1087	14.1	65501	81257	0.169
6371.3714	14.1	65501	81197	-0.044
5260.387	20	20333	39344	-1.719
5261.704	20	20333	39339	-0.579
5512.98	20	23656	41796	-0.464
5581.965	20	20349	38265	-0.555
5588.749	20	20374	38267	0.358
5590.114	20	20333	38222	-0.571
5594.462	20	20349	38225	0.097
5601.277	20	20374	38227	-0.523
5857.451	20	23656	40729	0.24
5867.562	20	23656	40700	-1.57
6102.723	20	15155	31542	-0.793
6122.217	20	15211	31546	-0.316
6156.0231	20	20333	36578	-2.521
6161.297	20	20349	36580	-1.266
6162.173	20	15316	31545	-0.09
6163.755	20	20333	36557	-1.286
6166.439	20	20333	36550	-1.142
6169.042	20	20349	36560	-0.797
6439.075	20	20374	35904	0.39
6449.808	20	20333	35838	-0.502
6455.598	20	20349	35840	-1.29
6462.567	20	20349	35823	0.262
6471.662	20	20374	35826	-0.686
6493.781	20	20333	35733	-0.109
6499.65	20	20349	35735	-0.818
6572.779	20	0	15214	-4.24
5083.731	21	11614	31285	0.284
5356.091	21	15042	33713	0.168
5484.626	21	14929	33162	0.148
5520.497	21	15042	33157	0.293
5671.821	21	11679	29310	0.495
5686.847	21	11614	29199	0.376
6210.658	21	0	16101	-1.529
5239.813	21.1	11735	30820	-0.765
5318.349	21.1	10945	29748	-2.015
5334.24	21.1	12074	30821	-2.203
5526.79	21.1	14260	32354	0.024
5641.001	21.1	12098	29826	-1.131
5657.896	21.1	12155	29829	-0.603
5658.361	21.1	12074	29747	-1.208
5667.149	21.1	12098	29744	-1.309

TABLE F7 — *Continued*

Wavelength (Å)	Species	Lower χ_l (cm ⁻¹)	Upper χ_l (cm ⁻¹)	log(<i>gf</i>)
5669.042	21.1	12098	29738	-1.2
5684.202	21.1	12155	29748	-1.074
6245.6366	21.1	12155	28166	-1.022
6300.6977	21.1	12155	28026	-1.898
6320.8513	21.1	12098	27919	-1.816
6604.601	21.1	10945	26086	-1.309
5009.645	22	169	20131	-2.2
5062.1026	22	17421	37177	-0.39
5071.467	22	11775	31494	-0.99
5113.44	22	11638	31195	-0.7
5145.4596	22	11775	31211	-0.54
5147.478	22	0	19427	-1.94
5152.184	22	169	19579	-1.95
5173.742	22	0	19328	-1.06
5210.385	22	387	19580	-0.82
5219.701	22	169	19328	-2.22
5223.62	22	16873	36017	-0.49
5224.3	22	17212	36354	0.13
5230.968	22	18059	37176	-1.19
5247.29	22	16962	36020	-0.64
5282.3758	22	8493	27424	-1.81
5295.7752	22	8606	27489	-1.59
5300.0107	22	8493	27361	-2.3
5338.3054	22	6662	25395	-2.73
5384.6299	22	6662	25234	-2.77
5426.25	22	169	18598	-2.95
5429.1379	22	18914	37333	-0.55
5448.907	22	18825	37178	-1.25
5449.15	22	11638	29990	-1.87
5453.6425	22	11638	29975	-1.6
5460.4986	22	387	18700	-2.748
5465.7724	22	8606	26902	-2.91
5471.1926	22	11638	29916	-1.42
5474.2232	22	11775	30043	-1.23
5490.1479	22	11775	29990	-0.84
5490.846	22	387	18599	-3.35
5503.8953	22	20793	38962	-0.05
5511.7786	22	11775	29919	-1.6
5514.3433	22	11533	29668	-0.66
5514.5335	22	11638	29773	-0.5
5565.4728	22	18034	36003	-0.22
5648.5653	22	20123	37828	-0.161
5662.15	22	18696	36357	0.01
5689.46	22	18526	36103	-0.36
5702.66	22	18486	36022	-0.59
5716.45	22	18526	36020	-0.72
5739.4689	22	18139	35563	-0.61
5866.4512	22	8606	25652	-0.79
5953.1596	22	15220	32018	-0.273
5965.8281	22	15155	31918	-0.353
5978.5406	22	15107	31833	-0.44
6064.6262	22	8436	24926	-1.888
6091.1713	22	18285	34702	-0.32
6092.7924	22	15220	31633	-1.38
6098.6583	22	24697	41094	-0.01
6121.0011	22	15155	31493	-1.42
6126.216	22	8606	24929	-1.368
6258.1015	22	11638	27618	-0.39
6261.0975	22	11533	27505	-0.53
6303.7557	22	11638	27502	-1.58
6312.2359	22	11775	27618	-1.55
6336.0985	22	11638	27421	-1.69
6395.4717	22	12122	27759	-2.54
6497.6838	22	11638	27029	-2.02
6554.2229	22	11638	26896	-1.15
6556.0617	22	11775	27029	-1.06
5013.6861	22.1	12759	32705	-2.14
5069.0921	22.1	25197	44925	-1.62
5129.1562	22.1	15260	34757	-1.34
5185.9018	22.1	15268	34551	-1.41
5211.5304	22.1	20890	40078	-1.41
5336.771	22.1	12759	31498	-1.6
5381.015	22.1	12630	31215	-1.97
5418.751	22.1	12759	31214	-2.13

TABLE F7 — *Continued*

Wavelength (Å)	Species	Lower χ_l (cm ⁻¹)	Upper χ_l (cm ⁻¹)	log(<i>gf</i>)
5490.6928	22.1	12630	30843	-2.43
6606.9498	22.1	16623	31759	-2.79
6680.1346	22.1	24963	39933	-1.89
5240.8621	23	19148	38229	0.242
5349.465	23	24640	43334	-7.114
5592.9716	23	322	18202	-3.23
5604.9312	23	8412	26254	-1.28
5627.6326	23	8719	26488	-0.363
5632.4615	23	556	18311	-3.22
5646.1083	23	8477	26188	-1.19
5657.4351	23	8581	26258	-1.02
5668.3608	23	8719	26361	-1.03
5670.8527	23	8719	26353	-0.42
5703.575	23	8477	26010	-0.211
5727.048	23	8719	26180	-0.012
5727.6517	23	8477	25936	-0.87
5737.0589	23	8581	26012	-0.74
6002.2953	23	9824	26484	-1.78
6002.6233	23	8477	25136	-1.58
6039.7219	23	8581	25139	-0.65
6081.441	23	8477	24920	-0.579
6090.2139	23	8719	25139	-0.062
6111.6445	23	8412	24775	-0.715
6119.5233	23	8581	24923	-0.32
6135.3608	23	8477	24776	-0.746
6199.1967	23	2314	18446	-1.3
6213.8658	23	2427	18521	-1.925
6216.3542	23	2218	18305	-1.29
6242.8285	23	2113	18131	-1.55
6243.1053	23	2427	18445	-0.98
6245.2191	23	2113	18125	-2.005
6251.8273	23	2314	18310	-1.34
6256.8865	23	2218	18200	-2.01
6274.6488	23	2153	18091	-1.67
6285.1499	23	2218	18128	-1.51
6531.4146	23	9824	25135	-0.84
6565.8777	23	9541	24772	-2.07
5380.3252	23.1	69357	87943	-5.627
5200.173	24	27302	46533	-0.58
5206.037	24	7589	26798	0.02
5214.1314	24	27173	46352	-1.206
5238.961	24	21850	40938	-1.27
5241.459	24	21858	40937	-1.92
5243.354	24	27383	46455	-0.58
5247.565	24	7751	26808	-1.59
5272	24	27818	46787	-0.42
5287.178	24	27729	46644	-0.87
5296.691	24	7928	26808	-1.36
5298.272	24	7928	26803	-1.14
5300.745	24	7928	26794	-2
5304.18	24	27939	46793	-0.67
5312.856	24	27818	46641	-0.55
5318.771	24	27729	46531	-0.67
5329.1381	24	23503	42268	-0.064
5340.447	24	27729	46455	-0.73
5344.757	24	27818	46529	-0.99
5345.796	24	8097	26804	-0.95
5348.315	24	8097	26795	-1.21
5409.784	24	8307	26793	-0.67
5628.643	24	27600	45367	-0.74
5702.306	24	27818	45355	-0.67
5719.816	24	24302	41785	-1.58
5781.167	24	24285	41583	-1
5783.0635	24	26802	44094	-0.375
5787.918	24	26794	44072	-0.083
5788.382	24	24302	41578	-1.49
5838.669	24	24285	41413	-1.82
5844.595	24	24302	41412	-1.77
5982.8738	24	25552	42266	-1.734
6330.091	24	7589	23387	-2.787
6537.9212	24	8097	23393	-3.718
6630.0109	24	8307	23390	-3.56
5246.768	24.1	29956	49015	-2.466
5249.437	24.1	30311	49361	-2.489

TABLE F7 — *Continued*

Wavelength (Å)	Species	Lower χ_l (cm ⁻¹)	Upper χ_l (cm ⁻¹)	log(<i>gf</i>)
5305.8526	24.1	30867	49715	-2.363
5369.356	24.1	31222	49847	-3.045
5420.922	24.1	30311	48758	-2.458
5117.93	25	25277	44817	-1.204
5255.33	25	25269	44298	-0.858
5377.6073	25	31004	49600	-0.166
5394.6698	25	0	18537	-3.503
5399.4745	25	31077	49598	-0.345
5407.4172	25	17284	35778	-1.743
5420.3508	25	17284	35734	-1.462
5432.5392	25	0	18408	-3.795
5457.4568	25	17454	35778	-2.891
5516.7659	25	17567	35694	-1.847
6013.51	25	24777	41407	-0.354
6016.67	25	24785	41406	-0.181
6021.82	25	24802	41408	-0.054
6440.9342	25	30423	45949	-1.16
5054.6425	26	29359	49143	-1.921
5060.0784	26	0	19762	-5.431
5068.7657	26	23713	43442	-1.041
5079.2227	26	17728	37416	-2.068
5079.7397	26	7985	27671	-3.221
5083.3382	26	7726	27399	-2.939
5107.6407	26	12558	32137	-2.358
5127.3592	26	7380	26883	-3.306
5131.4684	26	17930	37418	-2.515
5141.7389	26	19551	39000	-1.978
5150.8392	26	7985	27399	-3.008
5151.9108	26	8154	27565	-3.322
5166.2819	26	0	19356	-4.192
5187.9142	26	33416	52692	-1.371
5194.9414	26	12558	31808	-2.021
5197.9358	26	34690	53929	-1.54
5198.7108	26	17930	37166	-2.135
5215.1803	26	26342	45517	-0.871
5216.2739	26	12969	32140	-2.082
5217.3893	26	25899	45066	-1.1
5223.1827	26	29318	48464	-1.783
5225.5261	26	887	20024	-4.789
5232.94	26	23713	42823	-0.07
5235.3867	26	32875	51977	-0.859
5236.2022	26	33763	52861	-1.497
5242.4907	26	29310	48386	-0.967
5247.0501	26	701	19760	-4.949
5250.2089	26	975	20023	-4.933
5250.6456	26	17728	36774	-2.18
5253.0211	26	18381	37418	-3.84
5253.4617	26	26479	45515	-1.573
5262.8809	26	26229	45231	-2.56
5263.3062	26	26342	45342	-0.879
5267.2693	26	35255	54240	-1.596
5273.1635	26	26552	45516	-0.993
5281.7897	26	24511	43445	-0.833
5288.5247	26	29802	48712	-1.508
5295.3121	26	35610	54495	-1.59
5300.403	26	37045	55912	-1.65
5302.3003	26	26479	45339	-0.72
5307.3607	26	12969	31811	-2.912
5321.1079	26	35771	54565	-1.089
5322.0407	26	18381	37172	-2.802
5324.1787	26	25899	44681	-0.103
5326.1424	26	28818	47594	-2.071
5339.9293	26	26342	45069	-0.667
5364.8709	26	35860	54500	0.228
5365.3987	26	28818	47457	-1.02
5367.4659	26	35610	54241	0.444
5369.9612	26	35255	53877	0.536
5379.5736	26	29802	48392	-1.514
5383.3685	26	34787	53363	0.632
5386.3331	26	33505	52070	-1.67
5389.4788	26	35610	54165	-0.41
5393.1672	26	26141	44683	-0.715
5395.2174	26	35860	54395	-2.07
5397.1279	26	7380	25908	-1.991

TABLE F7 — *Continued*

Wavelength (Å)	Species	Lower χ_l (cm ⁻¹)	Upper χ_l (cm ⁻¹)	log(<i>gf</i>)
5398.2791	26	35860	54385	-0.63
5401.2665	26	34843	53358	-1.782
5405.7746	26	7985	26484	-1.849
5410.9097	26	36078	54559	0.339
5412.7838	26	35771	54246	-1.716
5415.1989	26	35384	53851	0.643
5429.6964	26	7726	26144	-1.879
5434.5235	26	8154	26555	-2.121
5436.5878	26	18381	36776	-2.964
5445.042	26	35384	53750	-0.02
5455.6091	26	8154	26484	-2.093
5464.2796	26	33416	51717	-1.402
5466.3958	26	35255	53549	-0.63
5466.9871	26	28818	47110	-2.233
5472.7087	26	33948	52221	-1.495
5476.5642	26	33093	51353	-0.453
5481.243	26	33093	51338	-1.243
5483.0987	26	33505	51743	-1.406
5491.8315	26	33763	51972	-2.188
5501.4649	26	7726	25904	-3.046
5506.7787	26	7985	26144	-2.795
5522.4461	26	33948	52056	-1.45
5525.5436	26	34126	52224	-1.084
5543.9356	26	34021	52059	-1.04
5546.5058	26	35255	53285	-1.21
5560.2115	26	35771	53756	-1.09
5567.3911	26	21043	39005	-2.568
5569.618	26	27560	45515	-0.486
5572.8423	26	27399	45343	-0.275
5576.0888	26	27665	45599	-0.9
5577.0247	26	40594	58525	-1.543
5586.7555	26	27165	45065	-0.114
5600.2242	26	34360	52216	-1.42
5615.6438	26	26875	44682	0.05
5618.6323	26	33948	51746	-1.275
5636.6958	26	29359	47100	-2.51
5638.2621	26	34037	51773	-0.77
5646.6839	26	34360	52069	-3.618
5651.4689	26	36078	53772	-1.9
5652.3176	26	34360	52052	-1.85
5653.8651	26	35384	53071	-1.54
5658.8163	26	27399	45071	-0.807
5661.3447	26	34553	52217	-1.756
5662.5161	26	33698	51359	-0.573
5667.5179	26	33698	51343	-1.575
5678.3788	26	31327	48938	-3.241
5678.6006	26	19551	37161	-5.293
5679.0229	26	37521	55130	-0.82
5696.0892	26	36691	54247	-1.72
5701.5442	26	20640	38179	-2.193
5704.733	26	40594	58124	-1.409
5705.4642	26	34690	52218	-1.355
5731.7618	26	34327	51774	-1.2
5732.296	26	40256	57701	-1.46
5741.8477	26	34327	51744	-1.672
5752.0319	26	36691	54076	-1.177
5775.0805	26	34037	51353	-1.297
5778.4533	26	20874	38180	-3.43
5784.658	26	27399	44686	-2.532
5793.9147	26	34037	51297	-1.6
5811.9144	26	33416	50622	-2.33
5814.8071	26	34545	51743	-1.87
5835.1	26	34327	51465	-2.27
5845.2865	26	40594	57703	-2.424
5849.6833	26	29802	46898	-2.89
5853.1483	26	11977	29062	-5.18
5855.0758	26	37166	54246	-1.478
5856.0879	26	34634	51710	-1.327
5859.5863	26	36691	53757	-0.419
5861.1085	26	34545	51607	-2.304
5862.3564	26	36691	53749	-0.127
5905.6712	26	37521	54455	-0.69
5916.2473	26	19785	36688	-2.994
5927.7887	26	37521	54391	-0.99

TABLE F7 — *Continued*

Wavelength (Å)	Species	Lower χ_l (cm ⁻¹)	Upper χ_l (cm ⁻¹)	log(<i>gf</i>)
5929.6764	26	36691	53555	-1.31
5930.1799	26	37521	54385	-0.23
5956.694	26	6928	23716	-4.599
5969.5621	26	34545	51297	-2.789
6003.0111	26	31311	47969	-1.12
6012.2098	26	17930	34563	-4.038
6015.2435	26	17930	34554	-4.424
6019.3655	26	28818	45432	-3.31
6024.0575	26	36691	53291	-0.12
6027.0508	26	32875	49468	-1.089
6054.0733	26	35255	51773	-2.333
6056.0046	26	38175	54688	-0.46
6065.4821	26	21043	37530	-1.529
6078.491	26	38683	55135	-0.321
6079.0077	26	37521	53972	-1.02
6082.7101	26	17930	34370	-3.576
6093.6429	26	37166	53577	-1.4
6094.3728	26	37521	53930	-1.84
6096.6641	26	32133	48536	-1.83
6120.2464	26	7380	23719	-5.97
6127.9062	26	33416	49735	-1.399
6136.6149	26	19785	36081	-1.402
6136.9938	26	17728	34023	-2.95
6137.6913	26	20874	37167	-1.402
6151.6173	26	17551	33807	-3.295
6165.3598	26	33416	49636	-1.473
6173.3343	26	17930	34129	-2.88
6180.2026	26	22003	38184	-2.591
6187.3978	26	22842	39004	-4.148
6187.9892	26	31803	47963	-1.62
6191.5575	26	19623	35775	-1.416
6200.3125	26	21043	37172	-2.433
6213.4294	26	17930	34024	-2.481
6219.2805	26	17728	33807	-2.432
6226.7342	26	31327	47387	-2.12
6229.2259	26	22947	39000	-2.805
6230.7222	26	20640	36690	-1.281
6232.6403	26	29472	45517	-1.223
6240.6462	26	17930	33954	-3.23
6246.318	26	29060	45070	-0.779
6252.5549	26	19390	35383	-1.699
6265.1323	26	17551	33512	-2.55
6270.2234	26	23051	39000	-2.47
6271.2779	26	26875	42821	-2.703
6290.5431	26	20874	36771	-4.33
6297.7926	26	17930	33809	-2.737
6301.4999	26	29472	45341	-0.718
6311.4994	26	22842	38686	-3.141
6315.811	26	32875	48709	-1.61
6322.685	26	20874	36690	-2.43
6330.8478	26	38175	53971	-1.64
6335.3299	26	17728	33513	-2.177
6336.8234	26	29730	45511	-0.856
6344.1478	26	19623	35386	-2.919
6353.8362	26	7380	23119	-6.477
6355.0281	26	22947	38682	-2.34
6358.6967	26	6928	22655	-4.468
6380.7432	26	33763	49435	-1.375
6385.7176	26	38175	53835	-0.975
6392.5379	26	18381	34025	-4.682
6393.6004	26	19623	35264	-1.452
6400.0003	26	29060	44686	-0.29
6400.317	26	7380	23004	-4.318
6408.0174	26	29730	45336	-1.018
6421.3499	26	18381	33955	-2.012
6430.845	26	17551	33101	-2.005
6464.662	26	7726	23196	-6.636
6481.8698	26	18381	33809	-2.981
6494.9804	26	19390	34786	-1.268
6498.9383	26	7726	23114	-4.687
6518.3657	26	22842	38183	-2.438
6546.2381	26	22253	37529	-1.536
6574.2266	26	7985	23196	-5.004
6581.2092	26	11977	27172	-4.679

TABLE F7 — *Continued*

Wavelength (Å)	Species	Lower χ_l (cm ⁻¹)	Upper χ_l (cm ⁻¹)	log(<i>gf</i>)
6592.9124	26	22003	37171	-1.473
6593.8695	26	19623	34789	-2.42
6597.5592	26	38683	53840	-0.97
6609.1097	26	20640	35771	-2.691
6625.0215	26	8154	23249	-5.336
6627.5438	26	36691	51779	-1.58
6633.7487	26	36771	51846	-0.799
6648.0796	26	8154	23196	-5.918
6667.7103	26	36973	51971	-2.112
6699.1413	26	37045	51973	-2.101
5197.5675	26.1	26052	45292	-2.22
5234.6226	26.1	25979	45083	-2.18
5264.8024	26.1	26052	45046	-3.13
5316.6087	26.1	25431	44240	-1.87
5316.7812	26.1	25979	44788	-2.74
5325.5523	26.1	25979	44757	-3.16
5337.722	26.1	26052	44787	-3.72
5362.8613	26.1	25802	44449	-2.57
5414.0698	26.1	25979	44450	-3.58
5425.2485	26.1	25802	44235	-3.22
5427.8158	26.1	54233	72658	-1.581
5525.117	26.1	26350	44450	-3.97
5627.4888	26.1	27318	45088	-4.1
5991.3709	26.1	25431	42122	-3.647
6084.1017	26.1	25802	42238	-3.881
6149.2459	26.1	31367	47630	-2.841
6238.3859	26.1	31367	47397	-2.6
6369.459	26.1	23318	39018	-4.11
6432.6757	26.1	23318	38864	-3.57
6456.3796	26.1	31480	46969	-2.185
5176.076	27	16776	36096	-1.72
5212.6878	27	28342	47527	-0.11
5280.6258	27	29270	48208	-0.03
5287.5543	27	29294	48207	-1
5301.041	27	13792	32657	-1.94
5331.4532	27	14397	33154	-1.99
5352.0397	27	28843	47527	0.06
5369.5889	27	14034	32658	-1.59
5483.3535	27	13792	32029	-1.41
5483.9539	27	29294	47530	-0.48
5530.7752	27	13792	31873	-2.23
5590.738	27	16470	34357	-1.87
5647.2338	27	18389	36098	-1.56
6005.0264	27	13792	30445	-3.32
6093.1407	27	14034	30446	-2.44
6116.9902	27	14397	30745	-2.49
6188.9963	27	13792	29950	-2.45
6429.8966	27	17236	32789	-2.41
6454.9943	27	29294	44786	-0.25
6632.4394	27	18389	33467	-2
5003.7407	28	13518	33503	-2.8
5010.9381	28	29318	49275	-0.677
5084.0957	28	29673	49343	-0.084
5137.0738	28	13518	32984	-1.99
5157.976	28	29085	48472	-1.51
5424.5361	28	33609	52045	-1.151
5424.645	28	15736	34171	-2.77
5435.8576	28	16018	34415	-2.6
5476.9035	28	14728	32986	-0.89
5578.7183	28	13518	31443	-2.64
5587.8578	28	15607	33503	-2.14
5589.358	28	31440	49331	-0.938
5593.7355	28	31440	49317	-0.682
5625.3168	28	32980	50757	-0.549
5682.1987	28	33109	50709	-0.344
5748.3507	28	13518	30914	-3.242
5805.2166	28	33609	50836	-0.579
5846.9935	28	13518	30621	-3.21
6007.3098	28	13518	30164	-3.74
6086.2815	28	34408	50839	-0.41
6108.1158	28	13518	29890	-2.44
6111.0703	28	32972	49336	-0.865
6128.9731	28	13518	29834	-3.32
6175.3665	28	32980	49174	-0.389

TABLE F7 — *Continued*

Wavelength (Å)	Species	Lower χ_l (cm ⁻¹)	Upper χ_l (cm ⁻¹)	log(<i>gf</i>)
6176.807	28	32972	49162	-0.26
6186.7109	28	33109	49273	-0.88
6191.1783	28	13518	29670	-2.939
6204.6	28	32972	49090	-1.1
6223.981	28	33109	49177	-0.91
6327.5985	28	13518	29322	-3.15
6378.247	28	33505	49183	-0.83
6414.581	28	33505	49094	-1.18
6482.7983	28	15607	31032	-2.63
6532.873	28	15607	30914	-3.357
5105.537	29	11203	30790	-1.516
5153.2307	29	30536	49942	-0.016
5218.1975	29	30786	49951	0.264
5220.0659	29	30786	49944	-0.616
5700.2373	29	13243	30787	-2.33
5782.1269	29	13243	30538	-1.781
6362.338	30	46748	62466	0.14
5256.893	38	18317	37340	0.23
5087.416	39.1	8743	28400	-0.17
5119.112	39.1	8001	27536	-1.36
5200.406	39.1	8001	27230	-0.57
5289.815	39.1	8331	27236	-1.85
5402.774	39.1	14832	33342	-0.63
5544.611	39.1	14018	32054	-1.09
5728.8865	39.1	14832	32288	-1.15
5046.58	40	12340	32156	0.06
5385.14	40	4186	22756	-0.71
6127.44	40	1242	17562	-1.06
6134.55	40	0	16301	-1.28
6140.46	40	4186	20471	-1.41
6143.2	40	572	16851	-1.1
6445.74	40	8057	23572	-0.83
5112.27	40.1	13429	32990	-0.85
5350.35	40.1	14300	32991	-1.16
5095.293	41	693	20320	-1.048
5318.598	41	1588	20391	-1.085
5437.256	41	5299	23691	-1.108
5533.031	42	10767	28841	-0.069
5570.444	42	10767	28720	-0.337
5751.408	42	11453	28840	-1.014
5858.266	42	11856	28926	-0.996
6030.644	42	12348	28930	-0.523
5853.668	56.1	4871	21955	-0.907
6141.713	56.1	5678	21960	-0.032
6496.897	56.1	4871	20264	-0.407
5122.99	57.1	2589	22109	-0.85
5303.53	57.1	2589	21444	-1.35
5936.21	57.1	1395	18241	-2.036
6390.48	57.1	2589	18237	-1.41
5187.458	58.1	9775	29053	0.17
5274.229	58.1	8420	27381	0.13
5330.556	58.1	7009	25769	-0.4
6043.373	58.1	9727	26274	-0.48
6169.563	58.1	32883	49092	-3.22
5219.045	59.1	6412	25573	-0.053
5220.1079	59.1	6420	25577	0.298
5259.7279	59.1	5105	24118	0.114
5292.6194	59.1	5226	24121	-0.257
5322.771	59.1	3895	22683	-0.141
5092.79	60.1	3064	22701	-0.61
5130.59	60.1	10517	30009	0.45
5132.33	60.1	4508	23993	-0.71
5143.34	60.1	1467	20911	-1.57
5212.36	60.1	1653	20839	-0.96
5250.81	60.1	6008	25054	-0.72
5276.869	60.1	6928	25879	-0.44
5293.16	60.1	6638	25530	0.1
5306.46	60.1	6928	25773	-0.97
5311.45	60.1	7952	26780	-0.42
5319.81	60.1	4436	23234	-0.14
5356.97	60.1	10195	28862	-0.28
5361.17	60.1	4508	23161	-1.48
5431.52	60.1	9041	27453	-0.47
5485.7	60.1	10195	28424	-0.12

TABLE F7 — *Continued*

Wavelength (Å)	Species	Lower χ_l (cm ⁻¹)	Upper χ_l (cm ⁻¹)	$\log(gf)$
5533.82	60.1	4508	22579	-1.23
5548.45	60.1	4436	22459	-1.27
5618.99	60.1	14300	32097	-0.65
5740.86	60.1	9356	26775	-0.53
5811.57	60.1	6928	24135	-0.86
6365.54	60.1	7525	23235	-1.2
6637.19	60.1	11711	26778	-0.84
5818.746	63.1	9920	27107	-1.25
6049.51	63.1	10316	26846	-0.8
6173.029	63.1	10646	26846	-0.86
6437.64	63.1	10646	26180	-0.32
6645.094	63.1	11130	26179	0.12
6598.5978	69.1	38586	53741	-1.54

TABLE F8
PORTO LINE LIST

Wavelength (Å)	Species	χ_1 (eV)	$\log(gf)$
5247.06	26	0.09	-4.941
5855.08	26	4.61	-1.531
6056.01	26	4.73	-0.489
6200.32	26	2.61	-2.397
6733.15	26	4.64	-1.429
6750.16	26	2.42	-2.615
4523.40	26	3.65	-1.871
4531.62	26	3.21	-1.801
4537.67	26	3.27	-2.870
4551.65	26	3.94	-1.928
4554.46	26	2.87	-2.752
4556.93	26	3.25	-2.644
4561.41	26	2.76	-2.879
4566.52	26	3.30	-2.156
4574.22	26	3.21	-2.353
4574.72	26	2.28	-2.823
4579.33	26	2.83	-3.024
4593.53	26	3.94	-1.921
4596.41	26	3.65	-2.090
4602.00	26	1.61	-3.163
4602.95	26	1.49	-2.291
4607.65	26	3.98	-0.754
4625.05	26	3.24	-1.222
4630.12	26	2.28	-2.488
4631.49	26	4.55	-1.890
4635.85	26	2.85	-2.384
4661.54	26	4.56	-1.186
4690.14	26	3.69	-1.550
4741.53	26	2.83	-2.027
4749.95	26	4.56	-1.236
4757.58	26	3.27	-1.988
4772.82	26	1.56	-2.752
4779.44	26	3.42	-2.162
4780.81	26	3.25	-3.236
4787.83	26	3.00	-2.532
4788.76	26	3.24	-1.791
4789.65	26	3.55	-1.171
4793.97	26	3.05	-3.464
4794.36	26	2.42	-3.892
4799.41	26	3.64	-2.073
4802.52	26	4.61	-1.714
4802.88	26	3.69	-1.527
4808.15	26	3.25	-2.630
4809.94	26	3.57	-2.542
4811.05	26	3.07	-3.182
4885.43	26	3.88	-1.136
4905.14	26	3.93	-1.818
4924.77	26	2.28	-2.058
4946.39	26	3.37	-1.049
4952.65	26	4.21	-1.184
4961.92	26	3.63	-2.301
4962.58	26	4.18	-1.209
4967.90	26	4.19	-0.720
4993.70	26	4.21	-1.138
4994.14	26	0.92	-3.171
5049.82	26	2.28	-1.432
5044.22	26	2.85	-2.038
5054.65	26	3.64	-1.992
5067.15	26	4.22	-0.860
5068.77	26	2.94	-1.074
5072.68	26	4.22	-0.983
5074.76	26	4.22	-0.229
5083.34	26	0.96	-3.047
5088.15	26	4.15	-1.554
5090.78	26	4.26	-0.514
5107.45	26	0.99	-3.151
5107.65	26	1.56	-2.600
5109.65	26	4.30	-0.736
5127.36	26	0.92	-3.317
5129.63	26	3.94	-1.469
5141.74	26	2.42	-2.125
5143.73	26	2.20	-3.811
5151.91	26	1.01	-3.155

TABLE F8 — *Continued*

Wavelength (Å)	Species	χ_1 (eV)	$\log(gf)$
5159.06	26	4.28	-0.846
5180.06	26	4.47	-1.105
5187.91	26	4.14	-1.202
5194.95	26	1.56	-2.333
5195.48	26	4.22	-0.441
5196.06	26	4.26	-0.827
5197.94	26	4.30	-1.491
5198.72	26	2.22	-2.164
5217.40	26	3.21	-1.082
5223.19	26	3.63	-2.252
5225.53	26	0.11	-4.773
5228.38	26	4.22	-1.095
5229.86	26	3.28	-0.935
5242.50	26	3.63	-1.124
5243.78	26	4.26	-1.022
5250.21	26	0.12	-4.807
5253.02	26	2.28	-3.855
5253.47	26	3.28	-1.591
5263.31	26	3.27	-0.864
5288.53	26	3.69	-1.612
5293.96	26	4.14	-1.747
5294.55	26	3.64	-2.627
5295.32	26	4.42	-1.518
5361.62	26	4.42	-1.205
5373.71	26	4.47	-0.841
5376.83	26	4.29	-2.040
5379.58	26	3.69	-1.552
5386.34	26	4.15	-1.709
5389.48	26	4.42	-0.534
5395.22	26	4.45	-1.724
5398.28	26	4.45	-0.684
5401.27	26	4.32	-1.712
5406.78	26	4.37	-1.429
5409.14	26	4.37	-1.051
5417.04	26	4.42	-1.404
5432.95	26	4.45	-0.729
5436.30	26	4.39	-1.319
5436.59	26	2.28	-3.267
5441.34	26	4.31	-1.558
5461.55	26	4.45	-1.570
5464.28	26	4.14	-1.595
5466.99	26	3.65	-2.141
5473.17	26	4.19	-1.986
5481.25	26	4.10	-1.203
5491.83	26	4.19	-2.195
5522.45	26	4.21	-1.419
5534.66	26	4.15	-2.391
5538.52	26	3.63	-2.090
5543.94	26	4.22	-1.070
5546.51	26	4.37	-1.124
5547.00	26	4.22	-1.741
5553.58	26	4.43	-1.321
5560.22	26	4.43	-1.064
5567.40	26	2.61	-2.594
5577.03	26	5.03	-1.485
5584.77	26	3.57	-2.189
5587.58	26	4.14	-1.656
5594.66	26	4.55	-0.858
5618.64	26	4.21	-1.298
5619.60	26	4.39	-1.435
5633.95	26	4.99	-0.385
5635.83	26	4.26	-1.556
5636.70	26	3.64	-2.511
5638.27	26	4.22	-0.809
5641.44	26	4.26	-0.969
5649.99	26	5.10	-0.785
5651.47	26	4.47	-1.763
5652.32	26	4.26	-1.751
5653.87	26	4.39	-1.402
5661.35	26	4.28	-1.828
5662.52	26	4.18	-0.601
5667.52	26	4.18	-1.292
5679.03	26	4.65	-0.756
5680.24	26	4.19	-2.330

TABLE F8 — *Continued*

Wavelength (Å)	Species	χ_I (eV)	$\log(gf)$
5701.55	26	2.56	-2.162
5715.09	26	4.28	-0.847
5720.90	26	4.55	-1.805
5731.77	26	4.26	-1.124
5738.24	26	4.22	-2.164
5741.85	26	4.26	-1.626
5752.04	26	4.55	-0.917
5775.08	26	4.22	-1.124
5778.46	26	4.15	-1.967
5793.92	26	4.22	-1.622
5806.73	26	4.61	-0.877
5809.22	26	3.88	-1.614
5811.92	26	4.14	-2.333
5814.81	26	4.28	-1.820
5815.22	26	4.15	-2.364
5827.88	26	3.28	-3.147
5852.22	26	4.55	-1.190
5853.15	26	1.49	-5.130
5856.09	26	4.29	-1.572
5862.36	26	4.55	-0.404
5902.48	26	4.59	-1.797
5905.68	26	4.65	-0.775
5916.26	26	2.45	-2.920
5927.79	26	4.65	-1.057
5929.68	26	4.55	-1.211
5930.19	26	4.65	-0.326
5934.66	26	3.93	-1.091
5956.70	26	0.86	-4.526
5983.69	26	4.55	-0.719
5984.82	26	4.73	-0.335
5987.07	26	4.79	-0.478
6005.55	26	2.59	-3.479
6024.06	26	4.55	-0.124
6027.06	26	4.08	-1.178
6034.04	26	4.31	-2.306
6035.34	26	4.29	-2.476
6054.08	26	4.37	-2.237
6065.49	26	2.61	-1.616
6078.49	26	4.79	-0.364
6079.01	26	4.65	-1.008
6082.72	26	2.22	-3.566
6089.57	26	4.58	-1.273
6094.38	26	4.65	-1.566
6096.67	26	3.98	-1.776
6098.25	26	4.56	-1.755
6120.25	26	0.92	-5.894
6127.91	26	4.14	-1.417
6151.62	26	2.18	-3.298
6157.73	26	4.08	-1.238
6159.38	26	4.61	-1.878
6165.36	26	4.14	-1.502
6173.34	26	2.22	-2.877
6180.21	26	2.73	-2.632
6187.99	26	3.94	-1.620
6213.44	26	2.22	-2.580
6219.29	26	2.20	-2.463
6220.79	26	3.88	-2.330
6226.74	26	3.88	-2.069
6229.24	26	2.85	-2.866
6232.65	26	3.65	-1.240
6240.65	26	2.22	-3.292
6265.14	26	2.18	-2.559
6270.23	26	2.86	-2.573
6290.98	26	4.73	-0.576
6297.80	26	2.22	-2.777
6303.46	26	4.32	-2.492
6315.81	26	4.08	-1.645
6322.69	26	2.59	-2.368
6335.34	26	2.20	-2.339
6336.83	26	3.69	-0.858
6358.68	26	0.86	-3.907
6380.75	26	4.19	-1.322
6385.72	26	4.73	-1.828
6392.54	26	2.28	-3.942

TABLE F8 — *Continued*

Wavelength (Å)	Species	χ_I (eV)	$\log(gf)$
6430.85	26	2.18	-2.127
6481.88	26	2.28	-2.929
6498.94	26	0.96	-4.627
6581.21	26	1.49	-4.706
6593.88	26	2.43	-2.384
6608.03	26	2.28	-3.967
6609.12	26	2.56	-2.632
6625.02	26	1.01	-5.284
6627.55	26	4.55	-1.475
6646.94	26	2.61	-3.915
6653.86	26	4.15	-2.407
6699.15	26	4.59	-2.106
6703.57	26	2.76	-3.022
6705.11	26	4.61	-1.057
6710.32	26	1.49	-4.810
6713.05	26	4.61	-1.514
6713.20	26	4.14	-2.438
6713.74	26	4.79	-1.425
6725.36	26	4.10	-2.187
6726.67	26	4.61	-1.045
6732.07	26	4.58	-2.144
6739.52	26	1.56	-4.902
6745.11	26	4.58	-2.094
6745.97	26	4.08	-2.657
6752.71	26	4.64	-1.234
6786.86	26	4.19	-1.886
6793.26	26	4.58	-1.901
6806.85	26	2.73	-3.103
6810.27	26	4.61	-0.995
6820.37	26	4.64	-1.134
6828.60	26	3.57	-1.871
6833.23	26	4.64	-1.975
6837.01	26	4.59	-1.732
6839.84	26	2.56	-3.377
6842.69	26	4.64	-1.169
6843.66	26	4.55	-0.867
6855.72	26	4.61	-1.674
6857.25	26	4.08	-2.075
6858.15	26	4.61	-0.972
6861.94	26	2.42	-3.795
6862.50	26	4.56	-1.437
6864.32	26	4.56	-2.229
4508.28	26.1	2.86	-2.403
4520.22	26.1	2.81	-2.563
4534.17	26.1	2.86	-3.203
4541.52	26.1	2.86	-2.762
4576.34	26.1	2.84	-2.947
4620.51	26.1	2.83	-3.234
4629.34	26.1	2.81	-2.262
4656.98	26.1	2.89	-3.676
4670.17	26.1	2.58	-4.011
4923.93	26.1	2.89	-1.541
5132.67	26.1	2.81	-4.008
5197.57	26.1	3.23	-2.293
5234.63	26.1	3.22	-2.235
5256.94	26.1	2.89	-4.019
5264.81	26.1	3.23	-3.091
5284.11	26.1	2.89	-3.132
5414.07	26.1	3.22	-3.568
5425.25	26.1	3.20	-3.234
5427.81	26.1	6.72	-1.481
5525.12	26.1	3.27	-4.000
5534.85	26.1	3.25	-2.792
5991.38	26.1	3.15	-3.539
6084.11	26.1	3.20	-3.774
6113.32	26.1	3.22	-4.108
6149.25	26.1	3.89	-2.719
6238.39	26.1	3.89	-2.526
6239.94	26.1	3.89	-3.448
6247.56	26.1	3.89	-2.347
6369.46	26.1	2.89	-4.131
6407.29	26.1	3.89	-2.899
6416.93	26.1	3.89	-2.625
6432.69	26.1	2.89	-3.572

TABLE F8 — *Continued*

Wavelength (Å)	Species	χ_I (eV)	$\log(gf)$
6442.97	26.1	5.55	-2.399
6456.39	26.1	3.90	-2.11
6516.09	26.1	2.89	-3.279
—	—	—	—
5052.15	6	7.68	-1.303
5081.11	28	3.85	0.064
5094.41	28	3.83	-1.108
5122.12	24	1.03	-3.166
5214.14	24	3.37	-0.784
5238.97	24	2.71	-1.427
5247.57	24	0.96	-1.618
5287.18	24	3.44	-0.954
5348.33	24	1	-1.229
5380.32	6	7.68	-1.616
5392.33	28	4.15	-1.354
5435.86	28	1.99	-2.432
5462.5	28	3.85	-0.88
5480.51	24	3.45	-0.997
5517.54	14	5.08	-2.496
5587.87	28	1.93	-2.479
5589.36	28	3.9	-1.148
5625.32	28	4.09	-0.731
5628.35	28	4.09	-1.316
5638.75	28	3.9	-1.699
5641.88	28	4.11	-1.017
5643.08	28	4.16	-1.234
5645.61	14	4.93	-2.068
5684.49	14	4.95	-1.642
5694.99	28	4.09	-0.629
5701.11	14	4.93	-2.034
5711.09	12	4.35	-1.777
5748.36	28	1.68	-3.279
5753.64	14	5.62	-1.333
5772.15	14	5.08	-1.669
5781.18	24	3.32	-0.886
5783.07	24	3.32	-0.472
5787.92	24	3.32	-0.183
5797.87	14	4.95	-1.912
5805.22	28	4.17	-0.604
5847	28	1.68	-3.41
5853.69	56.1	0.6	-0.91
5948.54	14	5.08	-1.208
5996.73	28	4.24	-1.01
6086.29	28	4.27	-0.471
6108.12	28	1.68	-2.512
6111.08	28	4.09	-0.823
6119.76	28	4.27	-1.316
6125.02	14	5.61	-1.555
6128.98	28	1.68	-3.368
6130.14	28	4.27	-0.938
6141.73	56.1	0.7	-0.03
6142.49	14	5.62	-1.52
6145.02	14	5.62	-1.425
6154.23	11	2.1	-1.622
6158.17	8	10.74	-0.296
6160.75	11	2.1	-1.363
6175.37	28	4.09	-0.534
6176.82	28	4.09	-0.266
6177.25	28	1.83	-3.538
6186.72	28	4.11	-0.888
6195.46	14	5.87	-1.666
6204.61	28	4.09	-1.112
6223.99	28	4.11	-0.954
6230.1	28	4.11	-1.132
6237.33	14	5.61	-1.116
6243.82	14	5.62	-1.331
6244.48	14	5.62	-1.31
6300.304	8	0	-9.717
6319.24	12	5.11	-2.3
6322.17	28	4.15	-1.164
6327.6	28	1.68	-3.086
6360.81	28	4.17	-1.145
6362.35	30	5.79	0.14
6378.26	28	4.15	-0.83

TABLE F8 — *Continued*

Wavelength (Å)	Species	χ_I (eV)	$\log(gf)$
6496.91	56.1	0.6	-0.41
6527.21	14	5.87	-1.227
6587.62	6	8.54	-1.086
6598.6	28	4.24	-0.914
6635.13	28	4.42	-0.779
6645.13	63.1	1.38	0.2
6696.03	13	3.14	-1.571
6698.67	13	3.14	-1.886
6721.85	14	5.86	-1.156
6741.63	14	5.98	-1.625
6767.78	28	1.83	-2.136
6772.32	28	3.66	-0.963
6842.04	28	3.66	-1.496
6882.52	24	3.44	-0.392

TABLE F9
UPPSALA LINE LIST

Element	Wavelength (Å)
Al	5557.063
Al	6696.023
Al	6698.673
Ba	5853.669
Ba	6141.715
Ba	6496.898
C	5052.145
C	5380.325
C	6587.610
Ca	5261.704
Ca	5349.465
Ca	5512.980
Ca	5588.749
Ca	5590.114
Ca	5601.277
Ca	5857.451
Ca	5867.562
Ca	6102.723
Ca	6122.217
Ca	6156.023
Ca	6162.173
Ca	6166.439
Ca	6169.042
Ca	6169.563
Ca	6439.075
Ca	6449.808
Ca	6455.598
Ca	6471.662
Ca	6493.781
Ca	6499.650
Co	5212.646
Co	5301.022
Co	5325.328
Co	5331.412
Co	5352.051
Co	5359.245
Co	5483.310
Co	5483.876
Co	5523.241
Co	5647.207
Co	6093.121
Co	6188.938
Co	6429.914
Co	6455.040
Co	6632.406
Co	6771.092
Co	6814.918
Cr	5200.172
Cr	5214.131
Cr	5237.329
Cr	5238.961
Cr	5241.458
Cr	5279.876
Cr	5296.691
Cr	5300.745
Cr	5304.180
Cr	5305.853
Cr	5310.687
Cr	5312.856
Cr	5313.563
Cr	5318.771
Cr	5340.447
Cr	5344.756
Cr	5345.796
Cr	5348.314
Cr	5409.784
Cr	5420.922
Cr	5480.507
Cr	5502.067
Cr	5628.642
Cr	5642.359
Cr	5648.261
Cr	5702.306

TABLE F9 — *Continued*

Element	Wavelength (Å)
Cr	5719.815
Cr	5838.669
Cr	5844.595
Cr	5982.872
Cr	6129.226
Cr	6330.091
Cr	6501.185
Cr	6537.921
Cr	6661.075
Cr	6669.281
Cu	5218.192
Cu	5220.061
Cu	5700.268
Eu	6645.060
Fe	5060.079
Fe	5068.766
Fe	5083.338
Fe	5123.720
Fe	5127.359
Fe	5194.941
Fe	5216.274
Fe	5217.389
Fe	5225.526
Fe	5232.940
Fe	5234.625
Fe	5242.491
Fe	5247.050
Fe	5264.625
Fe	5269.537
Fe	5281.790
Fe	5284.103
Fe	5302.300
Fe	5307.361
Fe	5324.179
Fe	5325.553
Fe	5339.929
Fe	5364.871
Fe	5365.399
Fe	5367.467
Fe	5369.961
Fe	5383.369
Fe	5393.167
Fe	5398.279
Fe	5405.774
Fe	5414.073
Fe	5415.199
Fe	5424.068
Fe	5425.257
Fe	5434.523
Fe	5441.339
Fe	5445.042
Fe	5501.465
Fe	5506.779
Fe	5534.838
Fe	5543.936
Fe	5560.212
Fe	5569.618
Fe	5572.842
Fe	5576.089
Fe	5586.755
Fe	5615.644
Fe	5638.262
Fe	5651.469
Fe	5661.346
Fe	5679.023
Fe	5705.465
Fe	5731.762
Fe	5732.296
Fe	5741.848
Fe	5855.080
Fe	5856.090
Fe	5991.380
Fe	6003.011
Fe	6027.050

TABLE F9 — *Continued*

Element	Wavelength (Å)
Fe	6056.004
Fe	6065.482
Fe	6084.110
Fe	6136.990
Fe	6149.260
Fe	6151.620
Fe	6165.360
Fe	6173.330
Fe	6200.312
Fe	6213.430
Fe	6246.318
Fe	6247.560
Fe	6252.555
Fe	6271.280
Fe	6322.690
Fe	6358.697
Fe	6411.650
Fe	6430.845
Fe	6432.680
Fe	6494.980
Fe	6516.077
Fe	6546.238
Fe	6593.870
Fe	6609.110
Fe	6627.544
Fe	6633.750
Fe	6677.985
Fe	6739.520
Fe	6750.151
Fe	6793.260
Li	6707.764
Mg	5528.405
Mg	5711.088
Mn	5117.935
Mn	5377.622
Mn	5394.619
Mn	5399.475
Mn	5407.490
Mn	5420.423
Mn	5457.518
Mn	5516.821
Mn	5537.801
Mn	6013.475
Mn	6016.643
Mn	6021.801
Mn	6440.944
Na	5682.633
Na	5688.205
Nd	5319.810
Ni	5082.344
Ni	5084.096
Ni	5094.411
Ni	5099.930
Ni	5115.392
Ni	5137.074
Ni	5347.708
Ni	5392.331
Ni	5424.645
Ni	5462.493
Ni	5468.104
Ni	5682.199
Ni	5694.983
Ni	5748.351
Ni	5760.830
Ni	5846.994
Ni	5996.730
Ni	6007.310
Ni	6025.754
Ni	6086.282
Ni	6111.070
Ni	6128.973
Ni	6130.135
Ni	6133.962
Ni	6175.367

TABLE F9 — *Continued*

Element	Wavelength (Å)
Ni	6176.807
Ni	6177.242
Ni	6186.711
Ni	6191.178
Ni	6223.981
Ni	6223.981
Ni	6230.089
Ni	6322.166
Ni	6327.599
Ni	6378.247
Ni	6384.662
Ni	6414.581
Ni	6424.852
Ni	6482.798
Ni	6532.873
Ni	6586.310
Ni	6598.598
Ni	6635.123
Ni	6643.630
Ni	6767.772
Ni	6772.315
O	6300.304
O	6363.776
Sc	5239.813
Sc	5356.097
Sc	5484.629
Sc	5520.494
Sc	5641.001
Sc	5657.896
Sc	5667.149
Sc	5669.042
Sc	5684.202
Sc	5686.838
Sc	6210.645
Sc	6245.637
Sc	6604.601
Si	5665.555
Si	5684.484
Si	5690.425
Si	5701.104
Si	5708.399
Si	5793.073
Si	5948.541
Si	6155.134
Si	6237.319
Si	6347.109
Si	6741.628
Ti	5147.478
Ti	5210.384
Ti	5211.530
Ti	5219.702
Ti	5224.300
Ti	5295.776
Ti	5336.786
Ti	5338.306
Ti	5381.021
Ti	5384.630
Ti	5418.768
Ti	5426.250
Ti	5490.147
Ti	5662.150
Ti	5689.460
Ti	5716.450
Ti	5903.315
Ti	5922.110
Ti	5937.809
Ti	5953.160
Ti	5965.828
Ti	6091.171
Ti	6092.792
Ti	6126.216
Ti	6258.102
Ti	6261.099
Ti	6312.236

TABLE F9 — *Continued*

Element	Wavelength (Å)
Ti	6336.099
Ti	6554.223
Ti	6599.105
V	5604.955
V	5627.647
V	5657.436
V	5668.375
V	5670.868
V	5703.586
V	5727.016
V	5727.616
V	5737.031
V	6039.723
V	6081.441
V	6090.231
V	6111.673
V	6119.524
V	6135.361
V	6199.156
V	6216.315
V	6256.871
Y	5200.406
Y	5402.774
Y	5544.611
Y	5728.887
Zr	5385.140